Durham E-Theses

Exotic renormalisation group flows from black holes

SOSA-RODRIGUEZ, OMAR,FERNANDO

Exotic renormalisation group flows
from black holes

Omar Fernando Sosa Rodríguez

A thesis presented for the degree of

Doctor of Philosophy

Supervised by Dr. Aristomenis Donos

Exotic RG flows from black holes

Omar Fernando Sosa Rodríguez

Submitted for the degree of Doctor of Philosophy
Supervised by Dr. Aristomenis Donos

July 2018

ABSTRACT: In this thesis we construct a variety of black hole solutions that have planar horizons and are asymptotically Anti-de Sitter, thus relevant in the context of the gauge/gravity correspondence. We use the correspondence to investigate the renormalisation group flows of the corresponding dual field theories. Our solutions break translations along one or more spatial directions of the dual field theory, thus making them suitable for describing lattices in strongly coupled matter. After a brief introduction to the gauge/gravity duality, three different set-ups are considered. First, in the context of type IIB supergravity, our solutions are dual to anisotropic plasmas that arise from deforming an infinite family of CFTs. Second, we construct black holes in $D = 11$ supergravity, making our solutions relevant for ABJM theory. And finally, we take a bottom-up approach, designing a gravity model for which the black hole solutions allows us to model interesting phase transitions that are triggered by the strong breaking of translational invariance.

In each scenario, we observe boomerang-like RG flows, in which the UV fixed point reappears as the IR fixed point. Similarly, all of our constructions reveal one or more intermediate scaling regimes, and we show how this can affect the scaling of some transport coefficients. For the phenomenological boomerang flows, we show that the entropic c-function is not monotonic. Furthermore, this model will reveal a novel thermal insulating ground state that has non-power-law scaling. The relation between the thermal diffusivity and butterfly velocity of these novel ground states is also studied.

Para Carolina, Sergio y Abraxas.

Declaration

The work in this thesis is based on research carried out in the Department of Mathematical Sciences at Durham University. The results presented here are derived from the following collaborative works:

- A. Donos, J. P. Gauntlett and O. Sosa-Rodriguez, *Anisotropic plasmas from axion and dilaton deformations*, *JHEP* **11** (2016) 002, [1608.02970].

- A. Donos, J. P. Gauntlett, C. Rosen and O. Sosa-Rodriguez, *Boomerang RG flows in M-theory with intermediate scaling*, *JHEP* **07** (2017) 128, [1705.03000].

- A. Donos, J. P. Gauntlett, C. Rosen and O. Sosa-Rodriguez, *Boomerang RG flows with intermediate conformal invariance*, *JHEP* **04** (2018) 017, [1712.08017].

No part of this thesis has been submitted for a degree or qualification in this or any other institution. I also herewith certify that, to my best knowledge, all of the material in this dissertation which is not my own has been properly cited.

Acknowledgements for those that talk to me in English

Aristos, thank you for your exceptional supervision throughout the past four years. You've been a very inspiring person, not to mention that you always had the answers for all of my questions. I feel very lucky and proud of being your student.

To my little group of friends: Leo, Mike & Akash. Thank you for all the good times we had together and for making the office a fun place to be at. Thank you, Leo, for being there in the good moments[1] and also the bad ones. Thank you, Mike, for your patience dealing with this Mexican guy that has no clue of how things work in the UK[2]. And thank you, Akash, for the countless times in which you answered my stupid questions[3].

---

[1]Except on birthdays.
[2]Also thank you for never listening to me, btw.
[3]Except after our CFT exam.

Agradecimientos para los que no me hablan en inglés

Familia: Sergio, Carolina, y Sergito. Estoy infinitamente agradecido con Dios por tenerlos conmigo. Todos estos años lejos de ustedes han sido los años más duros de mi vida. Si he podido llegar hasta este punto es solo gracias a ustedes. Gracias por su apoyo y amor incondicional, y por cuidar de mí aun estando lejos. A donde quiera que voy, ustedes son mi fuente de alegría, de inspiración y de confianza. Este trabajo es de ustedes.

Marisa: Durham es un lugar mágico desde que te conozco. Gracias por tu amor y tus sonrisas. Gracias por tomarme de la mano todo este tiempo. Gracias por motivarme, por respaladarme, y por levantarme en los momentos difíciles. Y gracias por enseñarme tantas y tantas cosas; soy muy afortunado de tener la oportunidad de descubrir el mundo contigo.

Contents

1 | Motivation and outline

Quantum Field Theory (QFT) is one of the biggest achievements of theoretical physics. For decades now, it has been the framework of choice when tackling virtually any problem in fundamental physics. However, QFT has two major limitations:

1. So far, every attempt to include gravity into the QFT framework has failed. While the other known fundamental forces comply with the rules of the quantum world, our best approach when dealing with gravity remains classical, namely, Einstein's theory of general relativity.

2. QFT is most easily approached in a weak-coupling regime. When the interactions underlying the system of interest are strong, the perturbative methods based on Feynman diagrams are not applicable. Significant effort has been made throughout the years in order to better understand strongly coupled phenomena. Yet, until today, a generic approach for strongly-coupled phenomena remains to be found.

The above problems have, for many years now, seeded several research disciplines—String Theory among them. Initially forged to be a theory of strong interactions, String Theory was eventually put to a side in favour of non-abelian gauge theories as the correct framework. Years later, String Theory reemerged, when it was realised that it was a plausible candidate for a theory of quantum gravity. Hoewever, the field saw a sudden expansion in 1997 after Maldacena published his paper *The large N limit of superconformal field theories and supergravity* [4].

The analysis in [4], together with the follow-up work in [5], claimed that, under the light of String Theory, quantum gravity in a $d + 2$-dimensional spacetime is equivalent to a gauge theorie living in the boundary of such spacetime. Further more, it claimed that *strongly* coupled gauge theories with a large number of degrees of freedom can be equivalently described by classical gravity; essentially tackling both of the above problems in one go. The claim, now called the *gauge/gravity* duality, unleashed a myriad of deep implications. Nowadays, String Theory is being used to shed light upon longstanding problems in all corners of physics. At the time of writing this thesis, [4] is the most cited article on HEP inSpire.

A particular area of physics in which the gauge/gravity duality is being used to develop intuition is Condensed Matter Physics. The major goal of the condensed matter theorist, as put by P. Coleman in [6], is to explain the emergent properties of

different materials, as we move from the microscopic (UV) to the macroscopic (IR), i.e., along the *renormalisation group (RG) flow* [7]. For weakly-coupled systems, one can typically make use of perturbative techniques in order to understand the RG flow. It is fair to say that the possible phenomena of weakly coupled matter is now well understood. The main obstacle lies again in strongly coupled systems.

The gauge/gravity duality is a powerful tool to explore generic features of certain classes of strongly coupled theories. As we shall see, the RG flow of a gauge theory acquires a neat geometric interpretation when seen from the perspective of its gravity dual, hence allowing us to probe different energy scales without the use of perturbation theory. However, much of the exploration done in this regard has been aimed at modelling systems that posses translational invariance. This becomes an immediate issue if one wishes to make direct contact with real matter systems, for which translation invariance is often absent due to the presence of an ionic lattice or impurities. Furthermore, for unitary, Poincaré invariant QFTs in 2 and 4 spacetime dimensions there exist the *c-theorem* [8] and *a-theorem* [9, 10] respectively, which already impose strong restriction on the possible paths that an RG flow might take, but it is not known if these restrictions extend to theories that do not posses translation invariance. An analogous theorem, the *F-theorem* has also been proposed for 3-dimensional QFTs (see [11]), but it has already been shown that such theorem does not hold in general [12]. A c-theorem based on entanglement entropy has also been proposed in [13, 14]. One of the advantages of holography is that the 'c'-theorems are easily approached in any dimensionality [15, 16].

This thesis is an exploration of the possible features that, according to the gauge/gravity duality, strongly coupled matter may exhibit. To do so, we must first review the two main ingredients that are necessary for understanding the duality: Conformal Fields Theories and dynamics of gravity in Anti de-Sitter spacetimes. We do this in chapter 2, which is not meant to be a thorough treatment of these topics but rather a quick overview with emphasis on the main similarities between them. In chapter 3 we introduce the statement of the gauge/gravity duality. The stress of this chapter is on how to use the duality. We explain how to compute correlation functions from the gravity side which naturally entails a discussion on renormalisation. We go on to show how to model the gravity equivalent of a lattice in a field theory, we call this a *holographic lattice*. This, as we shall see, is a simple enough idea but its implementation will necessarily involve numerics. The first appendix of this thesis is dedicated to explain the main numerical method employed throughout this work.

The work done in [1–3] is the content of chapters 4 to 6. In chapter 4 we build holographic lattices by deforming an infinite class of Conformal Field Theories that arise in the context of type IIB string theory. The gravity dual of these theories is a truncation of type IIB supergravity. Following the RG flow for these models, we

will show that the same solution that describes the UV behaviour reemerges in the deep IR. This 'boomerang-like' path for an RG flow had already been observed in other constructions that break translations. However, for strong lattice deformations we will find that an intermediate scaling regime appears in the RG flow. This intermediate scaling is governed by Lifshitz-like type of scaling [17] and its effects can extend over arbitrarily large range of scales as the strength of the lattice is increased. We will also compute some transport coefficients and show how the intermediate scaling imprints itself in the scaling of these quantities. In chapter 5, we extend the techniques developed so far, this time to construct holographic lattices in the context of $D = 11$ supergravity. Again we will see the boomerang-like behaviour of the RG flow, and we will also find intermediate scaling regimes for strong lattice deformation. However, contrary to the model in chapter 4, we will observe *two* intermediate regimes, each with hyperscaling violation [18]. In chapter 6 we engineer a gravity model that allows us to construct boomerang RG flows with intermediate conformal invariance. By design, this model is more manageable than those in the previous chapters and so we will be able to make more precise computations. One of the most remarkable features of our model is that we will see a thermal conductor-to-insulator quantum phase transition for a critical value of the lattice strength, and the phase diagram of this model will also show phase transitions at finite temperature. We will further see that the entropy for the novel insulating ground states vanishes as the temperature goes to zero, but this does not happen as a power-law. The appendices B to D, contain further details for the respective chapters 4, 5 and 6; they have been delegated to the end of the thesis to avoid breaking the flow between chapters.

Finally, in chapter 7 we give a quick recap of the main results found in this thesis, together with interesting future directions that this work might take.

2 | Preliminaries

In this chapter we start by defining conformal field theories (CFTs) for $d > 2$ spacetime dimensions. The particular, much richer case of 2-dimensional CFTs will not play any direct role in this thesis. After pointing out some important facts about CFTs, we go on to highlight the restrictions that conformal symmetry imposes on correlation functions and on the dimension of operators. In section 2.2 we make a drastic change of topic to discuss the dynamics of classical gravity in anti de-Sitter (AdS) spacetimes, including classical field dynamics in *AdS* backgrounds and black hole thermodynamics. The review of these topics is not meant to be thorough. Instead, the content of this chapter has been chosen as to highlight the key similarities that play a role in the future chapters.

2.1 | Conformal field theories

2.1.1 Definitions

A conformal field theory (CFT) is a field theory that is invariant under conformal the conformal group, which we now define. Given a spacetime with a metric $g_{\mu\nu}$, a *conformal transformation* is a change of coordinates such that

$$g_{\mu\nu} \to g'_{\mu\nu}(x) = \Omega^2(x)g_{\mu\nu}(x), \tag{2.1}$$

for some function Ω. The set of transformations satysfaying (2.1) form a group called the *conformal group*. In $\mathbb{R}^{1,d}$ Minkowski spacetime, Poincaré transformations are trivial examples of conformal transormations with $\Omega^2 = 1$. In $d + 1 \geq 3$ dimensions the other continuous transformations that satisfy (2.1) are [19, 20]

$$x^\mu \to \lambda x^\mu \tag{2.2}$$

$$x^\mu \to \frac{x^\mu + a^\mu x^2}{1 + 2a_\mu x^\mu + a^2 x^2} \tag{2.3}$$

where λ and a^μ are the continuous parameters of the transformations. We refer to (2.2) as a *dilation* or *scale transformation*, and to (2.3) as a *special conformal transformation* (SCT). Looking at the infinitesimal version of the above transformations one finds

the corresponding generators:

$$D = -ix^\mu \partial_\mu \qquad \text{(for dilations)} \qquad (2.4)$$

$$K^\mu = i(g^{\mu\nu}x^2 - 2x^\mu x^\nu)\partial_\nu \qquad \text{(for SCT)} \qquad (2.5)$$

Together with the generators of the Poincaré algebra, $P_\mu = -i\partial_\mu$ (translations) and $J_{\mu\nu} = i(x_\mu \partial_\nu - x_\nu \partial_\mu)$ (boosts and rotations), dilations and SCTs form a closed algebra

$$[P_\mu, P_\nu] = 0 \quad [K^\mu, K^\nu] = 0, \quad [D, J_{\mu\nu}] = 0$$

$$[D, P^\mu] = iP^\mu, \quad [D, K^\mu] = -iK^\mu, \quad [K^\mu, P^\nu] = 2i(g^{\mu\nu}D - J^{\mu\nu})$$

$$[J^{\mu\nu}, K^\lambda] = -i(g^{\mu\lambda}K^\nu - g^{\nu\lambda}K^\mu), \quad [J^{\mu\nu}, P^\lambda] = -i(g^{\mu\lambda}P^\nu - g^{\nu\lambda}P^\mu)$$

$$[J^{\mu\nu}, J^{\lambda\rho}] = i(g^{\nu\lambda}J^{\mu\rho} + g^{\mu\rho}J^{\nu\lambda} - g^{\mu\lambda}J^{\nu\rho} - g^{\nu\rho}J^{\mu\lambda}) \qquad (2.6)$$

and one can show that this is isomorphic to the Lie algebra of $SO(2, d+1)$. It is called the conformal algebra in $d+1$ dimensions ($d+1 \geq 3$).

2.1.2 Representations of the conformal group

One then asks how conformal transformations act on fields. That is, given an element of g of the conformal group $SO(2, d+1)$, we look for the possible representations

$$(g \cdot \Phi)(x) = S(g, x)\Phi(g^{-1}x). \qquad (2.7)$$

where $S(g, x)$ is a matrix representation of the group element g. To construct these, one starts by constructing the representations of the little group (i.e. the subgroup that leaves the point $x = 0$ invariant)[21]. After taking into account the translations one finds

$$P_\mu \Phi(x) = -i\partial_\mu \Phi(x) \qquad (2.8)$$

$$J_{\mu\nu}\Phi(x) = i(x_\mu \partial_\nu - x_\nu \partial_\mu)\Phi(x) + S_{\mu\nu}\Phi(x) \qquad (2.9)$$

$$D\Phi(x) = -i(x^\mu \partial_\mu + \Delta)\Phi(x) \qquad (2.10)$$

$$K_\mu \Phi(x) = (-2i\Delta x_\mu - x^\nu S_{\mu\nu} - 2ix_\mu x^\nu \partial_\nu + ix^2 \partial_\mu)\Phi(x) \qquad (2.11)$$

where Δ is a number[1] called the *scaling dimension* of Φ, and $S_{\mu\nu}$ is the usual spin representation of the Lorentz group. A finite scaling transformation takes the form

$$\Phi(x) \to \Phi'(x) = \lambda^\Delta \Phi(\lambda x). \qquad (2.12)$$

---

[1] The fact that Δ is a number and not a non-trivial matrix follows from Schur's lemma, because $[D, J_{\mu\nu}] = 0$.

At the classical level Δ coincides with the engineering dimension of the field, but it might get corrections upon quantization.

In field theories without conformal invariance it is customary to label states by their mass, $P^\mu P_\mu = -m^2$. One can then evolve from one state to another by means of a unitary evolution given by the Hamiltonian operator. This is a useful classification because P^2 is a Casimir of the Poincaré algebra, that is, it commutes with all the generators. In CFTs, however, P^2 does not commute with the dilation operator D and thus it is neccesary to find a different way of labelling states. This is related to the fact that the conformal algebra is a bosonic extension of the Poincaré algebra and, as such, Coleman-Mandula thoerem forbids the existence of an S-matrix [22]. A approach is to label states by their scaling dimension and their spin[2]. Assuming a conformally invariant vacuum, $|0\rangle$, we use an operator of dimension Δ, $\mathcal{O}_\Delta$, to create the state $|\Delta\rangle \equiv \mathcal{O}_\Delta(0)|0\rangle$ so that

$$D|\Delta\rangle = -i\Delta|\Delta\rangle. \tag{2.13}$$

From this perspective, P_μ and K_μ can be seen as raising and lowering operators, with D playing the role of the Hamiltonian. After doing Wick rotation, $t \to it$, and moving to spherical coordinates, the Minkowski metric can be rewritten as

$$\mathrm{d}s_{d+1}^2 = \mathrm{d}r^2 + r^2\mathrm{d}\Omega_d^2 \tag{2.14}$$

The dilations D are then naturally seen as connecting the different hyper-surfaces of constant radius. Because of this, the formalism is known as radial quantisation. For systems that are relevant in physics, we expect that the spectrum is bounded from below. This means that there should exist some state $|\Delta\rangle \equiv \mathcal{O}_\Delta|0\rangle$ for which $K_\mu|\Delta\rangle = 0$ or, equivalently,

$$[K_\mu, \mathcal{O}_\Delta] = 0. \tag{2.15}$$

The operator $\mathcal{O}_\Delta$ satisfying (2.15) is called a *primary operator*. Taking a spinless primary operator $\mathcal{O}_\Delta$, one can show [23] that the norm $||P^\mu P_\mu \mathcal{O}_\Delta|0\rangle||^2$ is proportional to $\Delta - (d-1)/2$. Thus, if we want our theory to be unitary we must demand that

$$\frac{d-1}{2} \leq \Delta. \tag{2.16}$$

Similar bounds exist for higher spin operators.

To conclude this section we point out that in any quantum field theory one should specify an energy scale cut-off Λ up to which the theory is meant to be valid. In

---

[2]We will be mainly interested in Lorentz scalars so we will omit the representation.
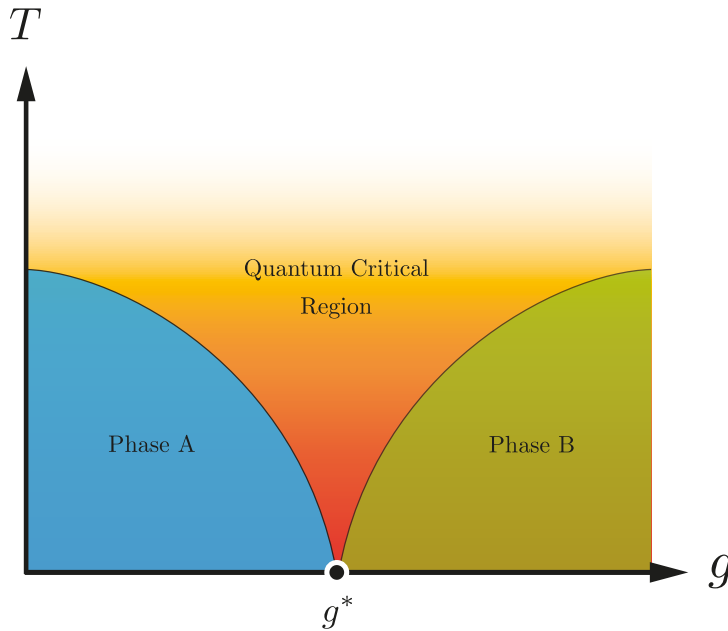
Figure 2.1: Illustration of a phase diagram in the vicinity of a quantum critical point, g^*. The critical point separates the two different phases with a fan-shaped region over which the effects of quantum critical fluctuations can be appreciated (see also [26]).

QFT the cut-off is introduced by hand to regulate the UV divergences of the theory, and explicit dependence on the cutt-off is then removed by means of renormalisation. Similarly, in condensed matter physics a cut-off naturally arises due to a finite lattice spacing in the underlying theory. In both scenarios the introduction of this cut-off gives a dimensionful quantity that *a priori* breaks scale invariance. The behaviour of the quantum theory under scale transformations is captured by the beta function

$$\frac{dg}{d\ln\Lambda} = \beta(g). \tag{2.17}$$

Thus, in a quantum theory we can recover scale invariance (and, carefully, conformal invariance) only in very particular circumstances. For example, it is possible that $\beta(g) \equiv 0$; this is the case in some supersymmetric theories such as in $\mathcal{N} = 4$ Super Yang-Mills [24]. Another possibility, of most interest for us, is at *quantum critical points* (QCP). These are special points in the space of coupling constants, $g = g^*$, for which a phase transition occurs at zero temperature [25]. Even though QCPs formally occur at zero temperature, they can still affect a vicinity of the finite temperature phase diagram and can give rise to exotic transport properties in such regimes (see figure 2.1).

2.1.3 Correlators and relevant operators

A distinctive feature of CFTs is that correlation functions take a simple form. We recall here that the standard procedure to compute correlation functions of an operator $\mathcal{O}_\Delta$ in a generic QFT involve derivatives of the generating functional

$$Z_{QFT}\left[j(x)\right] = \int \mathrm{d}\Phi \exp\left(iS_{QFT} + i\int \mathrm{d}^{d+1}x j(x)\mathcal{O}_\Delta(x)\right), \qquad (2.18)$$

so that the n-point correlator is given by

$$\langle \mathcal{O}_\Delta...\mathcal{O}_\Delta\rangle = \frac{(-i)^n}{Z\left[j\right]}\frac{\delta^n Z\left[j\right]}{\delta j^n} \qquad (2.19)$$

These n-point correlators are generically divergent; a regularisation procedure is needed to have a sensible description. On renormalising the theory, one can show that the effect of operators for which $\Delta < d+1$ becomes increasingly important as the energy is lowered - these are called *relevant* operators. Conversely, operators with $\Delta > d+1$ become negligible at low energies and are thus called *irrelevant*. Reversing the argument, relevant operators become negligible in the UV while the effect of irrelevant operators becomes more and more important. This simple distinction between operators has huge implications. While we could, in principle, deform our theory by adding operators with arbitrarily large dimensions, only the few operators for which

$$\frac{d-1}{2} \leq \Delta \leq d+1 \qquad (2.20)$$

are important for a low energy description[3]. Note also that the addition of the $j\mathcal{O}$ term to the CFT action explicitly breaks scale invariance (unless $\Delta \equiv d+1$), even before a cut-off is introduced. However, if we restrict ourselves to only modify the theory by relevant operators satisfying eq. (2.20), we are guaranteed to recover the CFT in the UV.

Within the conformal regime we can calculate 2 and 3-point functions without an explicit expression for the generating functional (2.18), simply appealing to the conformal symmetry. For example, taking two operators of scaling dimensions Δ_1 and Δ_2, their two-point function $\langle \mathcal{O}_1(x)\mathcal{O}_2(y)\rangle$ has to take the form

$$\langle \mathcal{O}_1(x)\mathcal{O}_2(y)\rangle = f(|x-y|) \qquad (2.21)$$

due to to Poincaré invariance. Then, scale invariance requires $f(x) = \lambda^{\Delta_1+\Delta_2}f(\lambda x)$.

---

[3]The lower bound comes from the unitarity bound for scalar operators mentioned in the previous section

Therefore, the two point function must be

$$\langle \mathcal{O}_1(x)\mathcal{O}_2(y)\rangle = \frac{C_{12}}{(x-y)^{\Delta_1+\Delta_2}}, \tag{2.22}$$

with C_{12} some constant that depends on the particular choice of normalisation for the operators. A similar expression can be found for the 3-point correlator. For future reference, we point out that the source $j(x)$ for the operator $\mathcal{O}_\Delta$ has engineering dimension $\Delta_j = d + 1 - \Delta$.

An important operator that should exist in any CFT is the stress tensor $T_{\mu\nu}$. If a Lagrangian description of the CFT is given, the stress tensor can be defined by the variation of the action with respect to the background metric

$$\delta S = \int \mathrm{d}^{d+1}x\sqrt{-g}T_{\mu\nu}\delta g^{\mu\nu}, \tag{2.23}$$

from where we see that $\Delta_{T_{\mu\nu}} = d+1$. In a CFT, Poincaré invariance implies that the stress tensor is conserved, while scale invariance implies that it should be traceless:

$$\nabla^\mu T_{\mu\nu} = 0 \tag{2.24}$$

$$T^\mu_\mu = 0. \tag{2.25}$$

Note that upon quantization, however, one can have $\langle T^\mu_\mu\rangle \neq 0$ [27] due to the presence of anomalies. Note that anomalies can only be present in even-dimensional QFTs. This is because $\langle T^\mu_\mu\rangle$ is a scalar quantity that does not depend on any particular state and thus can only be equal to a linear combination of curvature invariants of the background metric, which only exist in even dimensions. The equivalent of eq. (2.22) for the stress tensor is [28]

$$\langle T_{\mu\nu}(x)T_{\alpha\beta}(0)\rangle = \frac{c_{eff}}{x^{2(d+1)}}\left(\frac{A_{\mu\alpha}A_{\nu\beta}+A_{\mu\beta}A_{\nu\alpha}}{2}-\frac{1}{d}\eta_{\mu\nu}\eta_{\alpha\beta}\right) \tag{2.26}$$

$$A_{\mu\nu} \equiv \eta_{\mu\nu} - \frac{2}{x^2}x_\mu x_\nu \tag{2.27}$$

The proportionality constant, c_{eff}, is called the *effective central charge* and it is a rough measure for the number of degrees of freedom in the system, as it is the quantity that appears in (the generalised) Cardy's formula [29, 30]. In 2d CFTs it is equal to the central charge.

2.2 | Anti de-Sitter spacetime

2.2.1 Definitions

In the context of general relativity, anti de-Sitter spacetime of dimension $d + 2$, AdS_{d+2}, is the maximally symmetric spacetime of negative curvature. Maximal symmetry means that the number of independent isometries is $(d + 2)(d + 3)/2$. As a consequence of maximal symmetry, one finds that

$$R_{abcd} = k \left(g_{ad}g_{bd} - g_{ad}g_{bc} \right) \tag{2.28}$$

$$\implies R_{ab} = k(d + 1)g_{ab} \tag{2.29}$$

$$\implies R = k(d + 2)(d + 1), \tag{2.30}$$

and negative curvature means $k < 0$. Note in particular that, by (2.29), AdS_{d+2} is an Einstein manifold. The eqs. (2.29) and (2.30) also imply that AdS_{d+2} is a solution to Einstein equations with negative cosmological constant

$$R_{ab} - \frac{1}{2}Rg_{ab} + \Lambda g_{ab} = 0, \tag{2.31}$$

with

$$\Lambda = \frac{k}{2}d(d + 1). \tag{2.32}$$

The equation of motion (2.31) can be obtained from a variational principle with an action of the form

$$S = \frac{1}{2\kappa^2} \int \mathrm{d}^{d+2}x\sqrt{-g}\left(R - 2\Lambda\right) + S_\partial. \tag{2.33}$$

The term S_∂ refers to the boundary terms that are necessary to have a well defined variational set-up. As in the case for asymptotically flat spacetimes, S_∂ includes the Gibbons-Hawking-York term,

$$S_{GHY} = \frac{1}{\kappa^2} \int \mathrm{d}^{d+1}x\sqrt{-\gamma}K, \tag{2.34}$$

but additional terms will be necessary to counter volume divergences. We will come back to this point in due time.

In a particular set of coordinates known as *global coordinates* the AdS_{d+2} solution

of radius L reads[4]

$$ds^2 = L^2(-\cosh^2\rho\, d\tau^2 + d\rho^2 + \sinh^2\rho\, d\Omega_d^2), \tag{2.35}$$

where $\rho \in [0, \infty)$ and $\tau \in (-\infty, +\infty)$. The AdS radius, L, is related to the cosmological constant via

$$\Lambda = -d(d+1)/L^2. \tag{2.36}$$

There are two main properties of AdS spacetime that will be relevant for us [31]:

1 **Isometry group is SO(2, d + 1).** The easiest way to see this comes from the fact that one can define AdS_{d+2} through the embedding

$$-X_{-1}^2 - X_0^2 + X_1^2 + ... + X_{d+1}^2 = -L^2 \tag{2.37}$$

into a $(d + 3)$-dimensional manifold with metric

$$ds^2 = -dX_{-1}^2 - dX_0^2 + dX_1^2 + ... + dX_{d+1}^2. \tag{2.38}$$

The solution (2.35) is obtained by writing

$$X_{-1} = \cosh\rho\sin\tau\,,\;\; X_0 = \cosh\rho\cos\tau\,,\;\; X_k = \Omega_k\sinh\rho, \tag{2.39}$$

where $k = 1, ..., d + 1$ and Ω_k define the components of a unit vector. We then define AdS_{d+2} as the universal cover of the above solution, where τ is not identified with $\tau + 2\pi$.

The killing vectors of the metric (2.38) that also preserve the structure (2.37) are given by

$$L_{AB} = X_A\partial_B - X_B\partial_A. \tag{2.40}$$

Due to the antisymmetry, there are $(d + 3)(d + 2)/2$ of such Killing vectors and one can further check that they satisfy the Lie algebra of $SO(2, d + 1)$. Expressions for the Killing vectors in a specific coordinate patch are given in eq. (2.48).

2 **It is not globally hyperbolic.**   This is seen by changing to conformal coordinates, $\tan\theta = \sinh\rho$. The metric (2.35) becomes

$$ds^2 = \frac{L^2}{\cos^2\theta}(-d\tau^2 + d\theta^2 + \sin^2\theta d\Omega_d^2). \tag{2.41}$$

---

[4] $d\Omega_d^2 = d\chi^2 + \sin^2\chi d\Omega_{d-1}^2$
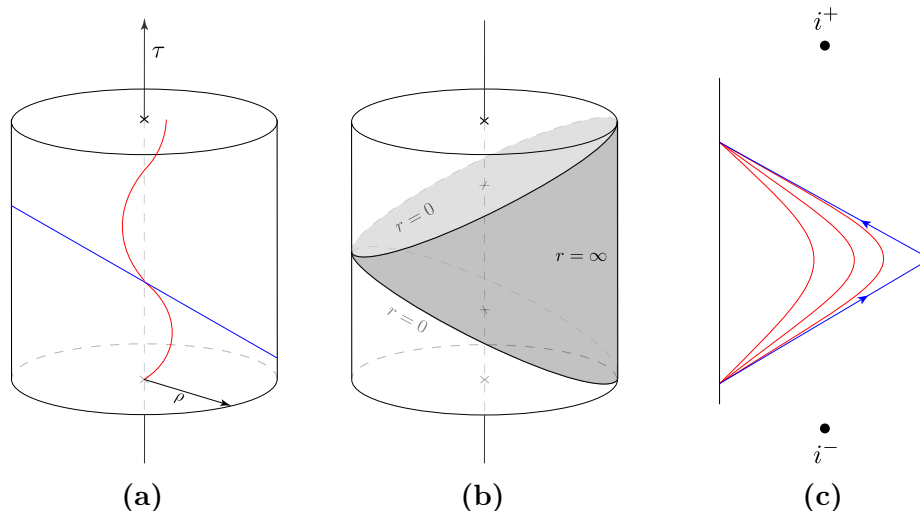
Figure 2.2: Schematic realisation of AdS spacetime showing some null (blue) and timelike (geodesics). Figure a shows the the universal cover of AdS in global coordinates. Figure b shows the section known as the Poincaré patch. Figure c shows the Penrose diagram for AdS; null geodesics travel to $\rho = \infty$ in finite coordinate time τ, while timelike geodesics always fall back to $\rho = 0$.

On the conformal boundary, now located at $\theta = \pi/2$, the metric is

$$\mathrm{d}s^2 = -\mathrm{d}\tau^2 + \mathrm{d}\Omega_d^2, \quad \text{at } \theta = \pi/2 \tag{2.42}$$

which is clearly time-like with the topology of $S^d \times \mathbb{R}$. Therefore, one cannot find a Cauchy surface[5] in AdS. This means that it is not enough to provide some initial data on a constant-time surface to fully determine the evolution of the system. In order to do classical dynamics it will be necessary to specify boundary conditions.

The above properties are the main hints for an AdS/CFT correspondence. The first point shows that the isometry group of AdS_{d+2} coincides with the conformal group of $(d+1)$-dimensional Minkowski. The second one states that in order to determine the dynamics of AdS one has to specify boundary conditions at the conformal boundary. The boundary values of fields in AdS will give rise to a conformal field theory that "lives" at the boundary.

In the context of the gauge/gravity correspondence, AdS spacetime is most often discussed in Poincaré coordinates, (r, t, x_i), in which the metric reads

$$\mathrm{d}s^2 = \frac{L^2}{r^2}\mathrm{d}r^2 + \frac{r^2}{L^2}\left(-\mathrm{d}t + \mathrm{d}\mathbf{x}_d^2\right). \tag{2.43}$$

with $r \in [0, \infty)$ and the conformal boundary now located at $r = \infty$. One arrives to

---

[5]A $d+1$ submanifold that intersects every inextensible causal curve exactly once.

this metric from (2.38) by defining

$$
\begin{aligned}
X^{\alpha} &= \frac{r x^{\alpha}}{L} \quad (\alpha = 0, 1, ..., d) && (2.44)\\
X^{(-1)} - X^{(d+1)} &= r && (2.45)\\
X^{(-1)} + X^{(d+1)} &= \frac{L^2}{r} + \frac{r}{L^2} \eta_{\alpha\beta} x^{\alpha} x^{\beta}\,. && (2.46)
\end{aligned}
$$

Similarly, taking $z = L^2/r$, the metric takes the rather simple form

$$
\mathrm{d}s^2 = \frac{L^2}{z^2} (\mathrm{d}z^2 + \eta_{\alpha\beta} \mathrm{d}x^{\alpha} \mathrm{d}x^{\beta})\,. \tag{2.47}
$$

We note that the Poincaré patch is conformally flat, and so we identify the Killing vectors to be[6]

$$
\begin{aligned}
t_{(\alpha)} &= \partial_{\alpha}\\
l_{(\alpha\beta)} &= x_{\alpha} \partial_{\beta} - x_{\beta} \partial_{\alpha}\\
k_{(\alpha)} &= (x^2 + z^2) \partial_{\alpha} - 2 x_{\alpha} x^{\beta} \partial_{\beta} - 2 x_{\alpha} z \partial_z\\
s &= z \partial_z + x^{\alpha} \partial_{\alpha} \tag{2.48}
\end{aligned}
$$

There are in total $(d+2)(d+3)/2$ Killing vectors, as it should be for a Maximally symmetric spacetime. Furthermore, we see that at the conformal boundary, located at $z = 0$, the Killing vectors k_{α} and s reduce to the generators for the conformal transformations in eqs. (2.2) and (2.3). Finally, one should keep in mind that, as oposed to the Global coordinates, Poincaré coordinates only cover a section of the whole AdS spacetime. This section is highlighted in **??**.

2.2.2 Fields in AdS

We now consider classical dynamics of a scalar field. Higher spin fields are interesting in their own right, but they will not play an important role in the rest of this thesis and thus we shall omit their discussion. Consider the action

$$
S = S_{\mathrm{EH}} + S_{\phi} + S_{\partial} \tag{2.49}
$$

where S_{EH} is the Einstein-Hilbert action introduced in the previous section and

$$
S_{\phi} = \frac{1}{2\kappa^2} \int \mathrm{d}^{d+2}x \sqrt{-g} \mathcal{L}_{\phi} = -\frac{1}{4\kappa^2} \int \mathrm{d}^{d+2}x \sqrt{-g} \left(g^{AB} \nabla_A \phi \nabla_B \phi + m^2 \phi^2 \right) \tag{2.50}
$$

---

[6]Here only, indices $\alpha, \beta (= 0, 1, ..., d)$ are raised with the Minkowski metric $\eta_{\alpha\beta} = \mathrm{diag}(-1, 1, ..., 1)$.

S_∂ is a boundary term to be discussed shortly. The equations of motion for this system read

$$R_{ab} - \frac{1}{2}Rg_{ab} + \Lambda g_{ab} = T_{ab} \tag{2.51}$$

$$\nabla^2 \phi = m^2 \phi. \tag{2.52}$$

where

$$T_{ab} \equiv -\frac{1}{\sqrt{-g}}\frac{\delta(\sqrt{-g}\mathcal{L}_\phi)}{\delta g^{ab}} \tag{2.53}$$

The rather unusual normalisation of the action is standard in holography. Note that, since $[\kappa^2] = [L]^d$ (in $d+2$ spacetime dimensions), the scalar field ϕ is in fact dimensionless.

The particular case for which $\phi \equiv 0$ admits the pure AdS_{d+2} spacetime as a solution to (2.51). In this set-up we can consider ϕ to be a small fluctuation so that there is no back-reaction on the metric. In such case the solution to (2.52) can be found in terms of Bessel functions. Analysis near the conformal boundary of AdS_{d+2}, located at $r \to \infty$, reveals that the solution is of the form

$$\phi(r,x) \to \frac{\alpha(x)L^{2\Delta_-}}{r^{\Delta_-}} + \cdots + \frac{\beta(x)L^{2\Delta_+}}{r^{\Delta_+}} + \cdots , \tag{2.54}$$

where

$$\Delta_\pm = \frac{d+1}{2} \pm \sqrt{L^2 m^2 + \frac{(d+1)^2}{4}} \tag{2.55}$$

The functions (also called *modes* or *fall-offs*) α and β correspond to the integration 'constants' that result from solving the differential equation (2.52). The term with $\alpha(x)$ is the slowest possible fall-off and the following terms, denoted by "...", are all determined by the value of α. The mode $\beta(x)$ is the next independent term and the following terms, again denoted by "...", are all determined in terms of it. Given that ϕ is dimensionless, it follows that the mass dimension of β is Δ_+, and the mass dimension of α is $\Delta_- = d + 1 - \Delta_+$. Hence one sees that the modes in (2.54) are related in the same way a CFT operator $\mathcal{O}_\Delta$ is related to its source (at least dimension-wise).

For the solution to be stable, it is required that $\Delta_\pm \in \mathbb{R}$, so

$$m^2 \geq m_{BF}^2 \equiv -\frac{(d+1)^2}{4L^2}, \tag{2.56}$$

which is known as the *Breitenlohner-Freedman bound* (or simply BF bound [32]). On saturating the BF bound, one has $\Delta_+ = \Delta_-$, and the asymptotic solution (2.54) in

fact takes a different form that involves logarithmic terms. We will not discuss this situation and assume that the mass of the scalar field is strictly above the BF mass.

Though independent in principle, $\beta(x)$ will also be determined in terms of $\alpha(x)$ because we will need to choose boundary conditions in the deep interior of the bulk. Note that when $m^2 > 0$ then Δ_- is negative and so the term proportional to α in fact diverges as $r \to \infty$. In such cases one can no longer have asymptotic an AdS boundary. This is a challenging situation from the point of view of holography; as it will become clear later on, it corresponds to studying field theories that have been deformed by irrelevant operators (see, for example, [33, 34]). However, we will not attempt to discuss such situations. We will always be interested in solutions for which we can recover the AdS geometry asymptotically, and thus we only consider field configurations for which

$$m_{BF}^2 \leq m^2 \leq 0. \tag{2.57}$$

If eq. (2.57) is satisfied, we will say that the field ϕ is *relevant*. Since $\Delta_+ > \Delta_-$, the modes β and α are usually referred to as the *fast (subleading) fall-off* and *slow (leading) fall-off* respectively.

Let us now briefly discuss the issue of imposing appropriate boundary conditions. A well defined phase space is only possible if the space of solutions is normalisable. This is the criteria we will use. Recall that the generalised Klein-Gordon inner product is

$$(\phi_1, \phi_2) = i \int_{\Sigma_t} \mathrm{d}S n^\mu (\phi_1^* \partial_\mu \phi_2 - \phi_2 \partial_\mu \phi_1^*) \tag{2.58}$$

where Σ_t is a slice of constant t, $\mathrm{d}S$ is the induced volume element on such a surface and n^μ is its unit normal vector. In the particular context of AdS_{d+2}, this means the a field which solves eq. (2.52) has a norm that behaves asymptotically as

$$||\phi||^2 \sim \int^\infty \mathrm{d}r r^{d-2-2\Delta_\pm}. \tag{2.59}$$

Thus, in order to have normalisable solutions we must demand that $d-2-2\Delta_\pm < -1$, or equivalently,

$$\frac{d-1}{2} < \Delta_\pm. \tag{2.60}$$

The above requirement is always true for Δ_+. In other words, the $\beta(x)$ mode is always *normalisable*. On the other hand, Δ_- satisfies eq. (2.60) only when $m_{BF}^2 \leq m^2 < m_{BF}^2 + L^{-2}$ and thus the α mode is often *non-normalisable*. With this criteria at hand, the *standard* choice is to fix by hand the value α and let

β be determined by the evolution of the system. The other boundary condition needed to solve the equation of motion will come from the demanding regularity in the bulk interior. For the special case in which α is normalisable, one has the *alternative* to fix the value of β instead as the boundary condition at infinity. This is important because each choice gives rise to different dynamics and hence, to a different interpretation via the AdS/CFT correspondence. Together with the BF bound (2.56), eq. (2.60) means that we should have

$$\frac{d-1}{2} \leq \Delta_- \leq \Delta_+ \leq d+1 \tag{2.61}$$

in order to have normalisable solutions (c.f with eq. (2.20)). A more detailed analysis of this topic can be found in [35].

2.2.3 Black holes in AdS_{d+2}

Finally, a black hole solution to the system (2.51) is given by $\phi \equiv 0$ and [36, 37]

$$ds^2 = \frac{L^2}{r^2 f(r)} dr^2 + \frac{r^2}{L^2} \left(-f(r) dt^2 + d\mathbf{x}_d^2 \right) , \tag{2.62}$$

$$f(r) = 1 - \frac{r_0^{d+1}}{r^{d+1}}. \tag{2.63}$$

The solution (2.62) is known as the AdS-Schwarzschild (SAdS) black hole. These are some of the main features of SAdS:

1. The black hole horizon is located at $r = r_0$. We see that the induced metric at the horizon is

$$ds^2 \Big|_{r_0,} = \frac{r_0^2}{L^2} d\mathbf{x}_d^2. \tag{2.64}$$

   Thus it is said that the SAdS black hole (2.62) has a planar horizon.

2. Note that $f(r) \to 1$ as $r \to \infty$. Hence the AdS metric (2.43) is recovered near the boundary. The discussion of the previous section remains valid in the presence of the SAdS black hole.

3. The Hawking temperature can be obtained as usual by switching to Euclidean signature and demanding regularity at the horizon. One finds

$$4\pi T = \sqrt{-g'_{tt} g^{rr'}} \Big|_{r_0} \tag{2.65}$$

So for the SAdS black hole in $d + 2$ dimensions we have

$$4\pi T = \frac{(d+1)r_0}{L^2} \tag{2.66}$$

Thus, the SAdS black hole has positive specific heat, as opposed to the asymptotically flat Schwarzschild black hole[7].

4. The entropy is given by the area of the horizon

$$S = \frac{A}{4G} = \frac{2\pi}{\kappa^2} \int_{r_0} \mathrm{d}^d x \sqrt{h} = \frac{2\pi r_0^d}{\kappa^2 L^d} V_d. \tag{2.67}$$

This is infinite because of the volume factor V_d, as expected for a non-compact horizon. However, the entropy *density* is finite and we can express it in terms of the temperature:

$$s \equiv \frac{S}{V_d} = \frac{2\pi(4\pi L)^d}{\kappa^2(d+1)^d} T^d \tag{2.68}$$

Note in particular that this power law relation is the same as for a CFT_{d+1} at finite temperature.

Having computed the entropy density in terms of temperature, one can use the first law, $\mathrm{d}\epsilon = T\mathrm{d}s$, to get

$$\epsilon = \frac{2\pi d(4\pi L)^d}{\kappa^2(d+1)^{d+1}} T^{d+1}, \tag{2.69}$$

and consequently the free energy *density*,

$$\omega = -\frac{2\pi(4\pi L)^d}{\kappa^2(d+1)^{d+1}} T^{d+1}. \tag{2.70}$$

One can further check that the free energy, F, is given by the total, euclidean, on-shell action, I_g, via

$$I_g = \beta F. \tag{2.71}$$

However, in order to use the above relation it is necessary that the total action I_g be finite. We will come back to this topic in section 3.3.

---

[7]Temperature increases with mass.

3 | The gauge/gravity duality

3.1 | Overview

The previous chapters show that there are several similarities between quantum field theories with conformal symmetry and classical gravitational dynamics in AdS spacetimes. The gauge/gravity duality [4] takes these similarities a step further, claiming that there is an actual correspondence between UV-complete QFTs and theories of quantum gravity. Also known as *holography* or *AdS/CFT correspondence*, the duality arose in the context of string theory and it can be thought of as a particular case of more general type of duality between open and closed strings.

The original argument in [4] considered a stack of N $D3$-branes in type IIB string theory, which involves both open and closed strings, as well as interactions between them. Maldacena realised that, in the low energy limit, open and closed strings decouple, and one is left with a system that admits two equivalent descriptions. On one hand, one can take the field theory living on the world volume of the $D3$-branes, which is an $U(N)$ gauge theory known as $\mathcal{N} = 4$ Super Yang-Mills, the closed strings playing the role of vertex operators. Alternatively, one can look at the dynamics of closed strings propagating in a background geometry that is backreacted by the stack of branes. The solution is given by [38]

$$\mathrm{d}s^2 = H^{-1/2}(-\mathrm{d}t^2 + \mathrm{d}\mathbf{x}_3^2) + H^{1/2}(\mathrm{d}r^2 + \mathrm{d}\Omega_5^2) \tag{3.1}$$

$$F_5 = (1 + \star)\mathrm{d}t \wedge \mathrm{d}\mathbf{x}_3 \wedge \mathrm{d}H^{-1} \tag{3.2}$$

where F_5 is the RR-field strength which we note is a self-dual five-form, and with

$$H(r) = 1 + \frac{R^4}{r^4}, \quad R^4 = 4\pi g_s l_s^4 N \tag{3.3}$$

where g_s and l_s are the usual parameters of string theory, coupling and length respectively. Maldacena argued that the low energy description of this picture is tantamount to taking the closed strings propagating in the near-brane geometry, that is, close to $r \approx 0$. From (3.1), we see that such geometry is $AdS_5 \times S^5$ each with radius R. This idea is depicted in section 3.1.

The parameters of the SYM theory, namely the effective coupling λ and the
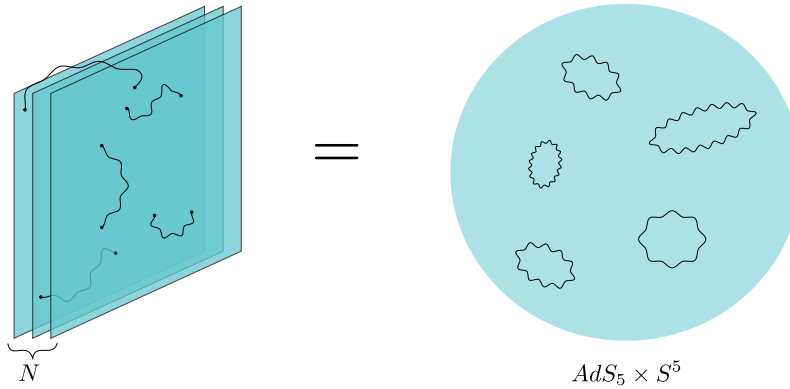
Figure 3.1: Schematic idea of the Open/Closed string duality in the low energy limit. To the left, a description in terms of open strings is given by the field theory theory living in the world volume of N parallel $D3$-branes. Alternatively, one can look at the open strings that propagate in the near brane geometry, in this case $AdS_5 \times S^5$.

number of degrees of freedom, N^2, translate to the closed string description as

$$\lambda \sim \left(\frac{L}{l_s}\right)^4, \quad N \sim \left(\frac{L}{l_p}\right)^4, \tag{3.4}$$

l_p is the Planck length. Hence one sees that on taking the classical limit for the closed string perspective

$$L \gg l_s \gg l_p \tag{3.5}$$

the dual description is given by SYM at large N and at strong coupling — this is the large N limit originally found by 't Hooft [39]. A very similar example (also considered in [40]) was given for the low energy limit of 11D-supergravity [41]. The dual field theory description is now known as ABJM theory. While the precise mapping between the parameters is different from (3.4), it remains true that the classical limit of the supergravity theory corresponds to taking ABJM at strong coupling and with a large number of degrees of freedom. This is in fact the case for all known examples of the duality. The upshot of this is that we can learn about the strongly coupled regime of certain quantum field theories by studying classical gravity in AdS backgrounds.

Top-Down and Bottom-Up

Many other examples of the gauge/gravity duality are now known (see, for instance, [40, 42–44]), with a precise and often intricate mapping between the parameters on each side of the correspondence. The many examples that have been found can help us to understand strongly coupled field theories. Given that the gravity theory and the field theory are obtained from a known string theory, the

field content on both sides of the correspondence is well understood. When studying the duality with string theory as the starting point one refers to this approach as *top-down*.

However, working with string theory has two major disadvantages. First, it is often too complicated because of the many fields involved and simplifying the set-up requires consistent truncations which are often tedious. And second, the field theories that one finds from string theory do not resemble the systems that we find in nature. To overcome these complications it is common to take the duality as a given: a theory of classical gravity is dual to some strongly coupled field theory with a large number of degrees of freedom. The hope is that such model can be somehow embedded in a string theory framework. Working with this point of view is called a *bottom-up* approach. Here one can study systems that are much simpler and, as we shall see in chapter 6, one can engineer the content of the gravity theory in order to replicate observed features of strongly coupled theories. However, one has to deal with the fact that the dual QFT might not be well defined and one will have to settle for qualitative results. Both perspectives, top-down and bottom-up, will be considered in this thesis.

Whilst the best known examples of the correspondence relate a strongly coupled QFT to classical gravity, the most ambitious claim of the correspondence is meant to hold beyond this regime but there is as yet no general proof of the duality. However, the evidence for a duality is such that the current status of the field is not how to prove the duality but rather how to use it. Along this line, the most useful proposal is that of Gubser, Klebanov and Polyakov [45] and Witten [5], which we now go on to elaborate on.

3.2 | The GKPW prescription

The GKPW proposal gives a very specific prescription for a gauge/gravity duality. Concretely, the idea is that the partition function of a quantum gravity in AdS is equal to the generating functional of a CFT. As it was discussed in section 2.2, the description of the physics in AdS should include boundary conditions such as

$$\phi(r, x) \xrightarrow[r\to\infty]{!} \frac{\alpha(x)L^{2\Delta_-}}{r^{\Delta_-}}. \tag{3.6}$$

As a result, we expect the partition function of a quantum theory of gravity must take this into account. We could schematically write

$$Z_{qg}\left[\Phi \to \alpha\right] = \int \mathrm{d}\Phi_\alpha \mathrm{Exp}\left(-S\left[\Phi\right]\right), \tag{3.7}$$

meaning that the path integral on the right hand side should be taken over those field configurations that satisfy our choice of boundary conditions. We have used Φ to denote all the fields in the gravitational theory. Whilst eq. (3.7) is a bit vague, it is there only to emphasize that the quantum gravity in AdS should somehow take into account the boundary conditions.

On the other hand, the generating functional for a QFT is defined thorough a set of sources and operators. We will write

$$Z_{CFT}\left[\mathbf{J}(x)\right] = \int \mathrm{d}\Phi \mathrm{Exp}\left(-S_{CFT} - \int \mathbf{J} \cdot \mathcal{O}\right), \tag{3.8}$$

using vector notation simply to emphasize that both $\mathbf{J}$ and $\mathcal{O}$ are a collection of sources and operators respectively.

Finally, GKPW claims that for a given quantum gravity theory in AdS_{d+2} it is possible to find a CFT_{d+1} such that

$$Z_{qg}\left[\Phi \to \alpha\right] = Z_{CFT}\left[\alpha(x)\right]. \tag{3.9}$$

In other words, the boundary conditions for the fields in AdS_{d+2} play the role of sources in a CFT_{d+1}. This relation is often phrased saying that the dual CFT "lives" in the boundary of AdS.

Moving onto the classical regime for gravity, the partition function is approximated with the low energy effective action evaluated at its saddle point,

$$Z_{qg} \approx e^{-I_g} \tag{3.10}$$

Thus, if we stay within the regime of classical gravity, the gauge/gravity duality is more accurately phrased in its classical version as

$$I_g\left[\Phi \to \alpha\right] = -\ln Z_{CFT}\left[\alpha(x)\right]. \tag{3.11}$$

It is in this limit that the statement of the duality acquires a precise meaning. As explained in the section above, taking the classical gravity description is only valid when the field theory description is taken at large N and strong coupling. Thus we are left with the following statement: The total, on-shell, gravity action is equal to the connected generating functional of a strongly coupled CFT with a large number of degrees of freedom.

3.3 | Correlation functions and holographic renormalisation.

According to eq. (3.11), we can compute CFT correlators by doing functional derivatives of the classical, on-shell, gravity action,

$$\langle \mathcal{O}_\Delta(x_1)...\mathcal{O}_\Delta(x_n)\rangle = (-1)^{n-1}\frac{\delta}{\delta\alpha(x_1)}...\frac{\delta}{\delta\alpha(x_n)}I_g\left[\alpha\right] \tag{3.12}$$

Let us take a bottom-up approach, considering a putative field theory that is dual to the scalar field model discussed in section 2.2.2. An immediate problem that arises trying to use eq. (3.12), is that the Euclidean action (2.49) is in fact divergent on-shell, so a regularisation procedure will be necessary. To see this, we first move to Euclidean signature, $t \to -it$ and $S \to iS$, we have

$$\text{(Euclidean)} \qquad S_{\text{EH}} = -\frac{1}{2\kappa^2}\int \mathrm{d}^{d+2}x\sqrt{g}\left(R-2\Lambda\right) \tag{3.13}$$

$$\text{(Euclidean)} \qquad S_\phi = \frac{1}{2\kappa^2}\int \mathrm{d}^{d+2}x\sqrt{g}\left(\frac{1}{2}(\partial\phi)^2 + \frac{1}{2}m^2\phi^2\right) \tag{3.14}$$

$$\text{(Euclidean)} \qquad S_\partial = -\frac{1}{\kappa^2}\int \mathrm{d}^{d+1}x\sqrt{\gamma}K + ... \tag{3.15}$$

Let us evaluate eqs. (3.13) to (3.15) on the AdS_{d+2} solution where ϕ is small and thus given in terms of Bessel functions. We will implicitly work in the Poincaré patch and use Poincaré coordinates. We will also abbreviate the integration measure as $\mathrm{d}r\mathrm{d}^{d+1}x = \mathrm{d}^{d+2}x$. To further declutter our notation we will denote the on-shell, Euclidean action S_X, by I_X. We start by looking at the Einstein-Hilbert sector which is relatively straight forward:

$$I_{\text{EH}} = +\frac{(d+1)}{L^2\kappa^2}\int \mathrm{d}^{d+2}x\sqrt{g} = \frac{V_{d+1}\Lambda_r^{d+1}}{L^{d+2}\kappa^2} \tag{3.16}$$

where V_{d+1} is the volume $\int \mathrm{d}^{d+1}x$ and we have introduced a radial cut-off at $r = \Lambda_r$ in order to keep track of the divergences. The final expression (3.16) is evidently divergent on taking the limit $\Lambda_r \to \infty$. Before attempting any regularisation, let us for now move on to evaluate I_ϕ. Integrating by parts equation 3.14, and using the equation of motion we get

$$I_\phi = \frac{1}{4\kappa^2}\int_{\partial\mathcal{P}} \mathrm{d}^{d+1}x\sqrt{\gamma}n_\mu\phi\nabla^\mu\phi. \tag{3.17}$$

Strictly speaking, $\partial\mathcal{P}$ is the boundary of the Poincaré patch, which is given by the hyper-surface $\{r = 0\}\bigcup\{r = \infty\}$. However, recall that to solve the equation of

motion for ϕ we demanded that the solution be regular at $r = 0$. This in fact implies that ϕ will have to vanish as $r \to 0$, and so the solutions of interest for us will not give any divergent contribution to the on-shell action coming from the Poincaré horizon. Hence, we will ignore the inner boundary for now and $\partial \mathcal{P}$ to denote exclusively the conformal boundary. One finds that[1]

$$
\begin{aligned}
I_\phi &= \frac{\Lambda_r^{d+2}}{4\kappa^2 L^{d+2}} \int_{\partial \mathcal{P}} \mathrm{d}^{d+1}x\, \phi \partial_r \phi \\
&= -\frac{1}{4\kappa^2 L^{d+2}} \int_{\partial \mathcal{P}} \mathrm{d}^{d+1}x \left(\Lambda_r^{2\nu} \Delta_- \alpha^2 L^{4\Delta_-} + (d+1)\beta\alpha L^{2(d+1)} \right)
\end{aligned}
\tag{3.18}
$$

This is also divergent, but there is an additional complication. If we evaluate on-shell the *variation* of the action we get

$$
\delta I_\phi = -\frac{V_{d+1}}{2\kappa^2 L^{d+2}} \left(\Lambda_r^{2\nu} \Delta_- \alpha\delta\alpha L^{4\Delta_-} + \Delta_+ \beta\delta\alpha L^{2(d+1)} + \Delta_- \alpha\textcolor{red}{\delta\beta} L^{2(d+1)} \right).
\tag{3.19}
$$

Now recall that our standard choice for boundary conditions is to fix the slow fall of, α, so that $\delta\alpha = 0$. In such case the term in red in eq. (3.19) is inconsistent with a variational set-up. To fix this, we include the counterterm

$$
S_{\phi,\mathrm{ct}} = \frac{\Delta_-}{2\kappa^2} \int_{\partial \mathcal{P}} \mathrm{d}^{d+1}x\, \sqrt{\gamma}\, \frac{\phi^2}{2L}
\tag{3.20}
$$

into the boundary action S_∂. Rather luckily, the counterterm (3.20) cancels the divergences coming from the scalar field and it simultaneously gives a well-defined variational problem[2]. One finds

$$
I_\phi + I_{\phi,\mathrm{ct}} = \frac{\Delta_- - \Delta_+}{4\kappa^2} \int_{\partial \mathcal{P}} \mathrm{d}^{d+1}x\, \sqrt{\gamma}\, \frac{\alpha\beta L^{2(d+1)}}{L r^{d+1}} = \frac{(\Delta_- - \Delta_+)L^d}{4\kappa^2} \int_{\partial \mathcal{P}} \mathrm{d}^{d+1}x\, \beta\alpha \,,
\tag{3.21}
$$

and

$$
\delta I_\phi + \delta I_{\phi,\mathrm{ct}} = \frac{\Delta_- - \Delta_+}{2\kappa^2} \int_{\partial \mathcal{P}} \mathrm{d}^{d+1}x\, \sqrt{\gamma}\, \frac{L^{2(d+1)}\beta\delta\alpha}{L r^{d+1}} = \frac{(\Delta_- - \Delta_+)L^d}{2\kappa^2} \int_{\partial \mathcal{P}} \mathrm{d}^{d+1}x\, \beta\delta\alpha \,.
\tag{3.22}
$$

The variation $\delta\beta$ no longer appears and the total action does not diverge with r.

As for the Gibbons-Hawking term (2.34), we know it is there to provide a well defined variational problem [46]. Indeed, when considering a variation of the

---

[1] Use $n^\mu \partial_\mu = \frac{r}{L}\partial_r$.

[2] this is not the case with the alternative $\delta\beta = 0$.

Euclidean gravitational sector with respect to the (inverse) metric one gets[3]

$$\delta(S_{\text{EH}} + S_{\text{GH}}) = \frac{1}{2\kappa^2} \int_{\mathcal{P}} \mathrm{d}^{d+2}x\sqrt{g}\left(-R_{\mu\nu} + \frac{1}{2}Rg_{\mu\nu} - \Lambda g_{\mu\nu}\right)\delta g^{\mu\nu}$$
$$+ \frac{1}{2\kappa^2}\int_{\partial\mathcal{P}}\mathrm{d}^{d+1}x\sqrt{\gamma}\left(K\gamma_{\mu\nu} - K_{\mu\nu}\right)\delta g^{\mu\nu} \tag{3.23}$$

Thanks to the Gibbons-Hawking term, there are no terms containing $\delta\partial g_{\mu\nu}$ in eq. (3.23), which would otherwise spoil the variational set-up. However, contrary to the counterterm (3.20) that we introduced for the scalar term, S_{GH} brings with it more divergences to the already-divergent gravitational action (3.16). Hence, additional counterterms are needed in order to regularise the action. An $r = constant$ hyper-surface embedded in AdS_{d+2} has $K = (d+1)/L$. We find that

$$I_{\text{EH}} + I_{\text{GH}} = -\frac{dV_{d+1}\Lambda_r^{d+1}}{\kappa^2 L^{d+2}}. \tag{3.24}$$

This divergence is cancelled by including the boundary term

$$S_{g,\text{ct}} = \frac{1}{2\kappa^2}\int_{\partial\mathcal{P}}\mathrm{d}^{d+1}x\sqrt{\gamma}\frac{2d}{L} \tag{3.25}$$

into S_∂. Putting all together we have that the boundary action we need is

$$S_\partial = -\frac{1}{2\kappa^2}\int_{\partial\mathcal{P}}\mathrm{d}^{d+1}x\sqrt{\gamma}\left(2K - \frac{2d}{L} - \frac{\Delta_-\phi^2}{2L}\right), \tag{3.26}$$

and now the total action is finite on-shell and provides a well defined variational problem. We emphasise that the validity of eq. (3.26) as an appropriate boundary term is limited to the analysis in the Poincaré patch, for which the conformal boundary of AdS_{d+2} is $\mathbb{R}^{1,d}$ Minkowski space. Furthermore, additional counterterms are needed for the scalar action if one decides for the alternative boundary conditions. The above example and more on how to renormalise the on-shell gravitational action are carefully discussed in [47].

Now that we have a finite Euclidean action, we can safely use it to compute correlation functions of the dual field theory. Having fixed our boundary conditions in (3.6), this corresponds to sourcing an operator with dimension $\Delta = \Delta_+$ in the dual CFT. The expectation value of this operator can be read-off from eq. (3.22):

$$\langle \mathcal{O}_\Delta \rangle = \frac{\delta I_g[\alpha]}{\delta\alpha} = \frac{(\Delta_- - \Delta_+)L^d}{2\kappa^2}\beta. \tag{3.27}$$

We see that the sub-leading fall off of the scalar field is giving us the expectation

---

[3]See `http://jacobi.luc.edu/Useful.html` for a list of formulas that will make this calculation a lot easier. Beware of the overall sign difference due to the Euclidean signature in this section.
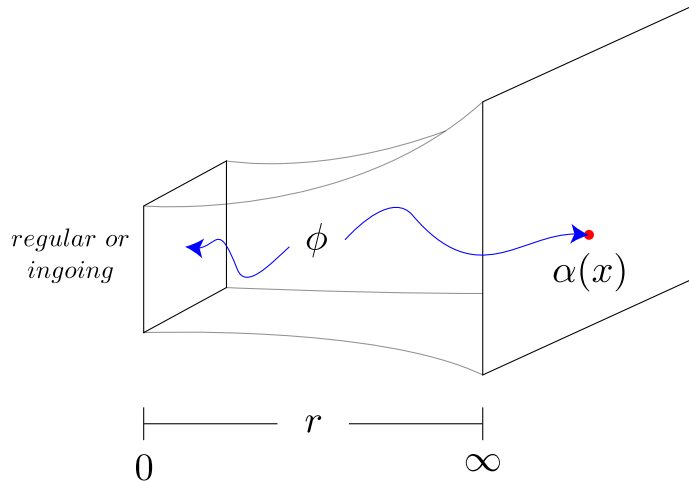
Figure 3.2: Typical illustration for the situation described in this section. Each slice of constant r in the Poincaré patch of AdS spacetime is drawn as a plane, illustrating the fact that these surfaces are conformally equivalent to Minkowski space. A field ϕ in the bulk will be subject to boundary conditions.

value of the operator $\mathcal{O}$ in the presence of a source. In fact, the relation

$$\text{Slow fall-off} \leftrightarrow \text{Source}$$

$$\text{Fast fall-off} \leftrightarrow \text{Expectation Value} \tag{3.28}$$

holds beyond the example of the scalar field. An important example is given by the bulk metric $g_{ab}(x)$. The boundary value of the bulk metric gives the metric for the dual field theory, which in turn sources the QFT stress tensor (2.23) [48, 49].

To calculate higher point correlators we simply calculate successive derivatives of the on-shell action. For example, the 2-point function is obtained from (3.27) as

$$\langle \mathcal{O}_\Delta(x_1)\mathcal{O}_\Delta(x_2)\rangle_j = -\frac{\delta\langle\mathcal{O}_\Delta(x_2)\rangle}{\delta\alpha(x_1)} = \frac{L^d(\Delta_+ - \Delta_-)}{2\kappa^2}\frac{\delta\beta(x_2)}{\delta\alpha(x_1)} \propto \frac{\beta(x_2)}{\alpha(x_1)} \tag{3.29}$$

where the last result follows from the fact that eq. (2.52) is a linear differential equation. The result (3.29) is possible because of the implicit relation that exists between α and β. As mentioned before, this dependence arises after imposing boundary conditions in the bulk interior. Typically, the requirement is to have a regular solution throughout the bulk. Note that, while we have carried out our discussion in Euclidean signature, analogous statements can be made working with real time, albeit more carefully [50]. In such situation, however, it turns out that demanding regularity in the bulk is not enough. Appropriate boundary conditions then have to be chosen based on physical grounds. For example, typical situations of interest for us will include a black hole in the bulk. Hence we will demand that the solution to the equation of motion of any field propagating in the bulk is expressed

in terms of purely in-going waves; nothing should come out of the black hole [51]. These discussion will become clear as we discuss the different scenarios in the rest of the thesis. For the case in which no back-reaction is induced in the *AdS* spacetime, it is a reassuring fact that (3.29) gives back the known result for an operator of dimension Δ_+ in a CFT (2.22).

It is a remarkable fact that one is able to regulate the field theory correlators by regulating the divergences of the dual gravitational model. This has strong implications. The regularisation procedure of the classical action is dual to the regularisation of the QFT. Furthermore, we saw that the cut-off in the gravity side is introduced via the radial coordinate, which means that the radial direction of the bulk captures information about the energy scale of the dual field theory. This fact provides an enormous simplification for understanding the behaviour of the QFT along the RG flow. All we need to do is follow the classical solution of the gravity action along the radial direction of the bulk. These ideas have been carefully developed and tested in the literature culminating in what we now call *holographic renormalisation* (see, for example, [47, 52, 53]).

To conclude this section, we recall that another way to probe the different energy scales of a QFT is to put it on a heat bath at some finite temperature and see how the system responds as the temperature is lowered. From the perspective of the gravity dual, this is achieved using a black hole in the bulk, such as the AdS-Schwarzschild black hole (2.62). The temperature of the black hole can be obtained by the time periodicity of its Euclidean continuation. Note, however, that the time coordinate in the bulk is the same as the time for the dual QFT. Thus, a periodic time coordinate in the bulk also introduces a temperature in the field theory.

Having obtained this geometrisation of the renormalisation group (RG), a follow-up question is if the gauge/gravity duality can assist us in describing the RG flows of strongly coupled matter. This is question in addressed in the next section.

3.4 | Holographic Lattices

There are many examples of quantum critical systems that seem to have a strongly coupled nature of which perhaps the best known examples are the high-T_c superconductors (see [25] for a broad discussion on these topics). Describing the RG flows of such systems is difficult by means of traditional techniques because one cannot make use of perturbative methods. It is then natural to ask if holography can provide any insights on these unsolved problems.

We are particularly interested in understanding the possible ground states and

its transport properties. From the field theory point of view, transport is described by linear response theory; one wishes to understand how the expectation value of an operator is affected as one introduces small variations to its source. This information is encoded in the retarded two point functions, from which the transport coefficients of the system can be obtained via Kubo's formula [54],

$$\sigma(\omega) = \frac{G^R_{\mathcal{O}\mathcal{O}}(\omega)}{i\omega}, \tag{3.30}$$

where $G^R_{\mathcal{O}\mathcal{O}}$ is the retarded Green function for the operator $\mathcal{O}$. If the gravity dual for the QFT at hand is known, one can compute (3.30) from holography by solving the gravity equations of motion. Alternatively, one can consider a bottom-up construction.

The typical example of this is the calculation of the AC electrical conductivity in [55] which uses an electrically charged black hole solution for an Einstein-Maxwell system,

$$S = \frac{1}{2\kappa^2} \int d^{d+2}x \sqrt{-g} \left(R - 2\Lambda - \frac{1}{4}F^2 \right), \tag{3.31}$$

where F is the field strength for the electromagnetic gauge field A_μ. The system (3.31) admits a pure AdS_{d+2} solution with $A_\mu \equiv 0$. For non-zero gauge field, a black hole solution, called the AdS-Reissner-Nordström, is given by

$$ds^2 = \frac{L^2}{r^2 f(r)} dr^2 + \frac{r^2}{L^2} \left(-f(r)dt^2 + d\mathbf{x}_d^2 \right), \tag{3.32}$$

$$A_t = \mu L \left[1 - \left(\frac{r_0}{r} \right)^{d-1} \right], \tag{3.33}$$

with

$$f(r) = 1 - \left(1 + \frac{(d-1)\mu^2 L^4}{2dr_0^2} \right) \left(\frac{r_0}{r} \right)^{d+1} + \frac{(d-1)\mu^2 L^4}{2dr_0^2} \left(\frac{r_0}{r} \right)^{2d} \tag{3.34}$$

and the other gauge field components vanishing. We can get the temperature and entropy density of these black holes using (2.65) and (2.68), to get

$$4\pi T = \frac{r_0}{L^2} \left(d + 1 - \frac{(d-1)^2 \mu^2 L^4}{2dr_0^2} \right), \tag{3.35}$$

$$\kappa^2 s = 2\pi \frac{r_0^d}{L^d}. \tag{3.36}$$

Via the gauge/gravity duality, the black holes (3.32) are dual to a field theory at finite temperature and finite chemical potential μ. For the extremal case, $T = 0$, these black holes interpolate between an AdS_{d+2} geometry in the UV, and an $AdS_2 \times \mathbb{R}^d$
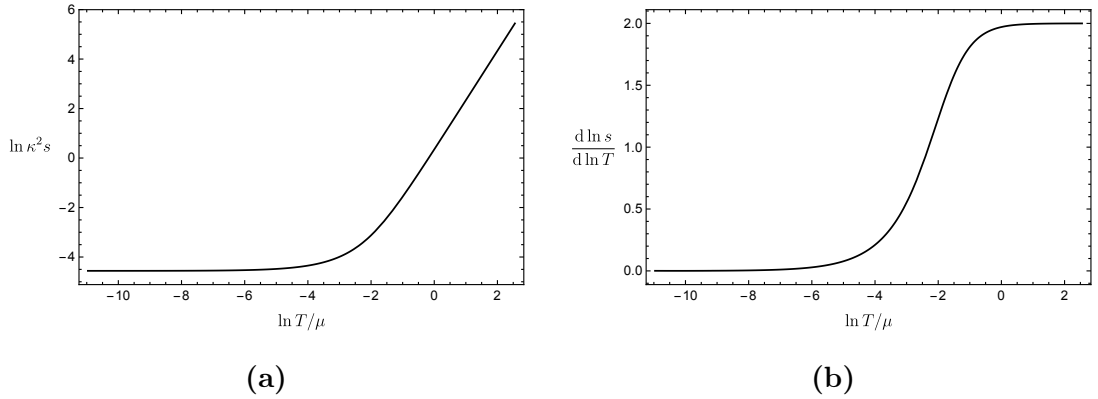
Figure 3.3: Entropy-temperature plot (figure 3.3a) for the *AdS-RN* black hole in 4 bulk dimensions, and its scaling behaviour (figure 3.3b). In figure 3.3b, regimes of power-law behaviour, $s \sim T^{\gamma}$, are plateaus at height γ. At very high temperatures, the entropy is scaling like $s \sim T^2$, corresponding to the behaviour in AdS_4. As the temperature decreases, the entropy decreases until it reaches a constant value, corresponding to the behaviour of the $AdS_2 \times \mathbb{R}^2$ geometry.

in the deep IR. Such interpolation is reflected in the behaviour of the entropy density as a function of the temperature. We illustrate this behaviour in figure 3.3 for the case $d + 2 = 4$.

To understand the transport properties of the field theories that are dual to the AdS-RN black holes, one must take these solutions and introduce a small time-dependent perturbation for the gauge field, with frequency ω. Solving the equation of motion for the perturbation one can ultimately compute the electrical conductivity using (3.29) and (3.30). Varying the temperatures, one can also probe the response of the system for different energy scales. We will shall not go through the details of this calculation, which can be found in [55]. The final result is is shown in figure 3.4. It is remarkable that these results have very similar properties as those observed in graphene experiments [56]. However, the graphene experiments show a finite rise in the real part of the AC counductivity as $\omega \to 0$, which is not seen in figure 3.4. This seemingly missing feature is called a Drude peak, and it is a common feature among many metals called *coherent metals*. In fact, a careful analysis reveals that the Drude peak is not absent in the holographic calculation but rather appears as a sharp delta function at $\omega = 0$. This infinite response at $\omega = 0$, which we call the DC conductivity, is a consequence of translation invariance of the solution in [55] along the field theory directions; momentum conservation prevents dissipation in the system [57, 58].

The DC conductivity is certainly not infinite for real-world materials, which exhibit dissipation due to the presence of impurities or an ionic lattice. In quantum field theory, introducing momentum dissipation can be achieved using a source with explicit spatial dependence that breaks translation invariance, $\mu(x)$ —for example, a
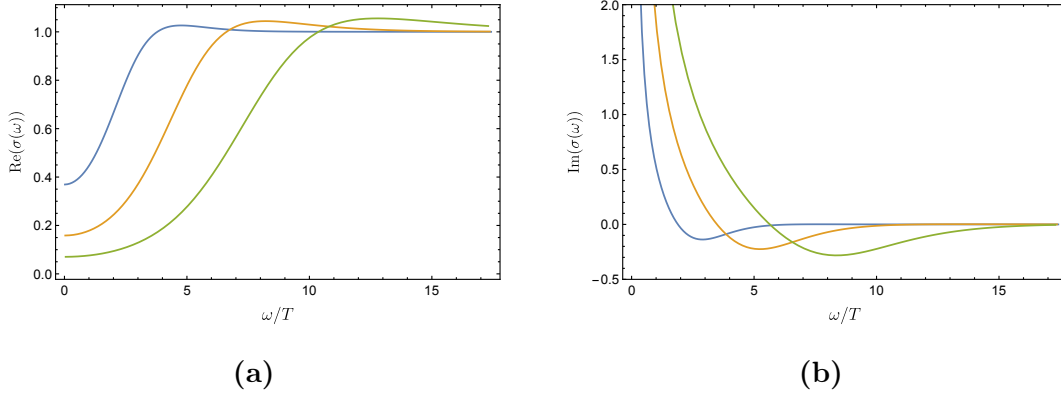
(a)

(b)

Figure 3.4: Plots for the holographic optical conductivity for the bottom-up model described by an AdS charged black hole at different temperatures. The gap in the real part deepens as the temperature is lowered. These plots are a replica of those in [55] and were obtained following the calculation therein presented.

periodic chemical potential,

$$\mathcal{L} \to \mathcal{L} + \mu(x)\mathcal{O}. \tag{3.37}$$

To address this from the perspective of holography, the gravity dual should be some field in the bulk with $\mu(x)$ as its boundary condition. However, building such type of gravity solutions represents an enormous challenge given the nature of Einstein equations. Explicit dependence on the spatial directions means that one will have to solve nonlinear PDEs in order to solve the equations of motion—a difficult task even numerically. This has been done explicitly done in [59] for the case of the AdS-RN black hole, by imposing a spatially modulated boundary condition on the Maxwell gauge field,

$$A_t(x, r) = \mu + A \cos kx + \mathcal{O}(r^{-1}), \tag{3.38}$$

as $r \to \infty$. The result is called a *holographic lattice*. On computing the conductivity for such backgrounds the Drude peak is now visible and finite, thus describing a coherent metal phase. All of the constructions using the above type of ansatz still flow down to an $AdS_2 \times \mathbb{R}^2$ geometry in the far IR.

In [60], Donos & Gauntlett presented a framework for constructing holographic lattices while circumventing the need to solve PDEs—these were called *Q-lattices*. Q-lattices exploit a global symmetry of the bulk in order to construct solutions to the equations of motion that break translations in the boundary directions while preserving homogeneity. The simplification provided by the Q-lattice constructions allows one to compute finite DC conductivities, and it also allows for more flexible constructions which might reveal novel ground states. Already in the original

reference, [60], Q-lattices were used to model coherent metals as well as insulators and transitions between them. The method is best illustrated with an example. Consider, for instance, this model of a complex scalar coupled to gravity[4], which for the purposes of this section we write as

$$\mathcal{L}_\tau = \sqrt{-g}\left(2\frac{\partial_\mu \tau \partial^\mu \tau^*}{(\tau - \tau^*)^2}\right), \tag{3.39}$$

with τ parametrising the upper half of the complex plane. It is customary to write $\tau = \chi + ie^{-\phi}$, with χ and ϕ real fields called the *axion* and *dilaton* respectively. The above Lagrangian arises in the context of type IIB supergravity [61] and one can check it is invariant under the transformations

$$\tau \mapsto \frac{a\tau + b}{c\tau + d} \tag{3.40}$$

with

$$\det\begin{pmatrix} a & b \\ c & d \end{pmatrix} = 1 \quad \text{and} \quad a, b, c, d \in \mathbb{R}. \tag{3.41}$$

That is, the model possesses global $SL(2, \mathbb{R})$ symmetry. This can be used to find a solution of equations of motion that break translations in the boundary while preserving bulk homogeneity. Take for instance the group element of $SL(2, \mathbb{R})$ given by

$$\mathcal{M} = \begin{pmatrix} 1 & ka \\ 0 & 1 \end{pmatrix} \tag{3.42}$$

All elements of this form leave ϕ unchanged and transforms χ as

$$\chi \mapsto \chi + ka \tag{3.43}$$

Hence, we can take the ansatz $\chi = kz$ and $\phi = \phi(r)$. This ansatz does not break bulk translations in the z-direction because $z \mapsto z + a$ acts on the solution exactly as an $SL(2, \mathbb{R})$ transformation would. In a sense, for this ansatz the translations are "aligned" with the $SL(2, \mathbb{R})$ transformation (3.43) and thus the bulk remains homogeneous. However, the boundary theory does not possess $SL(2, \mathbb{R})$ invariance and thus choosing $\chi = kz$ will break translations of the dual field theory. This ansatz was in fact used in [62] to construct an anisotropic plasma and to study its thermodynamics. More generally, it is known that each element $g \in SL(2, \mathbb{R})$ has a unique factorization as $g = kan$, with k, a and n being elements of the one-parameter

---

[4]This model will be further explored in chapter 4

subgroups given by

$$K = \left\{ \begin{pmatrix} \cos\theta & -\sin\theta \\ \sin\theta & \cos\theta \end{pmatrix} \right\} \quad A = \left\{ \begin{pmatrix} e^r & 0 \\ 0 & e^{-r} \end{pmatrix} \right\} \quad N = \left\{ \begin{pmatrix} 1 & x \\ 0 & 1 \end{pmatrix} \right\} . \tag{3.44}$$

This is known as the Iwasawa decomposition [63, 64]. The transformations generated by the subgroup N are the ones that shift the axion, as in (3.43), and thus suggest the linear axion ansatz that we just mentioned. We then ask if there is a parametrisation of τ in which the action of the subgroups A and K are naturally seen as a shift. Indeed, taking $\chi = 0$, elements of A generate a shift of the dilaton field ϕ, which suggests the linear dilaton ansatz that was studied in [65]. Finally, we are left with the action of the subgroup K. The appropriate ansatz for τ was introduced in [1] and it is the next chapter of this thesis.

Despite the simplification provided by the Q-lattice framework, the ODEs that arise still need to be tackled numerically in order to construct interesting solutions. All three different constructions studied in this thesis were solved by implementing a double-sided shooting in *Mathematica* which is detailed in appendix A.

4 | Anisotropic plasmas from axion and dilaton deformations

4.1 | Introduction

An interesting arena for studying holography is provided by the $AdS_5 \times X_5$ class of solutions of type IIB supergravity, where X_5 is a compact five-dimensional Einstein manifold. When $X_5 = S^5$ the four-dimensional dual conformal theory (CFT) is given by $N = 4$ supersymmetric Yang-Mills theory [4]. Furthermore, when $X_5 = SE_5$, where SE_5 is Sasaki-Einstein, the four-dimensional CFT has $N = 1$ supersymmetry and, starting with the work of [44, 66, 67], there are infinite classes of examples where both the geometry is explicitly known and the dual field theory has also been identified.

The vacua of these theories have a complex modulus, given by constant values of $\tau \equiv \chi + ie^{-\phi}$, where χ and ϕ are the type IIB axion and dilaton, respectively, corresponding to the fact that τ is dual to a marginal operator in the dual field theory. For the case of $N = 4$ supersymmetric Yang-Mills theory τ is simply identified with the theta angle, θ, and coupling constant, g_{YM}, via $\tau \sim \frac{\theta}{2\pi} + i\frac{4\pi}{g_{YM}^2}$. The identification for theories with $N = 1$ supersymmetry is a little less direct due to renormalisation scales and is discussed in [66].

In this chapter we will be interested in studying how the entire class of CFTs behave under deformations of τ, with the deformation having a non-trivial dependence on the spatial coordinates of the dual field theory. Such deformations trigger interesting RG flows which can, moreover, lead to novel IR ground states. Such spatially dependent deformations of CFTs are also of potential interest in seeking applications of holography with condensed matter systems. The deformations break translation invariance and hence they provide a mechanism to dissipate momentum in the field theory. This leads to finite DC conductivities and hence these deformations can be used to model various metallic and insulating behaviour (e.g. [59, 60, 68–72]).

An interesting setup, first studied in [73], involves a deformation in which the axion is linear in one of the spatial directions. It was shown that a novel ground state solution appears in the far IR of the RG flow which exhibits a spatially anisotropic Lifshitz-like scaling. These solutions were generalised to finite temperature in [62, 74], thus obtaining a dual description of a strongly coupled homogeneous and spatially

anisotropic plasma. One motivation for studying such plasmas is that they may provide some insights into the quark-gluon plasma that is seen in heavy ion collisions.

For the particular case of $N = 4$ SYM it has recently been shown [75] that the anisotropic plasma found in [62, 74] undergoes a finite temperature phase transition, demonstrating that the Lifshitz-like scaling ground state found in [73] is actually not realised in the far IR. A subsequent study [76] revealed additional phase transitions and it is not yet clear what the true ground state is. Furthermore, the modes that are responsible for these instabilities have an analogous in the SE_5 and X_5 classes. Thus, it is likely that these instabilities extend beyond the linear axion solutions associated to S^5, and it would be interesting to further investigate this matter.

From a technical viewpoint the solutions involving linear axions are appealing because they can be obtained by numerically solving a system of ODEs. This is also a feature of another class of deformations by τ that were studied in [65] involving a linear dilaton. For this class it was shown that at $T = 0$ the RG flow approaches an $AdS_4 \times R$ solution[1] in the IR. Note that unlike the linear axion solutions, the dilaton becomes large in the linear dilaton solutions and hence string perturbation theory will break down for a non-compact spatial direction. Both the linear axion and the linear dilaton solutions can be viewed as special examples of "Q-lattices", introduced in [60], where one exploits a global symmetry of the gravitational theory in order to break translation invariance using a bulk matter sector while preserving translation invariance in the metric. For deformations involving τ the relevant bulk global symmetry is the $SL(2, R)$ symmetry of type IIB supergravity which acts on τ via fractional linear transformations.

Generic spatially dependent deformations of τ will lead to solutions, which we refer to as holographic τ-lattices, that involve numerically solving PDEs. While it is certainly interesting to construct such solutions and explore their properties, it is natural to first ask if the linear axion and dilaton deformations exhaust the Q-lattice constructions. In fact they do not. The bulk global $SL(2, R)$ symmetry has three different conjugacy classes of orbits and, as we will explain, the linear axion and the linear dilaton deformations are associated with the parabolic and hyperbolic conjugacy classes, respectively. This leaves deformations associated with the elliptic conjugacy class that we study here. We can easily obtain a simple ansatz for these deformations by changing coordinates in field space. Instead of the upper half plane, the new coordinates naturally parametrise the Poincaré disc and the τ-deformation of interest is obtained by taking a polar coordinate on the disc to depend linearly, and hence periodically, on one of the spatial directions.

The τ-lattice solutions of [62, 65, 73, 74] and the new ones constructed here can

---

[1] This ground state is unstable for the case of $X_5 = S^5$ [65] and so it would be interesting to examine the associated finite temperature phase transitions generalising [75, 76].

all be found in a $D = 5$ theory of gravity which arises as a consistent KK truncation of type IIB supergravity on an arbitrary X_5. We will introduce this $D = 5$ theory in section 4.2 where we will also briefly review the Lifshitz-like scaling solution found in [73]. The new holographic τ-lattices will be presented in section 4.3. The finite temperature solutions depend on two dimensionless parameters T/k and λ, where T is the temperature, while k and λ are the wave-number and strength of the τ-deformation, respectively. We show that at $T = 0$ the new τ-lattices all approach domain walls interpolating between $AdS_5 \times X_5$ in the UV and the same $AdS_5 \times X_5$ in the far IR, thus recovering full four-dimensional conformal invariance. The underlying physical reason for this is that the operator which we are using to deform the CFT has vanishing spectral density at low energies for non-vanishing momentum. Similar domain walls have been seen in other settings involving deformations by marginal operators that break translation symmetry [77, 78] and, as in those examples, there is a renormalisation of relative length scales in moving from the UV to the IR.

A particularly interesting feature, for large enough values of λ, is that the solutions have an intermediate scaling regime, governed by the Lifshitz-like scaling solution found in [73]. At finite temperature this intermediate scaling appears for a range of T/k and we will show how it manifests itself in the temperature scaling of various physical quantities. For the $T = 0$ domain wall solutions the intermediate scaling will appear for a range of the radial variable. Since the Lifshitz-like scaling solution of [73] is singular the $T = 0$ domain wall RG flows can thus be viewed as a singularity resolving mechanism somewhat similar to some other singularity resolving flows, both bottom-up [79–82] and top-down [83]. An important difference is that here the RG flow is being driven by a deformation at non-vanishing momentum.

For the finite temperature plasmas we calculate some components of the shear viscosity tensor. The spin two components, $\eta_{||}$, with respect to the residual $SO(2)$ rotation symmetry, satisfy $4\pi\eta_{||}/s = 1$, where s is the entropy density, as usual [84, 85]. However, the spin one components $\eta_\perp$ behave differently. Defining $F \equiv 4\pi\eta_\perp/s$, for $T/k >> 1$ we find $F \to 1$ while for $T/k \ll 1$ we find that F approaches a constant given by the renormalised relative length scales in the IR. For intermediate values of T/k we have $F < 1$, as seen in other anisotropic examples e.g. [65, 86–89] (see [90] for an anisotropic example where $F > 1$).

We also calculate the DC thermal conductivity of the plasmas in the anisotropic direction. Using the results of [91–94] this can be expressed in terms of black hole horizon data and we find that it has the correct scaling associated with the different scaling regimes. For $T \ll k$ the Boltzmann behaviour of the thermal resistivity, κ^{-1}, is Boltzmann suppressed, which is expected because of the absence of low-energy excitations supported at the lattice momentum in the infrared, k_{IR} [68]. By contrast in the intermediate scaling regime, the lattice deformation gives rise to the power law

behaviour $\kappa \sim k^2(T/k)^{7/3}$. It is interesting to contrast these features with examples where power law behaviour occurs at low energies due to the non suppression of spectral density at finite momentum in the context of semi-local quantum critical points[68, 95].

We conclude the chapter with some comments in section 4.4 while appendix B discusses the connection between the $SL(2,R)$ conjugacy classes and Q-lattices.

4.2 | The set-up

Our starting point is $D = 5$ Einstein gravity with a negative cosmological constant, coupled to a complex scalar, Φ, with action given by

$$S = \int dx^5 \sqrt{-g} \left(R + 12 - 2 \frac{\nabla_\mu \Phi \, \nabla^\mu \Phi^*}{(1 - \Phi \Phi^*)^2} \right) .$$
(4.1)

The corresponding equations of motion are given by

$$R_{\mu\nu} + 4 \, g_{\mu\nu} - 2 \frac{\nabla_\mu \Phi \, \nabla_\nu \Phi^*}{(1 - \Phi \Phi^*)^2} = 0 \, ,$$

$$\nabla_\mu \left[\frac{\nabla^\mu \Phi}{(1 - \Phi \Phi^*)^2} \right] - 2 \frac{\nabla_\mu \Phi \, \nabla^\mu \Phi^*}{(1 - \Phi \Phi^*)^3} \Phi = 0 \, .$$
(4.2)

The complex scalar Φ parametrises the unit Poincaré disc $SU(1,1)/U(1) \cong SL(2,R)$. It will be helpful to introduce two other standard choices of coordinates for the scalar field manifold. For the first we write

$$\Phi = \frac{1 + i\,\tau}{1 - i\,\tau}, \qquad \tau = \chi + i\,e^{-\phi} \, ,$$
(4.3)

where ϕ is the dilaton, χ is the axion and τ parametrises the upper half plane. The metric on the scalar field manifold then takes the form

$$ds_2^2 \equiv 2 \frac{d\Phi \, d\Phi^*}{(1 - \Phi \Phi^*)^2} = \frac{d\tau d\bar{\tau}}{2(Im\tau)^2} = \frac{1}{2} \left(d\phi^2 + e^{2\phi} \, d\chi^2 \right) .$$
(4.4)

The second choice of coordinates

$$\Phi = \tanh \frac{\varphi}{2} \, e^{i\,\alpha} \, ,$$
(4.5)

resembles polar coordinates with $\varphi \geq 0$ and $0 \leq \alpha < 2\pi$ parametrising a circle. The

two coordinate systems are related through the non-linear field redefinition:

$$\chi = \frac{\sinh\varphi\,\sin\alpha}{\cosh\varphi + \sinh\varphi\,\cos\alpha}\,,$$

$$e^{\phi} = \cosh\varphi + \sinh\varphi\,\cos\alpha\,. \tag{4.6}$$

In these coordinates the metric on the scalar manifold is given by

$$ds_2^2 = \frac{2}{(1 - \Phi\Phi^*)^2}\,d\Phi\,d\Phi^* = \frac{1}{2}\left(d\varphi^2 + \sinh^2\varphi\,d\alpha^2\right). \tag{4.7}$$

The $D = 5$ theory (4.1) is a consistent truncation of type IIB supergravity on a general five dimensional Einstein manifold X_5. In this truncation the IIB dilaton and axion are precisely χ and ϕ, respectively, while the self-dual IIB five-form is proportional to the $D = 5$ volume form plus the volume form of X_5. The consistency of the truncation means that any solution of (4.2) can be uplifted on an arbitrary X_5 to obtain an exact solution of type IIB supergravity. In particular, the unit radius AdS_5 solution, given by

$$ds_5^2 = r^2\left(-dt^2 + d\mathbf{x}^2\right) + \frac{dr^2}{r^2}\,, \qquad \Phi = 0\,, \tag{4.8}$$

uplifts to the vacuum $AdS_5 \times X_5$ solution type IIB supergravity and is dual to a CFT in four spacetime dimensions. Thus, the solutions of this chapter are applicable to this infinite class of CFTs. For the special case when $X_5 = S^5$ the CFT is $N = 4$ supersymmetric Yang-Mills theory and when $X_5 = SE_5$ the dual CFT has $N = 1$ supersymmetry.

The complex scalar field τ is massless when expanded about the AdS_5 vacuum and is dual to an exactly marginal operator of the dual CFT. Indeed constant values of τ, which we write as $\tau^{(0)} \equiv \chi^{(0)} + ie^{-\phi^{(0)}}$, parametrise a complex moduli space of CFTs. For the special case when $X_5 = S^5$, the operators dual to χ and $e^{-\phi}$ are proportional to $\mathrm{Tr}F \wedge F$ and $\mathrm{Tr}F^2$ in $N = 4$ Yang-Mills, respectively, and furthermore, we also have a simple identification $\tau^{(0)} \sim \frac{\theta}{2\pi} + \frac{4\pi i}{g_{YM}^2}$. To be more precise using the conventions in section 4 of [74], which in particular means that for the AdS_5 vacuum solution we take $\phi^{(0)} = 0$ and identify, for $N = 4$ Yang-Mills theory,

$$\frac{1}{g_s}\tau^{(0)} = \frac{\theta}{2\pi} + \frac{4\pi i}{g_{YM}^2}\,, \tag{4.9}$$

where g_s is the string coupling constant. For general $X_5 = SE_5$ there is a less direct map because the dual field theory is described more implicitly, but nevertheless the complex modulus can easily be identified as described in [66] (see also [96]).

It is interesting to ask what happens to the field theory when we make the

deformation parameter $\tau^{(0)}$ depend on some or all of the spatial coordinates, $\mathbf{x}$, of the dual field theory. At strong coupling this can be addressed by constructing holographic solutions in which the bulk τ field behaves as $\tau(\mathbf{x}, r) \to \tau^{(0)}(\mathbf{x})$ as one approaches the AdS_5 boundary at $r \to \infty$. For the case of $N = 4$ Yang-Mills theory, this deformation corresponds to a spatially dependent θ and g_{YM}^2 via (4.9) (with g_s still a constant). The most general deformation parameter $\tau^{(0)}(\mathbf{x})$ would require the solution of a system of non-linear PDEs in the bulk. However, for a particular class of boundary deformations one can maintain enough homogeneity to reduce the problem to a system of ODEs involving only the radial coordinate r. Indeed since the scalar fields parametrise a group manifold $SL(2, R)$ the bulk equations of motion have a global $SL(2, R)$ symmetry and hence one can consider the Q-lattice constructions described in [60].

As we have already explained, and for which more details can be found in appendix B, there are three different Q-lattice constructions, associated with the three conjugacy classes of $SL(2, R)$. In each case the scalar fields trace out a one-dimensional orbit, parametrised by one of the spatial coordinates, which we take to be z. For all three cases the associated metric is anisotropic and given by

$$ds_5^2 = -U(r) \, dt^2 + \frac{dr^2}{U(r)} + e^{2\,V_1(r)} \, dz^2 + e^{2\,V_2(r)} \, (dx^2 + dy^2), \qquad (4.10)$$

with all metric components functions of r only. The hyperbolic conjugacy class is associated with a linear dilaton, namely $\chi = 0$ and $\phi = kz$, and these solutions were constructed in [65]. Solutions associated with the parabolic conjugacy class have the axion χ linear in z. These solutions were studied in [62, 73, 74] and some features will be briefly reviewed in the next subsection. The focus of this chapter is solutions associated with the elliptic conjugacy class in which the field α, introduced in (4.5), is linear in the z coordinate and will be discussed in the following section.

4.2.1 Brief review of linear axion solutions

The solutions obtained in [73] have

$$\phi = \phi(r), \qquad \chi = a \, z, \qquad (4.11)$$

where a is a constant, supplemented with the metric ansatz (4.10). It is simple to check that this gives a consistent non-linear ansatz for the equations of motion, leading to a system of ODEs which can be solved numerically. At the AdS_5 boundary the dilaton vanishes so that the only deformation parameter is given by a.

For the special case when $X_5 = S^5$, corresponding to $N = 4$ Yang-Mills theory,

the linear axion corresponds to a θ angle in (4.9) that is linear in the z direction. Also, recalling that the $AdS_5 \times X_5$ solutions arise from $D3$-branes sitting at the apex of the metric cone over X_5, the configurations with $\chi = a\,z$ are associated with the addition of $D7$-branes that are aligned along the x, y directions as well as wrapping X_5 and are smeared along the z direction. In fact it was shown in [62] that $a = (\lambda_{tH}/4\pi)(n_{D7}/N_c)$ where n_{D7} is the uniform density of D7-branes in the z-direction, N_c is the number of $D3$-branes and λ_{tH} is the 't Hooft parameter of the dual field theory.

By analysing the system of ODEs it was shown in [73] that for any deformation parameter a there is an RG flow from AdS_5 in the UV to a Lifshitz-like scaling solution in the far IR with

$$U = \frac{12}{11}\,r^2, \quad V_1 = \frac{2}{3}\,\ln r, \quad V_2 = \ln r, \quad e^\phi = r^{2/3}. \tag{4.12}$$

Notice that the metric of this IR solution admits the spatially anisotropic scaling symmetry $(t, x, y, z) \to (\nu t, \nu x, \nu y, \nu^{2/3} z)$ with $r \to \nu^{-1} r$. On the other hand the dilaton changes under this scaling. This means that some but not all observables will exhibit this scaling behaviour. The fact that we flow to a new fixed point in the IR demonstrates that the linear axion deformation is marginally relevant[2].

Finite temperature generalisations of these solutions were constructed and studied in some detail in [62, 74]. For the special case of uplifting these solutions on $X_5 = S^5$, an important subtlety is that in type IIB supergravity there are perturbative modes around the IR geometry (4.12) which are unstable [73] and hence, for this case, the true ground state cannot be described by the geometry (4.12). The unstable modes lie in the $\mathbf{20'}$ representation of the global $SO(6)$ R-symmetry and the back reaction of some of them have been studied recently using an enlarged consistent Kaluza-Klein truncation, valid just for the case when $X_5 = S^5$, in [75, 76]. By constructing finite temperature solutions it was shown in [75] that there is a phase transition at finite temperature leading to a low temperature ground state geometry which was again Lifshitz-like but with different scaling exponents [75]. However, subsequent work in [76] revealed additional instabilities and the current status is that the true ground state for this case is not yet clear. On the other hand for generic X_5 manifolds the instability of [73] is not present and one can hope that (4.12) will be the true ground state for an infinite sub-class of cases.

---

[2]Note that this is also true of the linear axion solutions constructed in [70] both at vanishing and non-vanishing charge density.

4.3 | A new holographic τ-lattice

We now turn our attention to a different non-linear ansatz associated with the parametrisation (4.5). It is simple to check that the ansatz for the scalars

$$\varphi = \varphi(r), \quad \alpha = k\, z\,, \tag{4.13}$$

combined with the metric given by (4.10) is consistent, leading to a system of ODEs. In particular, the scalar equation of motion can be written

$$\left(e^{V_1 + 2V_2} U \varphi'\right)' = \frac{1}{2} k^2 e^{2V_2 - V_1} \sinh 2\varphi\,. \tag{4.14}$$

The boundary deformations are now given by $\lambda \equiv \varphi^{(0)}$, where $\varphi^{(0)} \equiv \varphi(r = \infty)$, and the period k. An important difference in this parametrisation of the complex scalar, compared with those in [65, 73], is that the boundary deformation is periodic in the coordinate z with period $2\pi/k$. At fixed r, as we traverse a single period in the z direction it is clear from (4.5) that we traverse a circle in the Poincaré disc centred at the origin and with radius $\tanh \frac{\varphi}{2}$. Equivalently, in terms of χ, ϕ from (4.6) this corresponds to a circle in the upper half plane centred on the imaginary axis at $e^{-\phi} = (1 + \tanh^2 \frac{\varphi}{2})/(1 - \tanh^2 \frac{\varphi}{2})$ and with radius $2 \tanh \frac{\varphi}{2}/(1 - \tanh^2 \frac{\varphi}{2})$.

Notice, in particular, for the case of $N = 4$ Yang-Mills using (4.9) we see that both couplings θ and g_{YM}^2 are modulated by the same period. We also notice that provided φ is bounded in the bulk, which will turn out to be the case in the solutions we construct, then e^ϕ is also bounded and hence string perturbation theory is not breaking down for these solutions[3].

Like the linear axion deformation we can again interpret these deformations as arising from $D3$-branes at the apex of the metric cone over X_5 with a distribution of $D7$-branes aligned along the (x, y) directions, wrapping X_5 and smeared in the z-direction. A striking difference however is that the integral of $\chi^{(0)}$ along a period in the z-direction vanishes and so we have a distribution of both $D7$-branes and anti $D7$-branes.

Before constructing numerical solutions, we first develop some intuition about what will happen with the solutions in the two limits $\lambda \ll 1$ and $\lambda \gg 1$. For the small λ limit it is enough to examine small and static fluctuations of the scalar based on the ansatz (4.13) around the AdS_5 vacuum solution (4.8). By linearising the

---

[3]Recall that we are using conventions where string perturbation theory is governed by $g_s e^\phi$, where g_s is a free constant.

scalar equation of motion (4.14) we deduce that

$$\delta\phi(r) = \lambda \frac{k^2}{2\,r^2}\,K_2\left(\frac{k}{r}\right)\,,$$

(4.15)

where K_2 is a Bessel function, which close to the AdS boundary gives the desired falloff:

$$\delta\varphi(r) = \lambda - \frac{\lambda\,k^2}{4\,r^2} + \frac{\lambda\,k^4}{64\,r^4}\left(3 - 4\gamma - 4\ln\left(\frac{k}{2\,r}\right)\right) + \cdots\,.$$

(4.16)

By expanding the perturbation (4.15) close to the Poincaré horizon at $r = 0$ we find

$$\delta\varphi(r) = \lambda\,\sqrt{\frac{\pi}{8}}\,\left(\frac{k}{r}\right)^{3/2}\,e^{-k/r} + \cdots\,.$$

(4.17)

This perturbation will back react on the metric at order λ^2 and explicit expressions can be obtained in terms of Meijer G-functions. The behaviour in (4.17) demonstrates that when λ is small, the deformation of the boundary theory does not significantly affect the IR physics away from the AdS_5 vacuum (4.8). Indeed it is clear that k sets a scale in the bulk with the geometry rapidly returning to the AdS_5 vacuum at $r < k$. At finite temperature, similar statements can be made for the corresponding horizon at temperatures $T < k$.

We conclude that at $T = 0$, at least for small λ, the deformation gives rise to a domain wall solution interpolating between AdS_5 in the UV and the same AdS_5 in the IR. This behaviour should be contrasted with what occurs for the linear axion deformations [73] and the linear dilaton deformations [65], both of which modify the lR. As we will explain in more detail later there is a renormalisation of relative length scales as one moves from the UV to IR, which for small λ is of order λ^2. Note that similar domain walls have been shown to arise in other contexts involving deformations with spatially dependent marginal operators [77, 78].

We now turn our attention to deformations corresponding to large λ. In this case, one has to construct the full geometry either in closed form or, as we do in the next section, numerically. However, we can still obtain some insight based on analytic arguments. When λ is large, the scalar field $\varphi(r)$ close to the boundary of AdS_5 will also be large. In that region, the complex scalar target space metric in the (α, φ) coordinates given in (4.7) can be approximated by

$$ds_2^2 \approx \frac{1}{2}\left(d\varphi^2 + e^{2\varphi}\,d\left(\frac{\alpha}{2}\right)^2\right)\,,$$

(4.18)

which locally looks exactly like the metric (4.4) given in the (χ, ϕ) coordinates. It is natural to expect, therefore, that for the zero temperature solutions there will be

a large region where the metric scales according to (4.12) while the scalar behaves as $\varphi \approx \frac{2}{3} \ln r$. As we then move deeper in the bulk geometry, the scalar becomes smaller and this approximation breaks down. It is then plausible that as soon as soon as we are in the region $r < k$, we move quickly back to the horizon of AdS_5 with the scalar behaving as in (4.15).

Similar comments apply at finite temperature. For high temperatures we expect the entropy density, s, will scale as $s \sim T^3$ corresponding to the scaling associated with the AdS-Schwarzschild black hole. This will also be the behaviour for $T \ll k$ if the solution approaches the AdS_5 to AdS_5 domain wall, which we know happens for small λ, and we will shortly see also happens for large λ. To be more precise, due to the length renormalisation we expect this behaviour for $T \ll k_{IR} \equiv k/\bar{L}_1$ (with $\bar{L}_i$ defined below; see (4.25)).

In addition we expect an intermediate scaling region where s would scale according to $s \sim T^{8/3}$ associated with the finite temperature version of the scaling solution (4.12). The lower bound of this region should satisfy $1 \ll T/k_{IR}$, to ensure that we are not dominated by the $T = 0$ domain wall, while the upper bound will be fixed by ensuring that we are not dominated by the high T AdS-Schwarzschild solution. A consideration of the expansions of the functions in the UV that we give below (4.19) suggests that we should have $T/k \ll e^\lambda$.

4.3.1 Numerical construction

We consider the ansatz for the metric given in (4.10) supplemented with the ansatz for the complex scalar Φ given by (4.13) and (4.5). After substituting into the equations of motion (4.2) we obtain a system of ODEs for four functions, U, V_1, V_2 and φ, of the radial coordinate r. The function U satisfies a first order ODE, while the functions V_1, V_2 and φ satisfy second order ones. In order to find finite temperature solutions we use a standard double sided shooting technique which we now outline.

Close to the AdS_5 boundary, located at $r = \infty$, the expansion of the four functions

has the form

$$U(r) = r^2 \left(1 - \frac{k^2 \sinh^2 \lambda}{12r^2} + \frac{\mathcal{B}_1}{r^4} + \frac{\ln r}{72r^4} k^4 \sinh^2 \lambda (2 \cosh 2\lambda + 1) + \cdots \right),$$

$$V_1(r) = \ln r + \frac{k^2 \sinh^2(\lambda)}{12r^2} + \frac{\mathcal{B}_2}{r^4} - \frac{\ln r}{72r^4} k^4 \sinh^2 \lambda (2 \cosh 2\lambda + 1) + \cdots,$$

$$V_2(r) = \ln r - \frac{k^2 \sinh^2 \lambda}{24r^2} + \frac{k^4 (\cosh 2\lambda - \cosh 4\lambda) - 576 \mathcal{B}_2}{1152 r^4}$$

$$+ \frac{\ln r}{144 r^4} k^4 \sinh^2 \lambda (2 \cosh 2\lambda + 1) + \cdots,$$

$$\varphi(r) = \lambda - \frac{k^2 \sinh 2\lambda}{8r^2} + \frac{\mathcal{B}_3}{r^4} - \frac{\ln r}{96 r^4} k^4 (\sinh 2\lambda - 2 \sinh 4\lambda) + \cdots. \tag{4.19}$$

In particular, after fixing the scalar deformation parameter λ as well as the length scales of the asymptotic metric, we are left with the three constants of integration $\mathcal{B}_i$. Notice that if we rescale the radial coordinate $r \to \nu r$ as well as rescaling (t, x, y, z) by ν^{-1} the ansatz will be preserved by the following scaling of the UV parameters:

$$k \to \nu k, \qquad \lambda \to \lambda,$$

$$\mathcal{B}_1 \to \nu^4 \mathcal{B}_1 - \frac{(\nu k)^4}{72} \sinh^2 \lambda (2 \cosh 2\lambda + 1) \ln \nu,$$

$$\mathcal{B}_2 \to \nu^4 \mathcal{B}_2 + \frac{(\nu k)^4}{72} \sinh^2 \lambda (2 \cosh 2\lambda + 1) \ln \nu,$$

$$\mathcal{B}_3 \to \nu^4 \mathcal{B}_3 + \frac{(\nu k)^4}{96} (\sinh 2\lambda - 2 \sinh 4\lambda) \ln \nu. \tag{4.20}$$

The log terms are associated with anomalous scaling of physical quantities due to the conformal anomaly which is non-vanishing (see [74] for a related discussion).

We also demand that the solutions have a regular black hole event horizon located at some value $r = r_+$. This leads us to the following expansion near $r = r_+$:

$$U = h_{11}(r - r_+) + h_{12}(r - r_+)^2 + \dots,$$

$$V_1 = \mathcal{H}_2 + \mathcal{H}_1(r - r_+) + h_{22}(r - r_+)^2 + \cdots,$$

$$V_2 = \mathcal{H}_3 + h_{31}(r - r_+) + \cdots,$$

$$\varphi = \mathcal{H}_4 + h_{41}(r - r_+) + \cdots. \tag{4.21}$$

The expansion is specified by four free constants $\mathcal{H}_a$, with the remaining constants h_{ij} fixed in terms of those. We find that the temperature and entropy density of the black holes are given by

$$T = \frac{r_+}{\pi} \frac{16 + k^2 (1 - \cosh(2\mathcal{H}_4)) e^{-2\mathcal{H}_2}}{16(\mathcal{H}_1 r_+ + 1)},$$

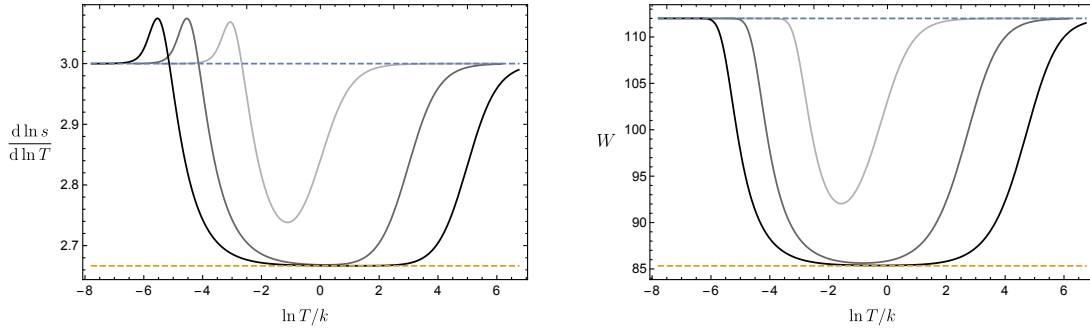$$s = 4\pi e^{\mathcal{H}_2 + 2\mathcal{H}_3}, \tag{4.22}$$

Figure 4.1: Plot of the logarithmic derivative of s, where s is the entropy density, and the Kretschmann scalar at the black hole horizon, W, for three values of the deformation parameter $\lambda = 2, 5$ and 7 (from lightest to darkest). At low temperatures the solutions are approaching domain walls interpolating between AdS_5 in the UV and the same AdS_5 in the IR. The dashed constant lines in the left panel are at 3 and at 8/3, while in the right panel they are at 112 and 256/3, and the intermediate scaling behaviour, parametrically large in λ, is clearly revealed for large λ.

respectively.

In total we have ten free constants: $\mathcal{B}_i$, λ, k, $\mathcal{H}_a$, and r_+, but one of these is redundant due to the scaling symmetry given in (4.20). By numerically solving the ODEs starting at both $r = r_+$ and $r = \infty$ we match the four functions at some point in the middle $r = r_m$ along with continuity of the first derivatives φ', V_1' and V_2'. This leads to seven conditions and thus the solution space is specified by two dimensionless parameters which we take to be λ and T/k.

We have constructed various black hole solutions for different values of the deformation parameter λ using a numerical implementation of the above technique. In figure 4.1 we plot the logarithmic derivative of s as a function of T/k for three different values of λ. Notice that when $d\ln s/d\ln T$ is equal to a constant γ the entropy is scaling with temperature according to $s \propto T^\gamma$. We also plot the value of W, the Kretschmann scalar at the black hole horizon:

$$W \equiv [R_{\mu_1\mu_2\mu_3\mu_4} R^{\mu_1\mu_2\mu_3\mu_4}]_{r=r_+} . \tag{4.23}$$

For each of the three branches we see that when $T/k \gg 1$, the entropy scales as $s \propto T^3$, as expected. Indeed, for $T/k \gg 1$ the temperature scale is much higher than the deformation scale set by λ and the solutions are approaching the standard AdS-Schwarzschild solution. This is also confirmed by the value of the Kretschmann scalar at the horizon which is approaching 112, the value for the AdS-Schwarzschild solution.

For $T/k \ll 1$, we see from figure 4.1 that the solutions behave similarly to the high temperature solutions. We conclude that at that low temperatures the solutions are approaching domain wall solutions that interpolate between the deformed AdS_5

in the UV and the AdS_5 vacuum in the IR. For small values of λ this was anticipated from our perturbative analysis and now we see that it also occurs for large λ.

As with other domain walls interpolating between the same AdS space (e.g. [77, 78, 97–99]), there can be a renormalisation of relative length scales between the UV and the IR. To extract this information we assume that the far IR of the domain wall solution at $T = 0$ has a metric as in (4.10) with $U = r^2$ and $e^{2V_i} = \bar{L}_i^2 r^2$. Since a rescaling of the radial coordinate in the IR would lead to a rescaling of both the time coordinate and the spatial coordinates, the invariant quantities, $\bar{L}_i$, are the relative length scales with respect to the scale fixed by the time coordinate. Since in the UV we approach a unit radius AdS_5, the $\bar{L}_i$ give the renormalisation of the relative length scales for the RG flow. It is slightly delicate to extract the $\bar{L}_i$ from the finite temperature solutions, because the constants $\mathcal{H}_2$ and $\mathcal{H}_3$ in (4.21) go to zero as $T \to 0$. After considering heating up the putative domain wall solution with a small temperature and examining the behaviour at the horizon, we deduce that the $\bar{L}_i$ can be obtained by taking the limit

$$\bar{L}_i = \lim_{T/k \to 0} L_i \,, \tag{4.24}$$

where we have defined[4]

$$L_i \equiv \frac{1}{\pi T} e^{V_i}|_{r=r_+} \,. \tag{4.25}$$

Since e^{V_1} and e^{V_2} are the norms of the Killing vectors ∂_z and ∂_x, ∂_y, respectively, we see that we can also write the L_i in a manifestly invariant way as:

$$L_1 = 2\left(\frac{|\partial_z|}{\kappa}\right)_{r=r_+} \,, \qquad L_2 = 2\left(\frac{|\partial_x|}{\kappa}\right)_{r=r_+} \,, \tag{4.26}$$

where here (only) κ is the surface gravity of the black hole.

We have plotted L_i as a function of T/k in figure 4.2. We see there is a significant relative length renormalisation in the anisotropic z direction, given by $\bar{L}_1$, that appears to monotonically increase with λ. By contrast we see that $\bar{L}_2 = 1$. The meaning of this is simply that the domain wall solution at $T = 0$ will preserve the symmetry of $\mathbb{R}^{1,2}$ along the full flow. Indeed it is easy to show that setting $e^{2V_2} = U$ is a consistent truncation of the equations of motion.

Returning to figure 4.1, we can also see, for sufficiently large λ, the clear emergence of an intermediate scaling behaviour with $s \propto T^{8/3}$, associated with the finite temperature Lifshitz-like scaling solution (4.12) (see [73]). To quantify this, we note that for the case of $\lambda = 7$, for example, our numerics show that the minimum of the

---

[4]In D spacetime dimensions we would have $L_i \equiv \frac{(D-1)}{4\pi T} e^{V_i}|_{r=r_+}$.
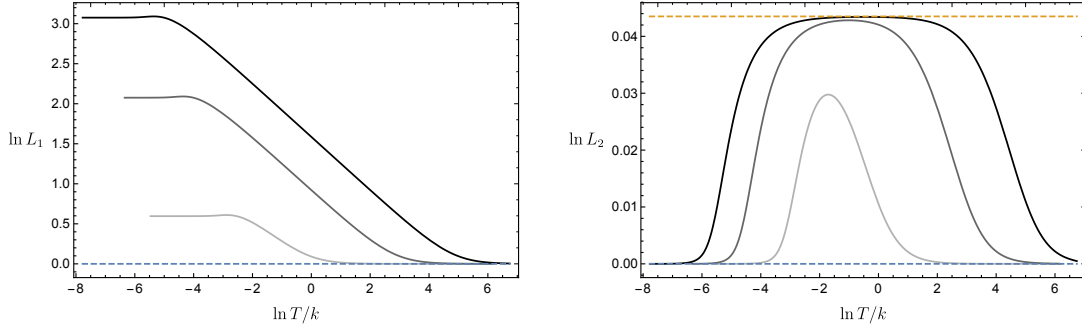
Figure 4.2: Plot of L_i, defined in (4.25) against T/k for three values of the deformation parameter $\lambda = 2, 5$ and 7 (from lightest to darkest). The values of $\bar{L}_1$ and $\bar{L}_2$, which are the values of L_1 and L_2 as $T/k \to 0$, give the relative length renormalisations in the z direction and the x, y directions, respectively, for the zero temperature AdS_5 to AdS_5 domain wall solutions. The dashed orange line at the top of the right plot is at $\ln \sqrt{12/11}$ associated with the intermediate scaling behaviour for large enough λ.

darkest curve in the left plot of 4.1 takes the value 2.6668 at $\ln T/k = 1.317$. We also see that the scaling region is becoming parametrically large as λ is increased. The lower bound is roughly given by $T/k_{IR} \gtrsim 1$ where $k_{IR} \equiv k/\bar{L}_1$. The upper bound satisfies $\ln T/k \ll \lambda$ and appears to scale with λ as anticipated. In the intermediate scaling region the value of the Kretschmann scalar at the horizon, W, defined in (4.23), is approaching $256/3$ which is the same as that of the black holes associated with heating up the Lifshitz-like scaling fixed point which were presented in equation (2.27) of [73]. It is also interesting to note that in the intermediate scaling regime we see from figure 4.2 that $\ln L_2 \sim \ln \sqrt{12/11} \sim 0.0435$. This is precisely the value associated with a domain wall solution approaching (4.12) at low temperatures.

Finally, for all T/k and for all deformation parameters λ, we find that the scalar field φ monotonically decreases as a function of the radius from λ at $r = \infty$ down to a constant at the black hole horizon. This behaviour can be established by multiplying (4.14) by φ' and then integrating in the radial direction from the horizon to r. The integral of the right hand side is positive and after integrating the the left hand side by parts one can establish $(\varphi^2)' \geq 0$. Notice, in particular, that the dilaton e^ϕ is bounded and so string perturbation theory does not break down in the bulk.

4.3.2 Shear viscosity and DC thermal conductivity

The viscosity shear tensor, $\eta_{ij,kl}$, is defined in terms of the DC limit of the imaginary part of the retarded, two point function of the stress tensor:

$$\eta_{ij,kl} = \lim_{\omega \to 0} \frac{1}{\omega} \mathrm{Im} G^R_{ij,kl}(\omega) \,, \tag{4.27}$$

where $G^R_{ij,kl}(\omega) = \langle T_{ij}(\omega, k = 0)T_{kl}(\omega = 0, k = 0)\rangle$. The procedure for calculating $\eta_{ij,kl}$ by studying the behaviour of metric perturbations is well known. Here we will import the results for anisotropic holographic lattices presented in [89] in order to calculate some of the components for our new anisotropic τ-lattice.

We define $\eta_\parallel \equiv \eta_{xy,xy}$, which is associated with spin 2 perturbations with respect to the residual $SO(2)$ rotation invariance in the x, y plane. By examining the behaviour of the metric perturbation involving δg_{xy}, as in [89], we obtain the standard result

$$\eta_\parallel = \frac{s}{4\pi} \ . \tag{4.28}$$

We next define $\eta_\perp \equiv \eta_{xz,xz} = \eta_{yz,yz}$, which is associated with spin 1 perturbations with respect to $SO(2)$. The equality arises because of the residual $SO(2)$ rotational symmetry in the x, y plane. These components of the shear viscosity can be obtained by examining metric perturbations involving $h_{x,z}$, $h_{y,z}$ which together carry spin 1 with respect to the $SO(2)$ symmetry. Following the calculation exactly as in [89], we obtain

$$\eta_\perp = \frac{s}{4\pi} \ e^{2(V_2 - V_1)}\Big|_{r=r_+} \ . \tag{4.29}$$

It is convenient to define the dimensionless quantity

$$F = \eta_\perp \frac{4\pi}{s} = e^{2(V_2 - V_1)}\Big|_{r=r_+} = \left(\frac{L_2}{L_1}\right)^2 , \tag{4.30}$$

where the L_i were defined in (4.25).

Our numerical results for F are presented in figure 4.3. For $T/k \gg 1$ our anisotropic solutions approach the standard AdS-Schwarzschild solution and hence in this limit we expect $F \to 1$, as we see in the figure.

Next, for $T/k \ll 1$ the solution is approaching a domain wall solution interpolating between AdS_5 in the UV and the same AdS_5 in the IR, but with a renormalisation of relative length scales. In this limit we thus expect F to approach a constant, but *a priori* it is not clear whether this constant is bigger or smaller than one. Figure 4.3 shows that as $T/k \to 0$ we have[5] $F \to F_0$ with $0 < F_0 < 1$. We also see that the value of F_0 monotonically decreases with increasing deformation parameter λ. Furthermore, as we decrease T/k, we see that F monotonically decreases from $F = 1$ down to $F = F_0$.

Finally, for large enough λ, in the intermediate scaling regime we expect that F

---

[5]This behaviour should be contrasted with the low temperature behaviour for other anisotropic models, where F is vanishing as result of different ground states at $T = 0$. For example, in the linear dilaton models $F \propto T^2$ [65], while for the linear axions solutions of [62, 73, 74] we have $F \propto T^{2/3}$ [86, 87].
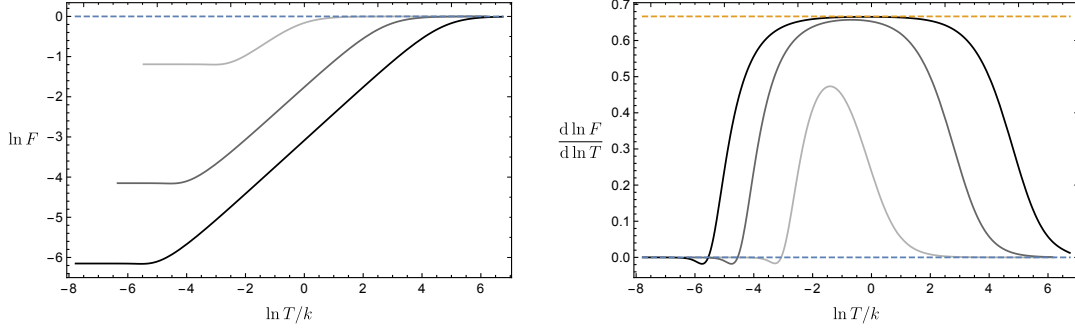
Figure 4.3: Behaviour the logarithm of $F \equiv \eta_\perp \frac{4\pi}{s}$, where $\eta_\perp$ is a component of the shear viscosity tensor, for three values of the deformation parameter $\lambda = 2, 5$ and 7 (from lightest to darkest). The left plot shows $\ln F$ monotonically decreasing from 0 at high temperatures to a finite negative constant at low temperatures. The right plot shows the intermediate scaling behaviour for large enough λ, with the dashed orange line at $2/3$.

will exhibit the same temperature scaling as for the Lifshitz scaling solution (4.12). An inspection of (4.12) reveals that the ratio of length scales imply $F \propto T^{2/3}$. This behaviour is also clearly visible in figure 4.3.

We conclude this section by calculating the DC thermal conductivity. The DC thermal conductivity is infinite in the x and y directions, due to translation invariance. However, our τ-lattice breaks translations in the z direction and hence the conductivity, κ, in this direction will be finite. It has been shown that κ can be obtained, universally, by solving a system of Stokes equations on the black hole horizon [92–94]. In fact these equations can be solved exactly for holographic lattices that depend on just one spatial direction giving results that were obtained earlier in [91]. For the case at hand we find that

$$\kappa = \left.\frac{4\pi sT}{k^2 \sinh^2 \varphi}\right|_{r=r_+} = \frac{16\pi^5 T^4 L_1 L_2^2}{k^2 \sinh^2 \varphi(r_+)}, \tag{4.31}$$

and our results are plotted in figure (4.4).

Given the understanding of the solutions that we have now gained, for $T/k \gg 1$ we expect that the scaling with temperature of κ will be the same as for the AdS-Schwarzschild solution and hence proportional to T^4. Indeed, from (4.31), with $L_1, L_2 \to 1$ and $\varphi(r_+) \to \lambda$ we explicitly see that we have $\kappa \sim k^2(T/k)^4$ for $T/k \gg 1$.

Similarly, for $T/k \ll 1$, we expect that the system will approach an ideal conductor associated with the momentum dissipating pole for the corresponding Green's function approaching the origin in the complex frequency plane. From the perturbative solution (4.17) we can deduce that

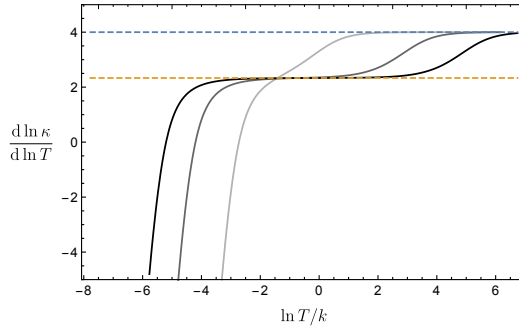$$\kappa \sim \frac{128\pi^7 T^7}{\lambda^2 k^5} e^{2k/\pi T}, \qquad T/k \ll 1, \quad \lambda \ll 1. \tag{4.32}$$

Figure 4.4: Scaling behaviour of the thermal conductivity κ as a function of $\ln T/k$ for three values of the deformation parameter $\lambda = 2, 5$ and 7 (from lightest to darkest). The dashed blue line is at 4 and the dashed orange line, associated with the intermediate scaling, is at $7/3$.

More generally by considering heating up a domain wall solution we expect

$$\kappa \sim (T^7/k^2 k_{IR}^3) e^{2k/\pi T} \tag{4.33}$$

for $T/k \ll 1$.

Finally, in the intermediate scaling regime, based on the result in [91], we expect that $\kappa \sim k^2 (T/k)^{7/3}$. This is exactly the behaviour that our numerics produces as we see in figure 4.4. For $T \ll k$ the Boltzmann behaviour of the thermal resistivity, κ^{-1}, can be understood as a consequence of the absence of low-energy excitations supported at the lattice momentum k_{IR}. More precisely, if we denote by $\mathcal{O}$ the operator dual to the axion and dilaton then the behaviour is a consequence of the vanishing of the spectral function $Im G_{\mathcal{O}\mathcal{O}}^R(\omega, k_{IR})$ as $\omega \to 0$, as explained in [68].

All of the above features for κ are clearly displayed in figure 4.4.

4.4 | Discussion

We have investigated a new class of anisotropic plasmas associated with the infinite class of CFTs that have $AdS_5 \times X_5$ holographic duals. The plasmas arise from periodic deformations of the axion and dilaton of type IIB supergravity that depend on just one of the spatial directions. While these deformations do not modify the far IR physics, apart from a simple renormalisation of relative lengths scales, for sufficiently large deformations there is a novel intermediate scaling regime governed by a Lifshitz-like solution with a linear axion that was found in [73].

The deformations that we have considered arise from a distribution of $D7$-branes and anti-$D7$-branes smeared along one of the spatial directions of the field theory. It is rather remarkable that one can construct back-reacted solutions for such

configurations. It is also suggestive that the solutions may suffer from instabilities and it would be worthwhile to investigate this issue in more detail.

For the particular case of $X_5 = S^5$, associated with $N = 4$ Yang-Mills theory, it is known that the Lifshitz-like solution is unstable [73]. At finite temperature it was shown that the linear axion solutions have phase transitions [75, 76] leading to new branches of solutions. It would be interesting to investigate whether similar instabilities and phase transitions occur for the τ-lattices we have constructed here. It seems plausible that there is a critical value of the deformation parameter where instabilities set in. For the case of the linear axion deformations, the addition of a gauge-field has been investigated in [76, 100]. Similarly incorporating a gauge field with the new τ-lattices is another topic for further study.

The deformations that we have constructed are periodic in the spatial direction. Indeed as one moves along a period in the spatial direction the field configuration traverses a circle in the Poincaré disc. One can construct other periodic configurations by utilising the exact $SL(2, Z)$ symmetry of type IIB string theory. More precisely, as one moves along a period in the spatial direction, one can demand that while τ itself is not periodic, it is periodic after acting with a non-trivial element of $SL(2, Z)$. Examples of such solutions can easily be obtained from the solutions we have presented here by taking $SL(2, Z)$ quotients of the circle on the Poincaré disc. Notice that integrating along the periodic spatial direction would then lead to a net (p, q) D7-brane charge. There are many more possibilities when additional spatial directions are involved and it would be interesting to explore such constructions in more detail.

5 | Boomerang RG Flows in M-theory with intermediate scaling

5.1 | Introduction

The AdS/CFT correspondence provides us with powerful tools to investigate the behaviour of strongly coupled conformal field theories that have been deformed by operators that explicitly break spatial translations. Indeed, by solving suitable gravitational equations we can study how such systems evolve under the renormalisation group as well as study their properties at finite temperature.

From the previous chapter, we see that in type IIB supergravity there is a rich class of examples associated with the family of $AdS_5 \times X_5$ vacuum solutions, where X_5 is an Einstein space . Motivated by these type IIB constructions, in this chapter we will construct examples of Q-lattices of $D = 11$ supergravity which are associated with the $AdS_4 \times S^7$ vacuum solution. While we find some similarities with the type IIB solutions we also find many new features. The new constructions will be made in the $N = 2$ STU gauged supergravity theory in four dimensions [101]. Recall that this theory arises from a consistent truncation of $N = 8$ gauged supergravity and hence any solution can be uplifted on the seven sphere, or a quotient thereof, to obtain a solution of $D = 11$ supergravity [101–103]. As such our solutions are directly relevant to ABJM theory [42].

The new $D = 4$ solutions involve two complex scalar fields each of which parametrises $SL(2, R)/SO(2)$. The Lagrangian has a potential term which breaks the $SL(2, R)$ symmetry down to $SO(2)$ and we use the latter for our Q-lattice construction. When expanded about the AdS_4 vacuum these scalar fields are dual to relevant operators in the dual CFT; this can be contrasted with the type IIB axion-dilaton which is massless and dual to a marginal complex operator (for any choice of X_5). Within the ABJM theory the scalar fields are dual to certain scalar and fermion bilinear operators and the RG flows are thus being driven by spatially modulated mass deformations.

An additional difference with the type IIB flows is that having two complex scalars allows us to break translation invariance in both spatial directions. Furthermore, this is achieved with a bulk metric that preserves spatial isotropy in the field theory directions. We will construct a one parameter family of solutions, parametrised by
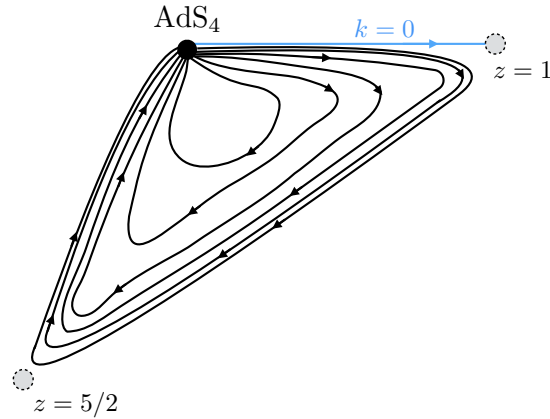
Figure 5.1: Schematic picture of the family of boomerang RG flows, parametrised by Γ/k which fixes the strength of the relevant UV deformation. They all flow from the AdS_4 vacuum in the UV to the same AdS_4 vacuum in the IR. For sufficiently large Γ/k the solutions exhibit two intermediate scaling regimes in the bulk geometry. Both regions are of hyperscaling violation form given in (5.12): the first is Lorentz invariant with $z = 1$, $\theta = -2$ while the second has $z = 5/2$, $\theta = 1$. Neither of the two intermediate scaling regimes are associated with exact solutions of $D = 11$ supergravity. The blue '$k = 0$' line is associated with a Lorentz invariant RG flow from AdS_4 in the UV to approximate hyperscaling behaviour with $z = 1$, $\theta = -2$ in the far IR.

the dimensionless ratio Γ/k, where Γ governs the strength of the deformation of the relevant operators in the UV and k is the wave number of the periodic spatial modulation.

Similar to the type IIB solutions, the new RG solutions are again boomerang flows, flowing from the AdS_4 vacuum solution in the UV down to the same AdS_4 solution in the IR with renormalised relative length scales. In addition, for large enough values of Γ/k we find that on the way to IR the RG flow exhibits intermediate scaling behaviour, similar to the $D = 5$ flows in the elliptic class. Interestingly, however, in contrast to the $D = 5$ flows there are now two distinct intermediate scaling regimes and both exhibit hyperscaling violation [104–106]. The first regime is Lorentz invariant with dynamical exponent $z = 1$ and hyperscaling violation exponent $\theta = -2$, while the second has $z = 5/2$ and hyperscaling violation exponent $\theta = 1$. A schematic picture of the RG flows is presented in figure 5.1.

This first intermediate scaling regime is directly related to the fact that we are deforming by a relevant operator. Indeed, the dimensionless deformation parameter, Γ/k, necessarily involves k and hence one can anticipate that the $\Gamma/k \to \infty$ behaviour should approach that of RG flows with $k = 0$ and $\Gamma \neq 0$. This simple observation indicates that Poincaré invariant intermediate scaling will be a more general phenomena in systems with deformations of relevant operators that break translations. Note that it did not occur in the type IIB flows [1] because the deformations by the axion and dilaton are associated with marginal operators. The existence of the

second intermediate scaling regime is less obvious, *a priori*, and furthermore it is an interesting fact that this regime appears for the same values of Γ/k for which the first intermediate scaling appears.

Another difference with the $D = 5$ flows, is that neither of the intermediate scaling behaviours are governed by fixed point solutions of the $D = 4$ gauged supergravity theory. Indeed the fact that there is hyperscaling violation means that there is a scalar field that is still running and hence they cannot be fixed point solutions. In fact, there are no exact hyperscaling violation solutions to the equations of motion which are determining the scaling behaviour. To elucidate the first regime, we construct a Poincaré invariant RG flow with $\Gamma \neq 0$ and $k = 0$, which flows from AdS_4 in the UV and approaches a hyperscaling violation behaviour in the far IR, without the far IR behaviour being itself a solution to the equations of motion. It is the far IR scaling behaviour of this RG flow, which we call the '$k = 0$ flow', that governs the first intermediate scaling of the RG flows with broken translation invariance shown in figure 5.1.

To understand the second scaling regime, we show that there is a hyperscaling violation solution with broken translation invariance and $z = 5/2$, $\theta = 1$ of an *auxiliary* theory of gravity, which has equations of motion that agree with the STU theory for large values of the modulus of the complex scalar fields. It is this solution which governs the second intermediate scaling of our RG flows shown in figure 5.1.

We are unaware of other RG flows in holography which exhibit such novel intermediate scaling behaviour and anticipate that these, or closely related flows, will have interesting applications. It is worth highlighting that using an auxiliary theory of gravity to govern intermediate scaling is rather simple and natural from the gravity side, but it is less so from the field theory point of view. Roughly speaking, it is associated with moving to the boundary in the space of coupling constants.

We have organised the chapter as follows. In section 5.2 we introduce the $D = 4$ theory of gravity that we will study, as well as the ansatz for the new RG flow solutions. In section 5.3 we pause to discuss both the $k = 0$ RG flow and also the scaling solution of an auxiliary theory of gravity, each of which governs an intermediate scaling behaviour of the boomerang RG flows. The main results for the RG flows with intermediate scaling are presented in section 5.4. In this section we also discuss how the intermediate scaling manifests itself in the behaviour of thermodynamic quantities at finite temperature, as well as in the behaviour of spectral functions of certain operators in the dual CFT at zero temperature. Using a matched asymptotics argument[1], which provides sufficient conditions for the appearance of intermediate scaling behaviour, we will expose an interesting type of universality

---

[1]Matching arguments were also discussed in the context of intermediate scaling of the optical conductivity in [82].

whereby scalar operators with different scaling dimensions, Δ, in the dual CFT, up to some maximum value set by the details of the flow, can have spectral functions with the same intermediate scaling behaviour for a certain range of frequency. We conclude with some final comments in section 5.5. In appendix B we discuss the $D = 4$ STU theory and also present an ansatz that can be used to construct charged anisotropic Q-lattice solutions.

5.2 | The set-up

Our starting point is the $N = 2$ truncation of maximal $N = 8$ $SO(8)$ gauged supergravity in four dimensions, whose bosonic field content consist of the metric, four $U(1)$ gauge-fields and three neutral complex scalar fields Φ_i which we write as

$$\Phi_i = X_i + iY_i = \lambda_i e^{i\sigma_i} \,. \tag{5.1}$$

The Lagrangian is given in appendix C. The X_i are components of the 35 scalars and the Y_i are components of the 35 pseudoscalars transforming in the $\mathbf{35_v}$ and $\mathbf{35_c}$ of the $SO(8)$ global symmetry of the $N = 8$ theory, respectively [107]. Using the formula given in [101–103], any solution of the $N = 2$ theory can be explicitly uplifted on a seven sphere to obtain an exact solution of $D = 11$ supergravity.

In the bulk of this chapter we will be interested in solutions with vanishing gauge-fields and we will also truncate $\lambda_1 = \sigma_1 = 0$, which we can do consistently. Thus, we consider the Lagrangian

$$\mathcal{L} = R - \frac{1}{2} \sum_{i=2}^{3} \left[(\partial \lambda_i)^2 + \sinh^2 \lambda_i (\partial \sigma_i)^2 \right] + 2(1 + \cosh \lambda_2 + \cosh \lambda_3) \,. \tag{5.2}$$

The AdS_4 vacuum solution, with unit radius and $\lambda_2 = \lambda_3 = \sigma_2 = \sigma_3 = 0$, uplifts to the maximally supersymmetric $AdS_4 \times S^7$ solution.

We now introduce the following ansatz, which breaks translation invariance in both spatial directions (x, y) of the dual field theory:

$$\mathrm{d}s^2 = -U(r)\mathrm{d}t^2 + U(r)^{-1}\mathrm{d}r^2 + e^{2V(r)}(\mathrm{d}x^2 + \mathrm{d}y^2) \,,$$
$$\sigma_2 = kx, \quad \sigma_3 = ky, \qquad \lambda_2 = \lambda_3 = \gamma(r) \,. \tag{5.3}$$

Notice that the ansatz for the metric preserves the spatial isotropy in the (x, y) directions. Also, since the σ_i are periodic variables, the dependence on the spatial coordinates is periodic in x, y with period $2\pi/k$. This ansatz solves the equations of motion for σ_2 and σ_3 and moreover because $(\partial \sigma_2)^2 = (\partial \sigma_3)^2$ it is consistent to have

$\lambda_2 = \lambda_3 = \gamma$. The remaining equations of motion lead to a first order ODE for U and two second order ODEs for V and γ given by:

$$U' = \frac{1}{2V'} \left(2(1 + 2\cosh\gamma) - e^{-2V} k^2 \sinh^2\gamma + U(\gamma'^2 - 2V'^2) \right),$$

$$V'' = -V'^2 - \frac{1}{2}\gamma'^2,$$

$$U\gamma'' = (-2 + e^{-2V} k^2 \cosh\gamma)\sinh\gamma - (U'\gamma' + 2UV')\gamma'. \tag{5.4}$$

As $r \to \infty$ we demand that the solutions approach the AdS_4 solution with the following asymptotic behaviour

$$U = r^2 + ..., \qquad e^{2V} = r^2 + ..., \qquad \gamma = \frac{\Gamma}{r} + ... \tag{5.5}$$

It will be convenient to refer to Γ and k as 'deformation parameters' in the following. For fixed dimensionless parameter Γ/k, by solving the ODEs with prescribed boundary conditions in the IR, we can then obtain the sub-leading terms in the expansion (5.5) and these can be used to parametrise 'expectation values' of the dual operators. Viewing (5.2) from a bottom-up context this is the appropriate language to describe the RG flow when γ is dual to an operator with scaling dimension $\Delta = 2$. However, in the top-down context it is important to note that the ansatz for the complex scalars is written in terms of the X_i and Y_i as

$$X_2 = \gamma(r)\cos(kx), \qquad Y_2 = \gamma(r)\sin(kx),$$

$$X_3 = \gamma(r)\cos(ky), \qquad Y_3 = \gamma(r)\sin(ky), \tag{5.6}$$

with $X_1 = Y_1 = 0$. Now supersymmetry implies that the scalars X_i and the pseudoscalars Y_i are associated with operators of scaling dimension $\Delta = 1$ and $\Delta = 2$, respectively. The parameter Γ therefore describes deformations of two pseudoscalar operators with spatial dependence given by $\sin kx$ and $\sin ky$. However, the deformations of two scalar operators, which have spatial dependence $\cos kx$ and $\cos ky$, are given by the sub-leading terms in (5.5). It is precisely this tuning of the deformation parameters of these operators that allows us to construct the RG flows by solving a system of ODE's. It would be interesting to extend our solutions away from this tuned situation, but that will necessarily involve solving partial differential equations and this will be left for future work. We also return to this issue below when we discuss finite temperature solutions.

The solutions that we construct are in the $U(1)^4$ invariant bosonic sector of $N = 8$ gauged supergravity. As such, after being uplifted on the S^7 to obtain solutions of $D = 11$ supergravity, they will survive the cyclic quotient of the S^7 and hence are

relevant for the $N = 6$ ABJM theory [42]. The scalar fields X_i are dual to operators that are scalar bilinears, while the pseudoscalar fields Y_i are dual to operators that are fermion bilinears. More precisely, under the $SU(4) \times U(1) \subset SO(8)$ holographically identified with the global symmetries of the ABJM theory, the X_i and Y_i each transform in a $\mathbf{15_0}$ representation and are thus dual to operators schematically of the form

$$\mathcal{O}_{\phi\phi} \sim \mathrm{Tr}\left(\phi^\dagger_{\tilde{A}} \phi^B - \frac{1}{4}\delta^B_{\tilde{A}} \phi^\dagger\phi\right), \qquad \mathcal{O}_{\psi\psi} \sim \mathrm{Tr}\left(\psi^\dagger_{\tilde{A}} \psi^B - \frac{1}{4}\delta^B_{\tilde{A}} \psi^\dagger\psi\right), \qquad (5.7)$$

respectively, where ϕ, ψ are scalar and fermion fields of the ABJM theory, respectively. The RG flows are being driven by spatially modulated deformations of these operators and (5.6) shows that this breaks spatial isotropy in the (x, y) directions.

5.2.1 Perturbative deformations

The RG flow solutions that we have constructed depend on the dimensionless deformation parameter Γ/k. For small deformations, $\Gamma/k \ll 1$, we obtain some important insight by solving the equations as a perturbative expansion about the AdS_4 vacuum. At leading order in Γ/k we can easily solve the linearised equation of motion for γ. Choosing the integration constants so that the solution is both regular at the Poincaré horizon and with boundary conditions as in (5.5) we find

$$\gamma(r) = \frac{k}{r}e^{-k/r}(\Gamma/k) + \mathcal{O}(\Gamma/k)^2. \qquad (5.8)$$

This solution will back react on the metric at order $(\Gamma/k)^2$ and explicit expressions can be obtained subject to the appropriate boundary conditions. We find

$$U = r^2[1 + \left(\frac{k}{4r}e^{-2k/r}\right)(\Gamma/k)^2 + \mathcal{O}(\Gamma/k)^3],$$

$$e^{2V} = r^2[1 + \frac{1}{8}\left(1 - e^{-2k/r}(1 + \frac{2k^2}{r^2})\right)(\Gamma/k)^2 + \mathcal{O}(\Gamma/k)^3]. \qquad (5.9)$$

In the far IR, as $r \to 0$, the metric rapidly approaches the same AdS_4 solution that appears in the UV, with the scale of the approach set by k. The only difference between the AdS_4 solutions in the UV and the IR is that there is a renormalisation of relative length scales. In the UV we can define the ratio $\chi_{UV} = \lim_{r\to\infty} U^{1/2}/e^V$ and similarly $\chi_{IR} = \lim_{r\to 0} U^{1/2}/e^V$ in the IR, both of which are invariant under scalings of the radial coordinate. Following [108] we can then define the RG flow invariant, n, (sometimes called the 'index of refraction' for the RG flow) as $n \equiv \frac{\chi_{UV}}{\chi_{IR}}$. Since in the parametrisation we are using $U \to r^2$ both as $r \to \infty$ and $r \to 0$ we

have

$$n = \frac{e^V(r \to 0)}{e^V(r \to \infty)} = 1 + \frac{1}{16}\frac{\Gamma^2}{k^2} + \mathcal{O}\left(\Gamma/k\right)^3 . \tag{5.10}$$

The recovery of conformal invariance that we see[2] for small values of Γ/k is associated with the fact that the operators used in the deformation have vanishing spectral weight at low energies. To determine what happens for larger values of Γ/k it is necessary to solve the equations of motion numerically. Our numerical results, summarised below, indicate that for arbitrarily large values of Γ/k the RG flows are all boomerang flows. In addition, we find that for large enough Γ/k all of the RG flow solutions successively approach, for intermediate values of the radial coordinate r/k, two intermediate scaling behaviours before hitting the AdS_4 behaviour in the far IR.

5.3 | Intermediate Scaling Solutions

The two intermediate scaling behaviours that we observe in the boomerang RG flows are, somewhat surprisingly, not associated with exact hyperscaling solutions of the equations of motion coming from the Lagrangian $\mathcal{L}$ in (5.2). In this section we explain their origin.

5.3.1 First intermediate scaling regime: the $k = 0$ flow

The first intermediate scaling regime that we observe on the way to the IR is governed by large values of the field γ and, moreover, is such that the terms involving k play a sub-dominant role in the equations of motion. Since the breaking of translation invariance is sub-dominant the first intermediate scaling behaviour is approximately Lorentz invariant.

Let us therefore consider Lorentz invariant RG flow solutions of the equations of motion (5.4) with $k = 0$ (i.e. $\sigma_2 = \sigma_3 = 0$) and $e^{2V} = U$. We look for solutions that approach AdS_4 in the UV with expansion (5.5). While there are not any exact hyperscaling violation solutions to the equations of motion that we can map onto in the IR, we have numerically constructed RG flow solutions that approach the

---

[2]The perturbative argument we used above was also used to argue for boomerang RG flows in the context of other examples of CFT deformations which break translations [1, 77, 78]. One context it does not apply is if the linearised deformation gives rise at higher orders in the perturbative expansion to additional sources with non-vanishing zero modes (i.e. the integral of the source over a spatial period is non-vanishing). It also does not apply to the type IIB linear dilaton and linear axion solutions of [65] and [73], respectively.

following singular behaviour[3] in the far IR as $r \to 0$:

$$U = e^{2V} = L_I^{-2} r^{4/3} + \dots, \qquad e^\gamma = e^{\gamma_0} r^{-2/3} + \dots, \qquad (5.11)$$

where $L_I^2 = (10/9)e^{-\gamma_0}$. Notice that the field γ is diverging as $r \to 0$. In particular, the IR behaviour of the $k = 0$ flow is approaching that of solutions with hyperscaling violation, with a running scalar, similar to the flows in [109] (see also [110]). To see this more explicitly, we introduce a new radial coordinate $\rho = (1/3L_I)r^{-1/3}$ and, after suitably scaling t, x, y, we find that we can write the leading form of the IR metric, now located at $\rho \to \infty$ as:

$$ds^2 = \rho^{-(2-\theta)} \left(-\rho^{-2(z-1)} d\bar{t}^2 + d\rho^2 + d\bar{x}^2 + d\bar{y}^2 \right), \qquad (5.12)$$

with dynamical exponent $z = 1$, associated with Lorentz invariance, and hyperscaling violation exponent $\theta = -2$ (in the parametrisation of [106]). Note that under the scaling

$$t \to \mu^z t, \quad (x, y) \to \mu(x, y), \quad \rho \to \mu\rho, \qquad (5.13)$$

the general metric (5.12) scales as $ds^2 \to \mu^\theta ds$. Furthermore, if one heats up these solutions one finds that the entropy density scales like $s \propto T^{(2-\theta)/z} = T^4$, a scaling we will see in the finite temperature solutions that we discuss in section 5.4.1. Finally, we note that we have checked that the $k = 0$ flow does not preserve supersymmetry.

5.3.2 Second intermediate scaling regime

The second intermediate scaling regime that arises in the RG flows is governed by large values of the field γ but now the terms involving k play a comparable role in the equations of motion. Thus, in contrast to the first intermediate scaling regime, this scaling behaviour breaks translation invariance.

Perhaps the simplest way to describe this behaviour is to consider the following auxiliary Lagrangian, $\hat{\mathcal{L}}$, which approximately governs the behaviour of solutions in regions of spacetime where the field γ is getting large:

$$\mathcal{L} = R - \frac{1}{2}(\partial\lambda_2)^2 - \frac{1}{8}e^{\lambda_2}(\partial\sigma_2)^2 - \frac{1}{2}(\partial\lambda_3)^2 - \frac{1}{8}e^{\lambda_3}(\partial\sigma_3)^2 + (e^{\lambda_2} + e^{\lambda_3}). \qquad (5.14)$$

Within the ansatz (5.3), there exists an exact hyperscaling violation solution for this auxiliary theory, which was first given in [71] (see also [72]). It takes the form, for

---

[3]The subleading corrections are more easily obtained by switching radial coordinate so that the metric is of the form $ds^2 = dR^2 + e^{2W}(-dt^2 + dx^2 + dy^2)$ and we then find that as $R \to 0$ we have $e^{2W} = R^4[1 + \frac{2}{21}R^2 + o(R^4)]$ and $e^\gamma = \frac{10}{R^2}[1 + \frac{1}{42}R^2 + o(R^4)]$.

all values of r,

$$U = L_{II}^{-2} r^{8/3}, \qquad e^{2V} = e^{2v_0} r^{2/3}, \qquad e^{\gamma} = e^{\gamma_0} r^{2/3}, \tag{5.15}$$

where $L_{II}^2 = (28/9)e^{-\gamma_0}$ and $e^{\gamma_0} = 6e^{2v_0}/k^2$. By introducing a new radial coordinate $\rho = (9L_{II}^2/4)r^{-2/3}$ and suitably scaling t, x, y, we can write the metric in the form of (5.12) with dynamical exponent $z = 5/2$ and hyperscaling violation exponent $\theta = 1$. In the second intermediate scaling regime the RG flow solutions approach the behaviour as in (5.15) with large values of γ (i.e. with r in (5.15) going to ∞.) If one heats up these solutions one finds that the entropy density scales like $s \propto T^{2/5}$.

5.4 | The RG flows

We now summarise the RG flows that we have constructed numerically. They are solutions within the ansatz (5.3) and solve the equations of motion (5.4). In the far IR, as $r \to 0$, they approach AdS_4 with expansion given by

$$U = r^2 \left(1 + e^{-2\frac{k}{rc_V}} \left(\frac{c_V c_\gamma^2}{4kr} \right) + \cdots \right),$$

$$e^{2V} = r^2 c_V^2 \left(1 - e^{-2\frac{k}{rc_V}} \left(\frac{1}{4r^2} + \frac{c_V^2}{8k^2} \right) c_\gamma^2 + \cdots \right),$$

$$\gamma = \frac{c_\gamma}{r} e^{-\frac{k}{rc_V}} + \cdots, \tag{5.16}$$

depending on two integration constants, c_γ, c_V. In the UV, as $r \to \infty$, we assume that the solutions approach AdS_4 with the following expansion

$$U = (r + r_+)^2 \left(1 - \frac{1}{2} \frac{\Gamma^2}{(r + r_+)^2} + \frac{M}{(r + r_+)^3} + \cdots \right)$$

$$e^{2V} = (r + r_+)^2 \left(1 - \frac{1}{2} \frac{\Gamma^2}{(r + r_+)^2} - \frac{2}{3} \frac{\Gamma \hat{\Gamma}}{(r + r_+)^3} + \cdots \right)$$

$$\gamma = \frac{\Gamma}{r + r_+} + \frac{\hat{\Gamma}}{(r + r_+)^2} + \dots,, \tag{5.17}$$

with the appearance of r_+ related to the fact that we have set the IR at $r = 0$. Our boundary conditions will be to hold fixed the dimensionless ratio Γ/k. The three constants of integration $\hat{\Gamma}$, r_+ and M appearing in (5.17) will be fixed by demanding regularity in the IR part of the geometry. For example, the perturbative solution (5.9), which has a smooth IR limit at $r = 0$, has $r_+ = \Gamma^2/(8k)$, $\hat{\Gamma} = -k\Gamma$ and $M = k\Gamma^2/2$. More generally, for the solutions that we will obtain numerically these three constants can be fixed by shooting both from the UV and the IR and then
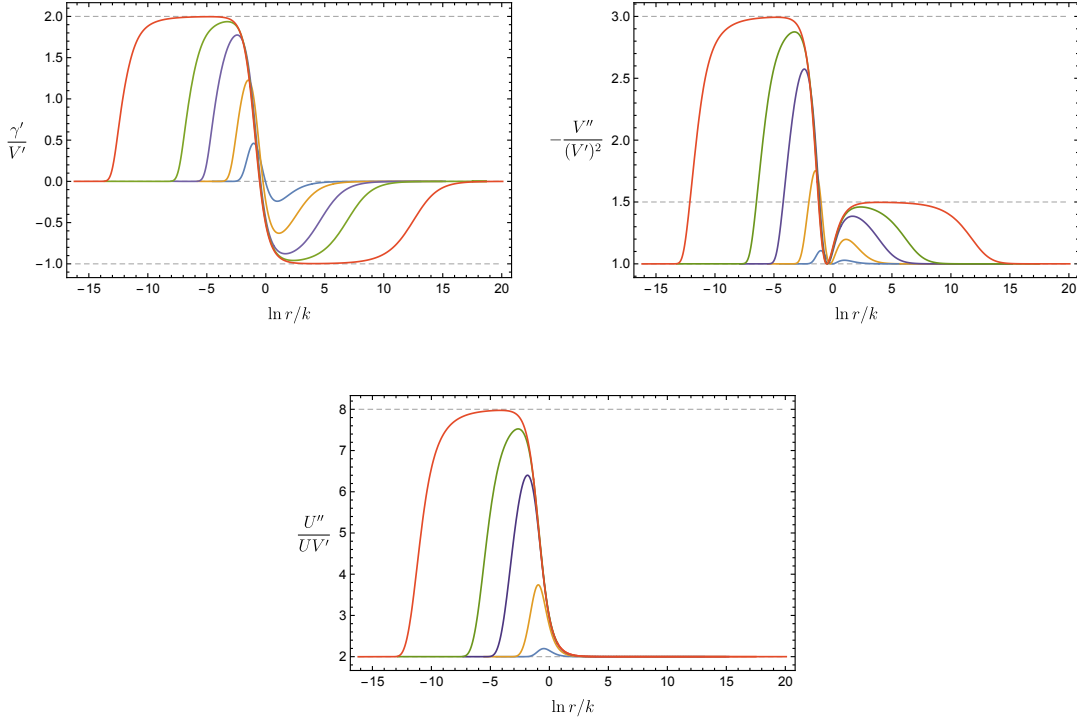
Figure 5.2: Plots of various functions associated with the RG flows, as functions of the dimensionless radial coordinate r/k, for various values of the dimensionless deformation parameter Γ/k: blue ($\Gamma/k = 1$), orange ($\Gamma/k = 10$), purple ($\Gamma/k = 10^2$), green ($\Gamma/k = 10^3$) and red ($\Gamma/k = 2.6 \times 10^5$). The plots demonstrate the boomerang RG flow from AdS_4 in the UV to AdS_4 in the IR for all values of Γ/k. For sufficiently large values of Γ/k, on the way to the IR the flows approach two intermediate scaling regimes.

matching at intermediate values of the radial coordinate. The equations of motion (5.4) that we will be integrating will require five constants to be fixed in this way. Therefore, two of them will have to come from the IR expansion. For the RG flows at $T = 0$ these two constants are c_γ and c_V in (5.16). For the finite temperature solutions, which we discuss in subsection 5.4.1, the two extra constants will come from an analytic expansion around a regular horizon which will be located at the fixed position $r = 0$, (again associated with the appearance of r_+ in (5.17)), which is convenient for the numerics.

For small Γ/k the solutions are well approximated by the perturbative solutions that we constructed in section 5.2.1. After sufficiently increasing the value of Γ/k we then start to approach the first intermediate scaling regime, governed by the IR behaviour of the $k = 0$ flow (5.11), thus approximately recovering Lorentz invariance. This first intermediate scaling regime arises because, since we are deforming by a relevant operator, the dimensionless deformation parameter, Γ/k, involves k. In particular, one can expect that the $\Gamma/k \to \infty$ behaviour should approach the $k = 0$ with $\Gamma \neq 0$.

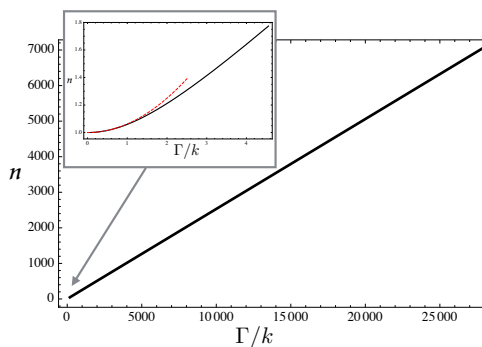Interestingly, for the same large values of Γ/k, as we go further into the IR,

Figure 5.3: Plot of the RG flow invariant n, defined in (5.10), versus deformation parameter Γ/k, for the boomerang RG flows. The inset shows excellent agreement with the perturbative result given in (5.10) for $\Gamma/k \ll 1$.

we also approach the second intermediate scaling region (5.15) with $z = 5/2$. A convenient way[4] of displaying the scaling behaviour is to plot γ'/V', $-V''/(V')^2$ and $U'/(UV')$ as functions of the dimensionless radial coordinate r/k. In particular, for the first intermediate scaling regime (5.11) these functions should approach -1, $3/2$ and 2, respectively. Similarly for the second intermediate scaling regime (5.11) these functions should approach 2, 3 and 8, respectively. Furthermore, for boomerang RG flows they should approach 0, 1 and 2, respectively, both in the UV and in the IR. In figure 5.2 we demonstrate the behaviour of these functions for several representative values of Γ/k and we clearly see the boomerang RG flows and the appearance of the intermediate scaling regimes.

By scanning over different values of Γ/k we can also determine the behaviour of the RG flow invariant n, as defined in (5.10), and our results are presented in figure 5.3. For small values of Γ/k we see that $n-1$ depends quadratically on Γ/k, as expected from the perturbative analysis. For large values Γ/k we find that n asymptotes to a linear dependence of the form $n \sim 0.253(\Gamma/k)$.

5.4.1 Finite temperature

The intermediate scaling regimes that we have found in the RG flows, for large enough values of Γ/k, should also manifest themselves at non-zero temperature T, for $T/k \ll \Gamma/k$. We have constructed finite temperature black hole solutions by changing the IR boundary conditions from AdS_4, as in (5.16), to a regular black hole

---

[4]The scaling behaviour displayed by these functions is invariant under shifts of the radial coordinate by a constant.
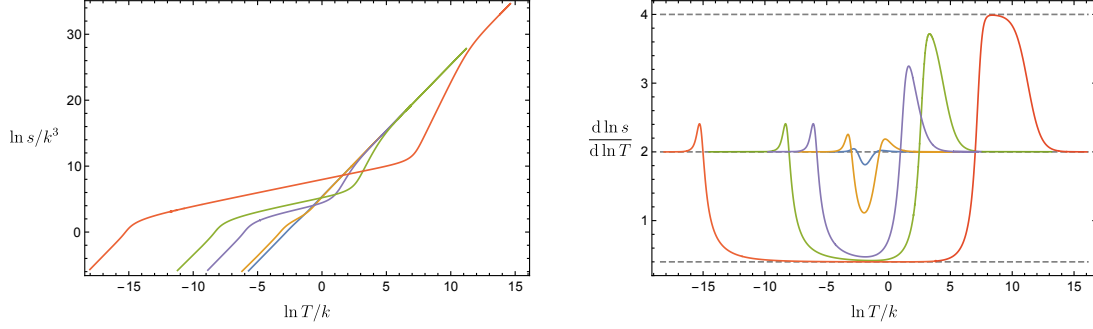
Figure 5.4: Behaviour of the entropy density, s, as a function of temperature, for various boomerang RG flows: blue ($\Gamma/k = 1$), orange ($\Gamma/k = 10$), purple ($\Gamma/k = 10^2$), green ($\Gamma/k = 10^3$) and red ($\Gamma/k = 10^6$). In the UV and in the IR we have $d \ln s / d \ln T$ approaching 2, associated with AdS_4. We also see, for large enough values of Γ/k, the appearance of two intermediate scaling regimes that are governed by the hyperscaling violation solutions which have $d \ln s / d \ln T = 4$ and $d \ln s / d \ln T = 2/5$.

Killing horizon located at $r = 0$, with

$$U = 4\pi T\, r + \frac{1}{2} e^{-2V_{1+}} k^2 \sinh^2 \gamma_+ \, r^2 + \cdots,$$

$$V = V_{1+} + \frac{1}{8\pi T} (2 + 4 \cosh \gamma_+ - e^{-2V_{1+}} k^2 \sinh^2 \gamma_+) \, r + \cdots,$$

$$\gamma = \gamma_+ + \frac{1}{8\pi T} (4 \sinh \gamma_+ - e^{-2V_{1+}} k^2 \sinh 2\gamma_+) \, r + \cdots, \tag{5.18}$$

where T is the temperature which we will be holding fixed. The two constants of integration γ_+ and V_{1+} are used to find a unique solution of the equations of motion (5.4) upon matching with the three constants that we discussed below (5.17).

For temperatures $T/k \ll \Gamma/k$ we can anticipate that there are intermediate regimes of low temperature where the solutions approach that of a hyperscaling violation black hole with $z = 5/2$, $\theta = 1$ and then, for large temperatures, a hyperscaling violation black hole with $z = 1$, $\theta = -2$. Correspondingly, this should give rise to an associated scaling of thermodynamic quantities. For example, the scaling of the entropy density should begin as $s \sim T^2$ for low temperatures, associated with the AdS_4 IR behaviour. Then, as we increase the temperature we should successively see $s \sim T^{2/5}$ followed by $s \sim T^4$, corresponding to the two hyperscaling regimes, and finally end up with $s \sim T^2$ for very high temperatures corresponding to the AdS_4 region in the UV. These features are clearly displayed for a range of Γ/k as shown in figure 5.4.

We would like to highlight an important subtlety concerning these finite temperature black hole solutions. By construction we find a one parameter family of black hole solutions, labelled by T/k, while holding the parameter Γ/k fixed. As we discussed below (5.6), this means that we are holding fixed the deformation parame-

ters for the two pseudoscalar operators, dual to the Y_i, as well as the expectation value of the two scalar operators, dual to the X_i. It is precisely for this particular mixed thermodynamic ensemble that we are able to construct black hole solutions by solving ordinary differential equations.

5.4.2 Spectral weight of operators in the RG flows

We now return back to the RG flows at zero temperature and analyse the behaviour of some correlation functions involving scalar operators. In particular, we will show how the intermediate scaling regimes can also lead to scaling behaviour appearing in various spectral functions of the dual field theory, for certain ranges of intermediate frequencies. We will also see that there can be an interesting kind of universality in which operators of different scaling dimensions in the UV exhibit the same scaling at intermediate scales. Some additional interesting features will be highlighted as we proceed.

In general, given that spatial translations have been explicitly broken, we need to consider linearised perturbations about the RG flows that involve solving partial differential equations. However, there are some correlation functions that can be obtained by solving ordinary differential equations, and this is what we will study here. Specifically, we start by considering a bulk scalar field ϕ whose linearised equation of motion in the background geometry is given by the Klein-Gordon equation

$$(\nabla^2 - m^2)\phi = 0 \,. \tag{5.19}$$

A specific case that we will focus on is when $m^2 = -2$: this arises in the STU model, given in (C.1), for the scalar field λ_1 with $\sigma_1 = 0$ (i.e. X_1 in (5.1)), which is dual to an operator with $\Delta = 1$ and also λ_1 with $\sigma_1 = \pi/2$ (i.e. Y_1 in (5.1)), which is dual to an operator with $\Delta = 2$. As usual, the retarded Green's function $G^R(\omega)$ can be obtained by writing $\phi = e^{-i\omega t} \tilde{\psi}(r)$ and then solving (5.19) with ingoing boundary conditions in the AdS_4 geometry in the far IR. This gives a radial equation for $\tilde{\psi}$ and the ratio of the normalisable to the non-normalisable solutions in the UV, then gives $G^R(\omega)$. For example, for the $\Delta = 1$ operator we can expand at $r \to \infty$ as $\tilde{\psi}(r) = \psi_1(\omega)/r + \psi_2(\omega)/r^2 + ...$ and we have $G^R(\omega) \propto \psi_1(\omega)/\psi_2(\omega)$, while for the $\Delta = 2$ operator we have the same expansion with $G^R(\omega) \propto \psi_2(\omega)/\psi_1(\omega)$.

It is convenient to introduce a new radial coordinate, z, defined by

$$z = -\int_r^{+\infty} \frac{dy}{U(y)} \,, \tag{5.20}$$

and we note that the UV is located at $z = 0$ and the IR at $z = -\infty$. We then have

that $v = t + z$ is the ingoing coordinate in Eddington-Finkelstein coordinate. Next, by writing $\tilde{\psi} = e^{-V}\psi$, we then deduce that the radial equation can be written in the Schrödinger form

$$-\partial_z^2\psi + \left(\mathcal{V} - \omega^2\right)\psi = 0\,, \qquad (5.21)$$

where we have defined the effective potential

$$\mathcal{V} = U\left(m^2 + e^{-V}\partial_r\left(U\partial_r e^V\right)\right)\,. \qquad (5.22)$$

Now for standard RG flows, which flow from the UV to another geometry with scaling behaviour in the far IR, matching arguments have been developed in [69], generalising earlier work, including [111], which show that for small frequencies the spectral function $\text{Im}G^R(\omega)$ is determined by the spectral function associated with the retarded Green's function[5] for the IR geometry, $\text{Im}\mathcal{G}^R(\omega)$.

We would like to know when something similar occurs for a background geometry with an intermediate scaling regime for $z_1 < z < z_2$. Specifically we want to determine when $\text{Im}G^R(\omega)$ exhibits scaling behaviour, for certain intermediate values of ω, that is fixed by spectral functions $\text{Im}\mathcal{G}_i^R(\omega)$, $i = 1, 2$, associated with one of the two intermediate scaling regimes. In order for this to occur we need to ensure that in the region $z_1 < z < z_2$, the solution of the radial equation (5.21), which has ingoing boundary conditions imposed in the far IR at $z \to -\infty$, is predominantly a solution in the intermediate scaling regime with ingoing boundary conditions imposed at $z = z_1$. In general this will not be the case[6] and the solution will also contain a significant admixture of a solution with outgoing boundary conditions imposed at $z = z_1$.

To proceed, for the scaling region $z_1 < z < z_2$ we assume

$$|\mathcal{V}(z_1)| \ll \omega^2 \ll |\mathcal{V}(z_2)|\,, \qquad (5.23)$$

and also demand that the potential satisfies

$$|\mathcal{V}(z)| < |\mathcal{V}(z_1)| \ll \omega^2\,, \qquad \text{for} \qquad z < z_1\,. \qquad (5.24)$$

To see that this is sufficient to have intermediate scaling of the spectral function, we

---

[5]As explained in [69], in general it is given by a sum of terms associated with various fields in the IR.

[6]For the solutions with intermediate scaling constructed in [82] it was numerically shown that the conductivity exhibited intermediate scaling. Some matching arguments were also discussed to explain this behaviour, but the sufficient conditions on the potential for when intermediate scaling appears, that we identify here, were not discussed.
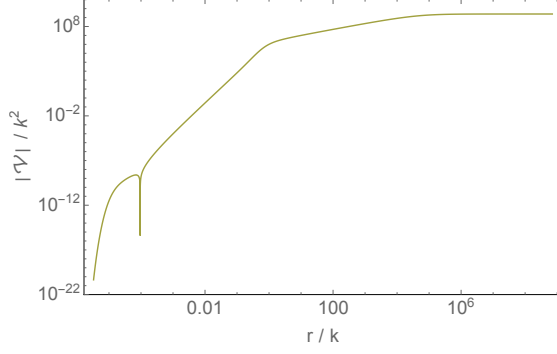
Figure 5.5: Plot of the Schrödinger potential $|\mathcal{V}|$, defined in (5.22), for a massive scalar field with $m^2 = -2$. Note that $\mathcal{V}$ has a zero at $r/k \sim 9.5 \times 10^{-5}$. The deformation parameter is $\Gamma/k = 0.7 \times 10^5$ and the intermediate scaling behaviour is between $10^{-4} < r/k < 1$ and $1 < r/k < 10^4$. The plot shows a clear separation of scales for the values of the potential in these regions.

next split the z interval into three regions:

$$\psi^{(}z) \approx \begin{cases} \psi^{(I)}(z), & z < z_1 \,, \\ \psi^{(II)}(z), & z_1 < z < z_2 \,, \\ \psi^{(III)}(z), & z > z_2 \,. \end{cases} \tag{5.25}$$

In the region $z < z_1$, using the perturbative expansion parameter $\epsilon = \frac{|\mathcal{V}(z_1)|}{\omega^2}$, we can develop the following perturbative solution

$$\psi^{(I)}(z) = C_{in}(\omega) \, e^{-i\omega z} + C_{out}(\omega) \, e^{i\omega z} + \epsilon \, \delta\psi^{(I)}(z) + \cdots \,, \tag{5.26}$$

where $C_{in}(\omega)$, $C_{out}(\omega)$ are constants. The in-falling boundary conditions at $z = -\infty$ require that $C_{out} = 0$. But this also shows that in the overlapping region around $z = z_1$, to leading order in ϵ, we should impose approximate in-falling boundary conditions on the matching solution $\psi^{(II)}(z)$. Thus, to leading order in ϵ, the solution $\psi^{(II)}(z)$ will be the usual perturbation in the scaling region $z_1 < z < z_2$, with ingoing boundary conditions at z_1. We can then invoke the matching arguments of [69] to match onto the solutions in region III and deduce that for $|\mathcal{V}(z_1)| \ll \omega^2 \ll |\mathcal{V}(z_2)|$, the spectral function $\mathrm{Im}G^R(\omega)$ will be determined by $\mathrm{Im}\mathcal{G}^R(\omega)$ where $\mathcal{G}^R(\omega)$ is the spectral function for the scaling solution in the region $z_1 < z < z_2$. It is important to appreciate that in making this argument we do not need to know about the properties of $\mathcal{G}^R(\omega)$ for other values of ω and, for example, it is possible that it has instabilities which do not play a role.

We can illustrate these ideas for the boomerang RG flows for the special cases mentioned above, with $m^2 = -2$ and quantised so that $\Delta = 1$ or $\Delta = 2$. In figure 5.5 we have plotted the Schrödinger potential $|\mathcal{V}|/k^2$ against r/k for the RG flow

with $\Gamma/k \sim 0.7 \times 10^5$. The plot shows that the potential has a power law behaviour for the intermediate scaling regions with $1 < r/k < 10^4$ and $10^{-4} < r/k < 1$. The plot also shows that the condition (5.24) is satisfied for both regions and hence we expect that there is an intermediate scaling behaviour for the spectral function that is governed by the two hyperscaling violation solutions.

For $1 < r/k < 10^4$ we have $10^6 < |\mathcal{V}|/k^2 < 10^9$ and hence we expect from (5.23) that there will be intermediate scaling governed by the hyperscaling violation geometry (5.11) (associated with the $k = 0$ flow) for the range of frequencies $10^6 \ll (\omega/k)^2 \ll 10^9$. It is important to notice that in the intermediate scaling regime, the mass term in the Schrödinger potential (5.22) is sub-dominant compared to the other term; this can easily be deduced by taking $r \to 0$ in (5.11). Taking this point into consideration, a straightforward calculation shows that for the hyperscaling violation geometry (5.11) we have $\mathrm{Im}\mathcal{G}_I^R(\omega) \sim \omega^{7/5}$ for small ω and hence in the boomerang flow we expect to have the scaling $\mathrm{Im}G^R(\omega) \sim \omega^{7/5}$ for $10^6 \ll (\omega/k)^2 \ll 10^9$.

Similarly, for $10^{-4} < r/k < 1$ we have $10^{-8} < |\mathcal{V}|/k^2 < 10^6$ and hence we expect intermediate scaling governed by the hyperscaling violation geometry (5.15) for the range $10^{-8} \ll (\omega/k)^2 \ll 10^6$. Once again the mass term in the Schrödinger potential (5.22) is sub-dominant compared to the other term in the intermediate scaling regime governed by the hyperscaling violation geometry (5.15). Now for (5.15) a calculation shows that $\mathrm{Im}\mathcal{G}_{II}^R(\omega) \sim \omega^5$ for small ω and hence for the boomerang flow we expect to have the scaling $\mathrm{Im}G^R(\omega) \sim \omega^5$ for $10^{-8} \ll (\omega/k)^2 \ll 10^6$.

We can now check these expectations by numerically constructing the spectral function $\mathrm{Im}G^R(\omega)$ of the full boomerang RG flow. A key technical point in solving (5.21), is that it is helpful to pull out an overall factor of $e^{-i\omega z}$ for ψ, where z is defined in (5.20). Indeed we find that this deals with the rapid oscillations of ψ throughout the whole of the flow, including the intermediate scaling regimes. Our results, which involved considerable numerical effort, are presented in figure 5.6 for various Γ/k. In particular, for the largest value of $\Gamma/k \sim 0.7 \times 10^5$ we see the spectral function exhibits the intermediate scaling behaviour exactly as predicted above.

An important point to emphasise in the above analysis is that in each of the intermediate scaling regimes (5.11),(5.15) the mass term appearing in the Schrödinger potential (5.22) is sub-dominant compared to the other term[7]. This means that the nature of the intermediate scaling that is displayed in figure 5.6 will be essentially the same for all scalar modes which have a simple mass term, provided that m^2 is much smaller than the second term inside the outer brackets of (5.22) when evaluated in

---

[7]As an aside we note that when considering the hyperscaling violation solutions (5.11) and (5.15) as UV complete solutions in themselves, one finds that the Schrodinger potential admits negative energy bound states, when $m^2 < 0$ and hence implies that the solutions are unstable for such scalars. However, as mentioned, this does not affect our conclusion concerning the intermediate scaling of the spectral functions on the boomerang RG flows.
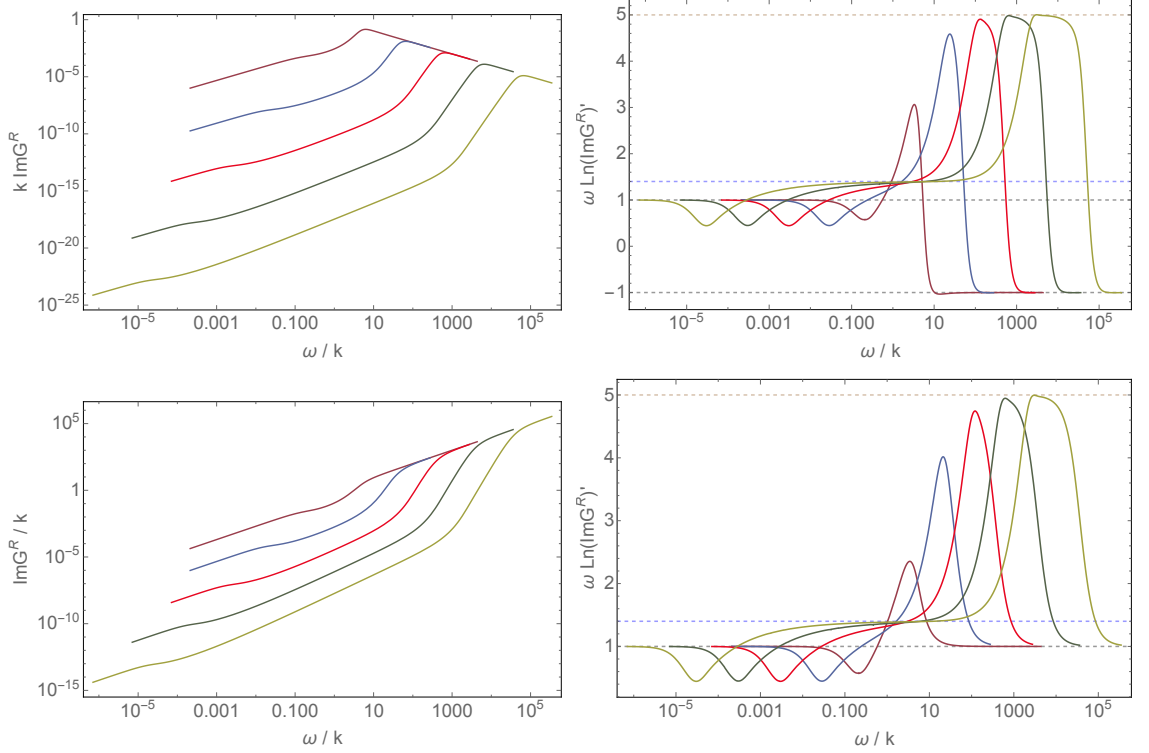
Figure 5.6: Plots displaying the behaviour of the spectral function $\mathrm{Im}G^R(\omega)$ for a scalar field with $\Delta = 1$ (top plots) and $\Delta = 2$ (bottom plots) for various values of $\Gamma/k = 0.7 \times 10^n$: purple ($n = 1$), blue ($n = 2$), red ($n = 3$), dark green ($n = 4$), light green ($n = 5$). In the left plot we see the build up of intermediate scaling regions as Γ/k increases with scaling behaviour governed by the spectral functions $\mathrm{Im}\mathcal{G}_I^R(\omega) \sim \omega^{7/5}$ and $\mathrm{Im}\mathcal{G}_{II}^R(\omega) \sim \omega^5$ of the two hyperscaling violation geometries. The right plot shows the more stringent test of scaling behaviour by plotting the derivative of the logarithm.

the intermediate regions. This implies an interesting type of universality for the intermediate scaling behaviour of a wide class of operators, irrespective of their UV scaling dimensions, up to some maximum bound set by (5.22). This is analogous to the universal scaling behaviour seen in standard RG flows in the far IR as $\omega \to 0$.

Furthermore, similar comments apply to scalar modes with different couplings to the background fields. For example, to illustrate the impact of different couplings, consider replacing the constant m^2 in (5.19) with an r-dependent term $m^2(r)$. If $m^2(r)$ is still sub-dominant to the other term in the Schrödinger potential there will be the same kind of universality in the intermediate scaling behaviour. Alternatively, it may be possible to have top-down couplings in which $m^2(r)$ is the dominant term in an intermediate scaling region which would again lead to intermediate scaling of the spectral function, but not with the same kind of universality.

To conclude this section, we would like to highlight one more interesting feature of the spectral functions displayed in figure 5.6, independent of the intermediate scaling. For both the $\Delta = 2$ quantisation and the $\Delta = 1$ quantisation we have $\mathrm{Im}G^R(\omega) \propto \omega$

as $\omega \to 0$ when $\Gamma/k \neq 0$. Indeed this is an example of the standard universal scaling in the far IR of RG flows that we mentioned above. Now, for the $\Delta = 2$ quantisation we also have $\mathrm{Im}G^R(\omega) \propto \omega$ as $\omega \to \infty$. For this case, as the lattice deformation is switched off, $\Gamma/k \to 0$, we continuously approach the AdS_4 result $\mathrm{Im}G^R(\omega) \sim \omega$ for all ω. On the other hand for $\Delta = 1$ quantisation, we have $\mathrm{Im}G^R(\omega) \propto \omega$ as $\omega \to 0$, but $\mathrm{Im}G^R(\omega) \propto \omega^{-1}$ as $\omega \to \infty$. This implies that $\mathrm{Im}G^R(\omega)$ has a maximum for some value of ω, as we see in figure 5.6. Furthermore, as $\Gamma/k \to 0$ this peak gets pushed closer and closer to $\omega \to 0$ and we do not continuously approach the AdS_4 result of $\mathrm{Im}G^R(\omega) \sim \omega^{-1}$ for all ω. It would be interesting to study this feature in more detail.

5.5 | Final Comments

In this chapter we have constructed a novel class of RG flows of $N = 2$ STU gauged supergravity theory that can be uplifted on the seven sphere to obtain solutions of $D = 11$ supergravity. The solutions break translations, periodically, in both spatial directions. The solutions flow from AdS_4 in the UV to the same AdS_4 in the IR and on the way to the IR, for large enough deformations, they approach two distinct intermediate scaling regimes with hyperscaling violation. It would be interesting to understand these novel RG flows directly from the dual field theory[8]. In this context the RG flows are driven by deformations of certain scalar and fermion bilinear operators of the dual CFT, with a specific periodic dependence on the spatial coordinates governed by a single wavenumber. The intermediate scaling that we have seen is associated with a class of deformations of the dual CFT within the framework of a Q-lattice construction. It would be interesting to determine whether this behaviour persists for more general deformations, by solving the associated partial differential equations.

We also constructed some finite temperature black hole solutions which lead to the RG flows in the $T \to 0$ limit. As we explained, these black hole solutions are associated with a thermodynamic ensemble of the dual field theory in which we hold fixed the deformation parameters of the pseudoscalar operators and the expectation values of the scalar operators. It is for this particular ensemble that we are able to construct the black hole solutions by solving a system of ODEs. It would be interesting to construct solutions in which the deformations of both sets of operators are held fixed, but to do this one will have to consider a more general ansatz and

---

[8]Of course, here we are implicitly assuming that if there are any other RG solutions of $D = 11$ supergravity with the same asymptotic boundary deformations then the ones we have constructed have the smallest free energy. It would be interesting to examine this issue in more detail: an analogous investigation at finite charge density was initiated in [112].

solve a system of partial differential equations. At this stage it is not clear to us whether the intermediate scaling that we have observed at $T = 0$ will persist for finite T in this other ensemble.

We have shown that for large enough deformations the spectral functions of certain scalar operators also exhibit scaling behaviour that is associated with the two intermediate scaling regimes, for certain intermediate values of frequency. Moreover, this intermediate scaling behaviour is independent of the mass of the bulk scalar field and hence independent of the conformal dimension of the scalar operator in the dual field theory. Another interesting feature is that the scaling of the spectral function governed by the hyperscaling violation solution can exist for a certain range of intermediate frequencies, even if the hyperscaling violation solution exhibits unstable behaviour for other frequencies.

It would be interesting to extend these investigations and calculate the thermoelectric conductivity for the solutions we have constructed. As usual this involves analysing perturbations of the metric and gauge-fields about the solutions with prescribed boundary conditions. However, there is an intricate coupling between the gauge-fields and the scalar and pseudoscalar fields, parametrised by the matrix $\mathcal{M}$ in (C.1), and as a consequence it will be a somewhat involved task to calculate the conductivities, unlike for other Q-lattices. In general, the thermoelectric DC conductivity can be obtained by solving Navier-Stokes equations on the black hole horizon [92]. For certain Q-lattice constructions these equations can be solved explicitly in terms of the horizon data [71, 91, 93]. Here, however, due to the coupling $\mathcal{M}$ it appears that this will not be the case and one will need to solve partial differential equations on the horizon.

We have argued that at least for Q-lattice constructions which involve relevant operators governed by a dimensionless parameter Γ/k, the appearance of a Poincaré invariant intermediate scaling regime should appear for large values of Γ/k. For example, using (5.2) we can construct anisotropic Q-lattices using just the fields λ_2, σ_2 with $\lambda_3 = \sigma_3 = 0$. Although we have not checked the details, it seems very likely that there will be an intermediate scaling regime governed by the same $k = 0$ flow that we discussed in section 5.3.1. Furthermore, it seems unlikely that this Q-lattice construction will have a second intermediate scaling regime. More generally, it is possible to make similar constructions in which the intermediate scaling regime is governed by an AdS fixed point [3].

The Q-lattice constructions of this chapter used a very specific global symmetry of the maximally supersymmetric $N = 8$ gauged supergravity theory. The 70 scalars of this theory parametrise the coset $E_{7(7)}/SU(8)$ and we utilised a specific truncation that kept scalars parametrising two $SL(2)/SO(2)$ factors in $E_{7(7)}/SU(8)$.

Furthermore, we exploited the fact that the scalar potential was invariant under $SO(2)^2$ and this was utilised to construct our Q-lattice ansatz. There are clearly many more Q-lattice constructions that could be made in the $N = 8$ theory and it would be interesting to explore their properties. For example, one specific avenue is to utilise the consistent truncations[9] that keep a single $SL(2)/SO(2)$ factor that were discussed in [113].

The solutions we have constructed all have vanishing gauge-fields and are associated with vanishing charge density in the dual field theory. Some of the analogous type IIB anisotropic flows that we discussed in the introduction have been generalised to finite charge density in [76, 100] using a straightforward consistent truncation. However, it is less clear how to add charge to the solutions that we have constructed with an isotropic metric in the spatial directions of the field theory. In appendix C we have identified a simple ansatz that is suitable for constructing charged solutions that are spatially anisotropic. Although our analysis has not been comprehensive, the constructions of some anisotropic RG flows that we have made did not reveal intermediate scaling behaviour. We think it would be worthwhile to investigate these charged solutions more systematically as well as looking for charged isotropic solutions.

---

[9]These truncations were used in [113] to construct supersymmetric Janus solutions. While the underlying physical set-up is different, it would be interesting to investigate whether there is any relationship with Q-lattice constructions of boomerang RG flows in some putative limit.

6 | Boomerang RG flows with intermediate conformal invariance

6.1 | Introduction

A boomerang RG flow starts at an RG fixed point in the UV and then flows to exactly the same RG fixed point in the IR [2]. A particularly interesting realisation is when the RG fixed point is conformally invariant. In this context, in order to be consistent with either the letter or the spirit of c-theorems, the deformations of the UV fixed point which are driving the RG flow should necessarily break Poincaré invariance.

The boomerang RG flows studied in [1, 2, 77, 78] all involve deformations with a single spatial Fourier mode and, for small enough deformations, a perturbative expansion can be used to argue for the existence of boomerang flows. Indeed, the perturbative deformation of the bulk field that is dual to the deforming operator exponentially dies out near the Poincaré horizon and hence is not expected[1] to modify the IR. An interesting feature of the specific top-down examples constructed in the previous chapters and in [2] is that the boomerang flows actually persist for arbitrarily large deformations, which *a priori*, is not guaranteed. Furthermore, it is particularly interesting that for sufficiently large deformations the boomerang flows [1, 2, 78] exhibit one or more intermediate scaling regimes, where the solution approaches, somewhere in the bulk, a configuration with scaling properties. In the constructions of [1], which involved deformations of the axion and dilaton in the context of $AdS_5 \times X_5$ solutions of type IIB supergravity, the intermediate scaling is dominated by a fixed point solution with Lifshitz-like scaling [73]. By contrast, the constructions in [2] were made in the context of $D = 11$ supergravity and are of relevance to ABJM theory. In these examples, for large enough deformations, the boomerang flows approach two intermediate scaling regimes in succession, each associated with hyperscaling violation.

The original aim of this chapter was to construct boomerang RG flows in $D = 5$ which have an intermediate scaling regime governed by another AdS_5 factor associated with approximate $d = 4$ conformal invariance. We have not yet been able to find

---

[1]A subtlety is that one needs to check that the expansion does not generate constant Fourier modes which can change the IR.

top-down examples but, as we will see, it is quite straightforward to construct bottom-up examples. As in [1, 2], we will utilise a Q-lattice construction [60] in which we exploit a global symmetry of the bulk spacetime in order to develop an ansatz for the bulk fields in which the dependence on the spatial directions of the CFT is solved exactly. This leads to a system of ordinary differential equations for a set of functions that just depend on the holographic radial coordinate which are then amenable to straightforward numerical integration.

A key ingredient in our construction is to have a bulk theory that admits a Poincaré invariant domain wall solution that flows between AdS_5^0 in the UV and another AdS_5^c in the IR. We demand that this domain wall flow is driven by deformations of relevant operators in the UV CFT, with scaling dimension Δ, and hence is parametrised by a dimensionful parameter Γ. By conformal invariance all values of Γ are physically equivalent for these Poincaré invariant RG flows. Within a Q-lattice ansatz, we then consider deformations by the same relevant operators which also have a dependence on the spatial directions of the CFT, parametrised by a wave number k. This gives rise to a one parameter family of associated RG flows, parametrised by a dimensionless number $\Gamma/k^{4-\Delta}$. For small values of $\Gamma/k^{4-\Delta}$ we can easily show that we must have boomerang RG flows using a perturbative construction. For larger values of $\Gamma/k^{4-\Delta}$ the existence of the boomerang flows must be established numerically. When they do exist, though, since large values of $\Gamma/k^{4-\Delta}$ can be achieved by holding Γ fixed and taking $k \to 0$, one can expect that the boomerang RG flows should start to track the Poincaré invariant flow and hence exhibit an intermediate scaling regime with conformal invariance that is governed by the AdS_5^c fixed point solution.

For holographic RG flows with intermediate scaling regimes, which have also been extensively studied in other contexts (e.g. [65, 79–81, 83, 114]), it is of interest to investigate to what extent the scaling regime imprints itself on the scaling behaviour of physical observables. For example, one might expect that the spectral weight of operators as a function of frequency, ω, should exhibit scaling for a range of ω dictated by the range of the radial region of the RG flow which has intermediate scaling. This issue was discussed in [2] using matching arguments (for a related discussion see [82]). It was shown that while intermediate scaling behaviour is not guaranteed it will manifest itself providing sufficient conditions on the effective potential for the bulk fluctuations about the RG flow solutions are met [2]. In this chapter we make a complementary discussion by examining how the holographic entanglement entropy behaves for the new boomerang RG flows. In particular, by calculating the entanglement entropy of a strip geometry of width l, we analyse the behaviour of the entropic 'c-function', $C(l)$ [14, 115, 116] (see also [117]). While $C(l)$ is not monotonic along the boomerang flow, as it is for Poincaré invariant RG flows, it does effectively encapsulate the correct scaling of the degrees of freedom of CFT

in the UV and IR as well as the CFT in the intermediate scaling regime.

We will study a class of $D = 5$ models with a quartic potential for the scalar fields that depend on two real parameters. The constructions summarised above are for certain values of the parameters, such that the models admit both the AdS_5^0 vacuum and also the AdS_5^c solution (in fact there will be two AdS_5^c related by a $\mathbb{Z}_2$ symmetry). Interestingly, for different values of the parameters there is no longer an AdS_5^c solution but there is an $AdS_2 \times \mathbb{R}^3$ solution which breaks translations in all of the spatial directions.

In the second part of the chapter, starting in section 6.5, we will investigate models with boomerang flows that have intermediate scaling governed by such locally quantum critical $AdS_2 \times \mathbb{R}^3$ solutions. While there are some similarities to the previous constructions there are also some interesting differences. The RG flows from AdS_5^0 in the UV to $AdS_2 \times \mathbb{R}^3$ in the IR now exist for a specific value of the dimensionless deformation parameter $\Gamma/k^{4-\Delta} \equiv \bar{\Gamma}$. Focussing on a specific model, we find that the boomerang RG flows only exist in the range $0 \leq \Gamma/k^{4-\Delta} \leq \bar{\Gamma}$, and moreover, have increasingly large intermediate scaling behaviour determined by the $AdS_2 \times \mathbb{R}^3$ solution as $\Gamma/k^{4-\Delta} \to \bar{\Gamma}$. In order to understand the RG flows for $\Gamma/k^{4-\Delta} > \bar{\Gamma}$ we construct finite temperature black holes and then cool them down to very low temperatures. This investigation reveals an interesting phase diagram schematically presented in figure 6.1. For a range of $\Gamma/k^{4-\Delta} \leq \bar{\Gamma}$ there is a line of first order phase transitions ending on the $AdS_2 \times \mathbb{R}^3$ fixed point at $T = 0$ and on a finite temperature critical point. Furthermore, the $T = 0$ ground states for $\Gamma/k^{4-\Delta} > \bar{\Gamma}$ are singular[2] and, by calculating the behaviour of the thermal DC conductivity, κ, as a function of temperature, we conclude that they are thermally insulating ground states.

The behaviour of the entropy as a function of temperature is not a power law for the new insulating ground states, in contrast to those constructed in [69, 71, 72, 118]. This in itself makes them worthy of further study. One additional calculation that we carry out here is motivated by the various investigations aiming to elucidate universal connections between diffusion and quantum chaos in holography [119–121] (see also [122–134]). We determine the thermal diffusion constant, D, using the Einstein relation $D \equiv \kappa/c$, where c is the specific heat. We also calculate the butterfly velocity, v_B, by analysing a shockwave on the black hole solution as in [135, 136] (see also [137]). Remarkably, we find

$$D = E \frac{v_B^2}{2\pi T} \, , \tag{6.1}$$

---

[2]Since these ground states are obtained by cooling down black hole solutions, they are necessarily "good singularities" in the sense of [109].
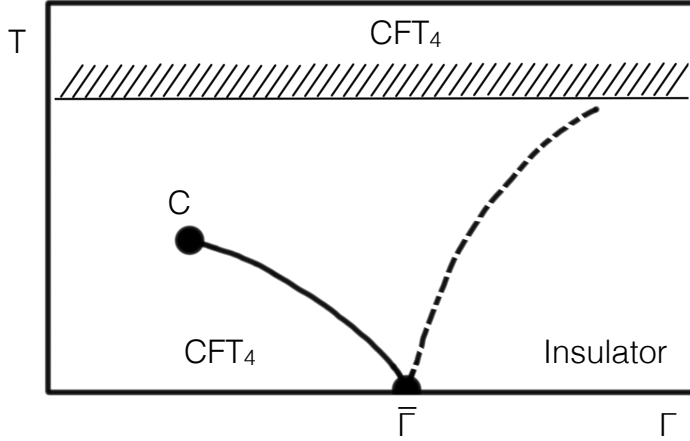
Figure 6.1: Schematic phase diagram as a function of the deformation parameter Γ for models with $m^2 = -15/4$, $\xi = -1/4$ discussed in section 6.5. The $T = 0$ ground states are RG flows from AdS_5 in the UV, dual to some CFT$_4$, to various behaviours in the IR: for $\Gamma < \bar{\Gamma}$ we have AdS_5 (boomerang RG flows), for $\Gamma = \bar{\Gamma}$ we have $AdS_2 \times \mathbb{R}^3$ (locally quantum critical ground states), and for $\Gamma > \bar{\Gamma}$ we have singular thermal insulating behaviour. There is line of first order phase transitions that end in the critical point C. Intermediate scaling governed by the $AdS_2 \times \mathbb{R}^3$ solution is present in the quantum critical wedge bounded by the first order line and the dashed line. For high temperatures the scaling is fixed by the AdS_5 solution in the UV.

with the dimensionless quantity $E(T) \to 0.5$ as $T \to 0$. This is the first example of such a relationship for ground states without power law behaviour. We have also made some other constructions for models with slightly different parameters[3] to those in figure 6.1, again finding insulating ground states with E unchanged.

6.2 | General set up

Consider an action in $D = 5$ spacetime dimensions of the form

$$S = \frac{1}{16\pi G} \int \mathrm{d}^5 x \sqrt{-g} \left(R + 12 + \mathcal{L}_z \right), \tag{6.2}$$

where $\mathcal{L}_z$ describes a sigma model for three complex scalars z^α. In order to construct the Q-lattice solutions of interest, we will take $\mathcal{L}_z$ to have a $U(1)^3$ global symmetry and consider

$$\mathcal{L}_z = \sum_\alpha \left(-\frac{1}{2} \partial_\mu z^\alpha \partial^\mu \bar{z}^{\bar{\alpha}} - \frac{1}{2} m^2 z^\alpha \bar{z}^{\bar{\alpha}} - \frac{1}{3} \xi \, (z^\alpha \bar{z}^{\bar{\alpha}})^2 \right), \tag{6.3}$$

---

[3]For certain models we also find a novel non-uniqueness of the boomerang RG flows which we discuss in appendix D.1.

where m^2, ξ are two free parameters. The equations of motion admit a unit radius AdS_5^0 vacuum solution with $z^\alpha = 0$ which is dual to a CFT in $d = 4$. In these units $1/16\pi G$ is a measure of the number of degrees of freedom in the dual CFT, scaling like N^2, at large N. In a slight abuse of notation we will set factors of $16\pi G$ to unity in the following since this simplifies some formulae and the factors can easily be reinstated in physical quantities as needed.

We are interested in studying specific isotropic deformations of this CFT that break translations in three spatial directions. To do this we exploit the $U(1)^3$ global symmetry and consider the Q-lattice ansatz

$$\mathrm{d}s^2 = -g(r)e^{-\chi(r)}\mathrm{d}t^2 + \frac{\mathrm{d}r^2}{g(r)} + r^2 dx^\alpha dx^\alpha \,,$$
$$z^\alpha = \gamma(r)e^{ik\,x^\alpha} \,, \tag{6.4}$$

where $x^\alpha \in \{x, y, z\}$ are the spatial directions of the field theory. Notice that a simultaneous translation and a $U(1)^3$ transformation preserves this ansatz. The associated equations of motion are given by

$$0 = \chi' + r\,\gamma'^2 \,,$$
$$0 = g' + g\left(\frac{1}{2}r\gamma'^2 + \frac{2}{r}\right) + \gamma^2\frac{(k^2 + m^2r^2)}{2r} + \frac{1}{3}\xi r\gamma^4 - 4r \,,$$
$$0 = \gamma'' + \gamma'\left(\frac{g'}{g} - \frac{\chi'}{2} + \frac{3}{r}\right) - \gamma\frac{(m^2r^2 + k^2)}{r^2g} - \frac{4\xi\gamma^3}{3g} \,. \tag{6.5}$$

In sections[4] 6.2-6.4, we will be focussing on boomerang flows from AdS_5^0 in the UV to AdS_5^0 in the IR that have an intermediate scaling behaviour governed by a different AdS_5 solution. We will choose the parameters m^2, ξ so that there are, in fact, three stable AdS_5 solutions with constant γ (and all with $k = 0$). Writing the AdS_5 metric in Poincaré coordinates as

$$\mathrm{d}s^2 = -r^2\mathrm{d}t^2 + r^2\mathrm{d}\vec{x}^2 + \frac{L^2}{r^2}\mathrm{d}r^2 \,, \tag{6.6}$$

the UV AdS_5 vacuum solution, which we call AdS_5^0, has

$$L_0^2 = 1 \qquad \text{and} \qquad \gamma_0 = 0 \,, \tag{6.7}$$

---

[4]In section 6.5 we will consider boomerang flows with an intermediate $AdS_2 \times \mathbb{R}^3$ solution and it is convenient to use a different radial coordinate to that of (6.4).

while the other two AdS_5 solutions, which we call AdS_5^c, have

$$L_c^2 = \frac{64\xi}{3m^4 + 64\xi} \qquad \text{and} \qquad \gamma_c = \pm\sqrt{\frac{-3m^2}{4\xi}}\,. \tag{6.8}$$

In order to have suitable relevant and irrelevant scalar operators in the UV and IR, with conformal dimensions Δ_0 and Δ_c, respectively, we demand that

$$\Delta_0 \equiv 2 + \sqrt{4 + m^2} < 4\,, \qquad \Delta_c \equiv 2 + \sqrt{4 - 2m^2 L_c^2} > 4\,. \tag{6.9}$$

In sections 6.2-6.4 we will focus the specific values of m, ξ given by

$$m^2 = -15/4\,, \qquad \xi = 675/512\,, \tag{6.10}$$

corresponding to having a relevant scalar operator with dimension[5] $\Delta_0 = 5/2$ in the CFT dual to the AdS_5^0 UV vacuum and an irrelevant scalar operator with dimension $\Delta_c = 5$ in the CFT dual to AdS_5^c. Furthermore, for the AdS_5^c vacuum we have $L_c^2 = 2/3$ and $\gamma_c = \pm(32/15)^{1/2}$.

6.2.1 Poincaré invariant domain wall flows: $AdS_5^0 \to AdS_5^c$

With the set up just described there are standard Poincaré invariant domain wall solutions, with $k = 0$ in (6.4), that approach the unit radius AdS_5^0 vacuum solution in the UV and then approach one of the two AdS_5^c solutions (6.8) in the IR. As there is a $\mathbb{Z}_2$ symmetry relating these IR vacua, without loss of generality we can focus on the solution with positive γ_c.

In the UV, as $r \to \infty$, the solutions have a radial expansion of the form

$$g = r^2 + \dots \qquad \chi = \chi_{UV} + \dots \qquad \gamma = \Gamma r^{\Delta_0 - 4} + \dots\,, \tag{6.11}$$

and we set $\chi_{UV} = 0$. In the IR, as $r \to 0$, we have the expansion

$$g = \frac{r^2}{L_c^2} + \dots \qquad \chi = \chi_0 + \dots \qquad \gamma = \gamma_c + f_0 r^{\Delta_c - 4} + \dots\,. \tag{6.12}$$

The boundary conditions (6.11) are associated with deformations of the CFT dual to AdS_5^0, parametrised by Γ, using the real parts of the three operators $\mathcal{O}_\alpha$ that are dual to the three complex scalars z^α. Note that within the ansatz (6.4), with $k = 0$, the deformation of all three operators are the same. There are additional domain wall solutions flowing to the same AdS_5^c solution in the IR that lie outside this ansatz,

---

[5]Note that, with this value of m^2 we can also, if we wish, do an alternative quantisation of the scalar field leading to $\Delta = 3/2$ [138].

but they will not play a role in the sequel. We also note that by conformal invariance, the $k = 0$ domain walls with different values of Γ are all physically equivalent.

We have explicitly constructed these domain wall solutions, for the specific values of m^2, ξ given in (6.10), using numerical shooting techniques. We did this both by shooting from the UV and the IR and then matching at an intermediate point, as well as shooting out just from the IR[6], with excellent numerical agreement.

6.3 | Boomerang RG Flows

We now want to consider RG flows, with $k \neq 0$ in the ansatz (6.4), that are seeded by deformations of the UV CFT by relevant operators which break translation invariance. Imposing the boundary conditions (6.11) in the UV now corresponds to deformations of the real and imaginary parts of the operators $\mathcal{O}_\alpha$ having spatial modulation of the form $\cos kx$ and $\sin kx$, respectively. For the specific values of m, ξ given earlier, with $\Delta_0 = 5/2$, we deduce that there is a one-parameter family of RG flows that are parametrised by the dimensionless number $\Gamma/k^{3/2}$.

6.3.1 Perturbative Analysis

For $\Gamma/k^{3/2} \ll 1$, it is straightforward to argue that the RG flows must be boomerang flows, returning to the same AdS_5^0 vacuum (with $\gamma = 0$) in the IR. Indeed we can construct the RG flows in a perturbative expansion about the AdS_5^0 vacuum solution. Starting with the linearised scalar equation of motion in the AdS_5^0 vacuum, we find that the leading order solution that satisfies the UV boundary conditions and is regular at $r = 0$, is of the form

$$\gamma = \frac{k^{3/2}}{r^{3/2}} e^{-k/r} \left(\frac{\Gamma}{k^{3/2}} \right) + \dots . \tag{6.13}$$

This solution back reacts on the metric at order $(\Gamma/k^{3/2})^2$ and the explicit form of the metric functions, satisfying the correct UV boundary conditions, are given at this order by

$$g = r^2 \left[1 - \frac{k^3}{r^3} e^{-2k/r} \frac{1}{4} \left(-3 + 2\frac{k}{r} \right) \left(\frac{\Gamma}{k^{3/2}} \right)^2 + \dots \right],$$

$$\chi = \frac{3}{16} \left(\frac{\Gamma}{k^{3/2}} \right)^2 - e^{-2k/r} \frac{1}{16} \left(3 + 6\frac{k}{r} + 6\frac{k^2}{r^2} - 8\frac{k^3}{r^3} + 8\frac{k^4}{r^4} \right) \left(\frac{\Gamma}{k^{3/2}} \right)^2 + \dots . \tag{6.14}$$

---

[6]In this approach the solutions generically reach the UV with non-vanishing constant parameter $\chi \to \chi_{UV}$, as $r \to \infty$, so a simple rescaling of the time coordinate is necessary to bring the asymptotic metric to the canonical form (6.6).

It is clear that in the IR as $r \to 0$, the metric exponentially approaches exactly the same AdS_5^0 solution as the UV, with the scale of approach set by k. The only difference is that there is a renormalisation of length scales, which is captured by the 'index of refraction' n [108] defined by

$$n \equiv e^{\frac{1}{2}(\chi_{IR} - \chi_{UV})} . \tag{6.15}$$

At leading order in the expansion we immediately deduce that

$$n = 1 + \frac{3}{32} \left(\frac{\Gamma}{k^{3/2}} \right)^2 + \dots . \tag{6.16}$$

That the index of refraction is bigger than one is an example of a more general result. Indeed returning to the equations of motion (6.5) we immediately deduce that $\chi' \leq 0$ and hence $\chi_{IR} \geq \chi_{UV}$, with the equality realised only for flows in which the scalar does not run.

6.3.2 Numerical Boomerang Flows

To determine what happens for larger values of $\Gamma/k^{3/2}$ we need to construct the solutions numerically. In the IR we develop the expansion

$$g = r^2 \left[1 - \frac{k^3}{r^3} e^{-2k/r} \frac{1}{4} \left(-3 + 2\frac{k}{r} \right) \left(\frac{C_\gamma}{k^{3/2}} \right)^2 + \dots \right] ,$$

$$\chi = \chi_0 - e^{-2k/r} \frac{1}{16} \left(3 + 6\frac{k}{r} + 6\frac{k^2}{r^2} - 8\frac{k^3}{r^3} + 8\frac{k^4}{r^4} \right) \left(\frac{C_\gamma}{k^{3/2}} \right)^2 + \dots ,$$

$$\gamma = \frac{k^{3/2}}{r^{3/2}} e^{-k/r} \left(\frac{C_\gamma}{k^{3/2}} \right) + \dots , \tag{6.17}$$

where C_γ, χ_0 are constants, and demand that the solutions match onto the UV boundary conditions (6.11). In the range $0 < \Gamma/k^{3/2} < 10^7$ we find that the RG flows are always boomerang flows, returning to the same AdS_5^0 in the IR. Furthermore, we have no reason to suspect that this behaviour will not persist for larger values of $\Gamma/k^{3/2}$. In figure 5.10 we have presented the index of refraction n for the flows. For small values of $\Gamma/k^{3/2}$ we recover the behaviour (6.16), as expected. For very large $\Gamma/k^{3/2}$ we find that n appears[7] to asymptote to a constant, with $n \sim 2.09$.

For sufficiently large $\Gamma/k^{3/2}$, the boomerang RG flow solutions start to exhibit intermediate scaling. Indeed, moving in from the UV, the solutions start to track the Poincaré invariant RG flow solutions with $k = 0$, for a range of the radial variable,

---

[7]This can be contrasted with the $D = 4$ boomerang flows constructed in [2], where it was unbounded.
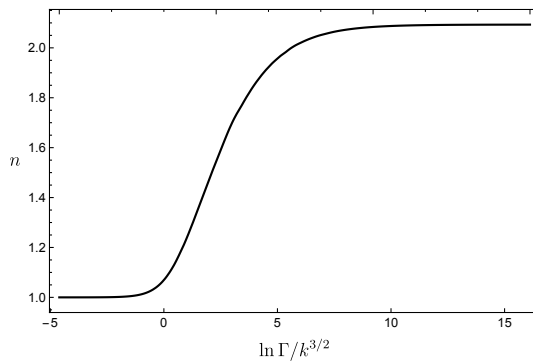
Figure 6.2: Plot of the refractive index n, defined in (6.15), as a function of the dimensionless deformation parameter $\Gamma/k^{3/2}$, for boomerang RG flows with $m^2 = -15/4$ and $\xi = 675/512$.

including a region where the geometry approaches the AdS_5^c solution, before heading off back to the original AdS_5^0 solution in the deep IR. This behaviour is displayed for four representative flows with $\Gamma/k^{3/2} = 10^2, 10^4, 10^5$ and 10^7 in figure 6.3. In this figure one can see the solution being dominated by the AdS_5^c solution for an intermediate range of r/k which one can make parametrically large by increasing $\Gamma/k^{3/2}$. Notice that for very large values of $\Gamma/k^{3/2}$, the function χ starts to take a kind of 'sliding' form, in which the only significant difference is the radial position in which χ increases to the first plateau. This behaviour gives rise to the asymptotic behaviour of n, but we have not been able to find a way to analytically extract the asymptotic value of n as $\Gamma/k^{3/2} \to \infty$.

6.4 | Entanglement Entropy

We now investigate how the intermediate scaling regime of the boomerang flows manifests itself in the entanglement entropy. Specifically we focus on calculating the holographic entanglement entropy for a "strip geometry" of width l in the x direction [139, 140]. We take a constant time slice and calculate the area, $\mathcal{A}$, of the minimal two-dimensional surface that is anchored to the strip on the boundary. The entanglement entropy, $\mathcal{S}_{\mathcal{A}}$, is then given by

$$\mathcal{S}_{\mathcal{A}} = 4\pi\mathcal{A}. \tag{6.18}$$

A standard calculation shows that the area can be expressed as

$$\mathcal{A} = \frac{2W^2}{r_\star{}^3} \int_{r_\star}^{\Lambda} \frac{r^5}{\sqrt{g\left(\frac{r^6}{r_\star{}^6} - 1\right)}} \mathrm{d}r\,, \tag{6.19}$$
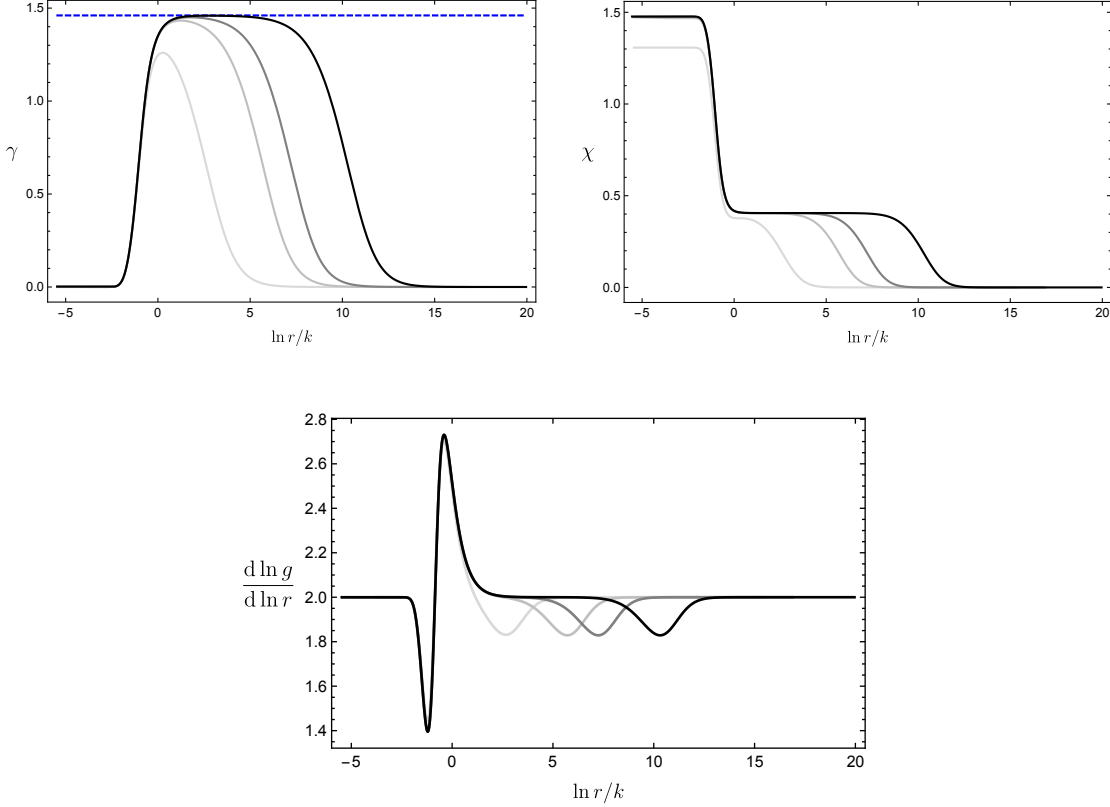
Figure 6.3: Boomerang RG flows with $\Gamma/k^{3/2} = 10^2$ (lightest), $10^4, 10^5$ and 10^7 (darkest) showing the build up of intermediate conformal invariance. The blue dashed line in the upper left plot shows the value of the scalar in the AdS_5^c solution, with $\gamma_c = \sqrt{32/15}$. The plots clearly reveal an intermediate scaling region, dominated by the AdS_5^c vacuum. The plots are for $m^2 = -15/4$ and $\xi = 675/512$.

where W^2 is the area of the boundary strip in the y, z, directions. We have integrated from a minimum radial position of the surface at $r_\star$ to a UV cut-off Λ, which will eventually be taken to infinity. We can relate r_* to l via the formula

$$l = 2 \int_{r_\star}^{\Lambda} \frac{\mathrm{d}r}{r\sqrt{g\left(\frac{r^6}{r_\star{}^6} - 1\right)}} . \tag{6.20}$$

At this point, setting $g = r^2/L^2$, we can easily recover the AdS_5 result of [139, 140]

$$\frac{\mathcal{A}}{L^3} = \Lambda^2 \frac{W^2}{L^2} - b\left(\frac{W}{l}\right)^2 . \tag{6.21}$$

where $b = 4\pi^{3/2} \left(\frac{\Gamma(\frac{2}{3})}{\Gamma(\frac{1}{6})}\right)^3$. Note that in the limit $\Lambda \to \infty$ the area of the minimal surface displays the expected UV divergence. As this term is scheme dependent, it is natural to define the renormalised entanglement entropy, $\bar{\mathcal{S}}_A$, after subtracting off the UV divergence, as $\bar{\mathcal{S}}_A = 4\pi(\mathcal{A} - \Lambda^2 W^2 L_0)$, and then take $\Lambda \to \infty$.

The expression (6.21) also motivates the definition of the so-called "entropic

c-function", defined for general bulk geometries via [115]

$$C(l) = \frac{l^3}{W^2} \frac{\mathrm{d}\mathcal{S}_\mathcal{A}}{\mathrm{d}l}.$$

(6.22)

In particular, for a bulk AdS_5 solution with radius L, we see that $C(l) = 8\pi b L^3 \approx 8.06L^3$ and hence, as it is proportional to the a central charge of the dual CFT, provides a measure for the number of degrees of freedom in the dual CFT. Furthermore, for Poincaré invariant RG flows, it has been shown that within two derivative gravity and with matter satisfying the null energy condition, $C(l)$ monotonically decreases along the RG flow [116].

We now want to investigate $\bar{\mathcal{S}}_\mathcal{A}$ and $C(l)$ for the Poincaré invariant domain wall and the boomerang RG flows. A preliminary issue is to first check whether the flows introduce any additional UV divergences into the calculation of the minimal area. This would be the case if, for example, there was a constant term g_0 in the near boundary expansion $g \approx r^2 + g_0 + O(1/r)$. For the specific values of $m^2 = -15/4$, $\xi = 675/512$, it is straightforward to demonstrate that the Einstein equations require $g_0 = 0$. Thus, when constructing a renormalised entanglement entropy from the numerical data we need only to account for the quadratic "area law" divergence of pure AdS_5.

We next discuss the Poincaré invariant $AdS_5^0 \to AdS_5^c$ domain wall solutions. For the usual values of $m^2 = -15/4$, $\xi = 675/512$, our results for $\bar{\mathcal{S}}_\mathcal{A}$ and $C(l)$ are shown in figure 6.4. Notice that for very large values of l, where the minimal surface is dipping deep into the AdS_5^c geometry in the IR, $\bar{\mathcal{S}}_\mathcal{A}$ is not falling off with increasing l but instead asymptotes to a constant negative value. This behaviour was first observed for Poincaré invariant domain wall solutions in [141]. Further insight into this phenomenon was also provided in [141] by showing how this result is expected at least in the case of very thin domain wall solutions. Figure 6.4 also shows that the entropic c-function $C(l)$ is a monotonically decreasing function of l, as expected, interpolating between the AdS_5^0 result, $C(l) \to 8\pi b L_0^3 \sim 8.06$, as $l \to 0$ and the AdS_5^c result, $C(l) \to 8\pi b L_c^3 \sim 4.39$, as $l \to \infty$.

Finally, we turn to the boomerang RG flows, and our main results are shown in figure 6.5. For a given RG flow, labelled by $\Gamma/k^{3/2}$, the entanglement entropy looks qualitatively similar to the Poincaré invariant domain wall solution: it is always negative and asymptotically approaches a negative constant for large l. For small values of $\Gamma/k^{3/2}$ we can easily understand this behaviour using the perturbative solutions given in (6.13),(6.14). Explicitly, starting from (6.14), writing $g = r^2 +$
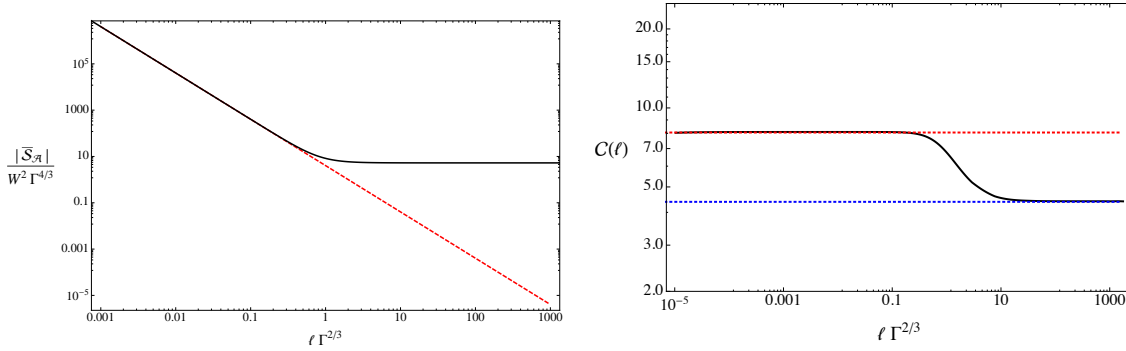
Figure 6.4: The entanglement entropy $\bar{\mathcal{S}}_{\mathcal{A}}$ (left) and entropic c-function $C(l)$ (right) evaluated in the $AdS_5^0 \to AdS_5^c$ domain wall flow. The pure AdS_5^0 results are shown as dashed red lines, and agree excellently with the numerically computed quantities for small values of l. The right plot shows that the entropic c-function $C(l)$ monotonically approaches the result for pure AdS_5^c (lower dashed, blue line) for large l.

$\Gamma^2 u(r) + \ldots$ and expanding the integrand in the scalar amplitude Γ yields

$$\mathcal{A} = \mathcal{A}_{AdS} - \frac{W^2}{r_\star^3}\Gamma^2 \int_{r_\star}^{\Lambda} \frac{r^2}{\sqrt{\frac{r^6}{r_\star^6} - 1}} u(r)\, \mathrm{d}r\,, \tag{6.23}$$

where $\mathcal{A}_{AdS}$ is the AdS_5^0 result, and the second term, which is finite in the limit $\Lambda \to \infty$, thus contains the entire finite contribution at large strip width. To isolate the relevant part of the integral, we next turn our attention to the small $r_\star$ behaviour of the second term in (6.23), since small $r_\star$ corresponds to large strip width in these backgrounds. The area in this limit is given by

$$\mathcal{A} = \mathcal{A}_{AdS} + \frac{W^2 k^3}{4}\left(\frac{\Gamma}{k^{3/2}}\right)^2 \int_{r_\star \to 0}^{\infty} \frac{e^{-2k/r}}{r^3}(2k - 3r)\mathrm{d}r\,, \tag{6.24}$$

and hence the renormalised strip entanglement entropy evaluated in the perturbative RG flows asymptotes to

$$\bar{\mathcal{S}}_{\mathcal{A}} \to -\pi W^2 k^2 \left(\frac{\Gamma}{k^{3/2}}\right)^2\,, \tag{6.25}$$

at large strip width. This analytic prediction can be verified by comparing to the numerical results, and shows excellent agreement. As we increase $\Gamma/k^{3/2}$, we find that $\bar{\mathcal{S}}_{\mathcal{A}}$ is always negative and from figure 6.5 shows that it approaches an increasingly negative asymptotic value.

In figure 6.5 we see that in the boomerang RG flows the entropic c-function reveals additional interesting features. In the figure we have plotted $C(l)$ for the same value as in the boomerang flows of figure 6.3. For small values of l we see the expected L_0^3 behaviour of the AdS_5^0 solution with $C(l) \to 8\pi b L_0^3 \sim 8.06$, as $l \to 0$. At intermediate length scales, and for boomerang flows with intermediate scaling,

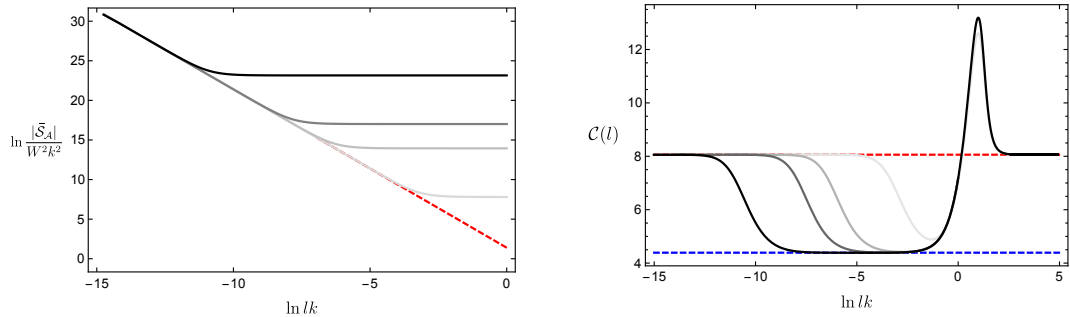**Figure 6.5:** The size of the entanglement entropy $|\bar{\mathcal{S}}_\mathcal{A}|$ (left) and the entropic c-function $C(l)$ (right) evaluated for the boomerang RG flows for $\Gamma/k^{3/2} = 10^2$ (lightest), $10^4, 10^5$ and 10^7 (darkest), as in figure 6.3. In the left plot, the pure AdS_5^0 result is a dashed red line. In the right plot, the pure AdS_5^0 and AdS_5^c results are given by the red and blue dashed lines, respectively.

the function dips to a second plateau, much like in the Poincaré invariant domain wall, with $C(l) \to 8\pi b L_c^3 \sim 4.39$ as one might have naively anticipated. Finally, far in the IR, the entropic c-function replicates the UV behaviour, as a consequence of the boomerang RG flow. Thus while $C(l)$ is certainly not a monotonic function along the RG flow, figure 6.5 shows that it does, nevertheless, provide a measure of the number of degrees of freedom in each of the three regions of the geometry where there is approximate conformal invariance, in the sense that for ranges of l it approaches the result for the corresponding AdS_5 geometry.

6.5 | Boomerang flows with intermediate $AdS_2 \times \mathbb{R}^3$ scaling and novel insulators

Within the same class of models (6.2), but for a different range of the parameters m^2 and ξ, we now investigate another interesting framework in which instead of a second AdS_5 solution there is now an $AdS_2 \times \mathbb{R}^3$ fixed point solution, which breaks translations. We will construct boomerang RG flows with locally quantum critical intermediate scaling, governed by the $AdS_2 \times \mathbb{R}^3$ solution, as well as novel ground states that are thermal insulators. It is illuminating to construct the associated black hole solutions describing the systems at finite temperature and, for the specific values $m^2 = -15/4$, $\xi = -1/4$, we find the phase diagram schematically shown in figure 6.1.

In this section (only) it will be convenient to use a slightly different radial variable

than that of (6.4) and consider the ansatz

$$ds^2 = -U dt^2 + U^{-1} d\rho^2 + e^{2V} dx^\alpha dx^\alpha \,,$$
$$z^\alpha = \gamma e^{ik\,x^\alpha} \,, \tag{6.26}$$

with U, V, γ functions of ρ. This ansatz can be used to construct both the RG flows and the black hole solutions. We start by noting that for certain parameter ranges, we can construct $AdS_2 \times \mathbb{R}^3$ solutions with $k \neq 0$, similar to the solutions discussed in the appendix of [60]. Specifically, we take $U = \rho^2/L_{(2)}^2$, $V = 0$, $\gamma = \gamma_{(2)}$ and

$$\gamma_{(2)}^2 = \frac{\sqrt{12}}{\sqrt{-\xi}}, \qquad k^2 = \frac{\sqrt{-\xi}}{\sqrt{3}L_{(2)}^2}, \qquad L_{(2)}^{-2} = 8 - \frac{m^2\sqrt{3}}{\sqrt{-\xi}} \,. \tag{6.27}$$

Clearly these solutions require models in which $\xi < 0$. Now recall from (6.9) that the requirement that there is a relevant scalar operator in the UV CFT with dimension $\Delta_0 < 4$, implies that $m^2 < 0$. From (6.8) we see that $m^2 < 0$ and $\xi < 0$ are not compatible with having the second AdS_5^c fixed point that we discussed in sections 6.2-6.4.

We next consider the spectrum of deformations about the $AdS_2 \times \mathbb{R}^3$ solution. Considering perturbations of the form

$$U = \frac{\rho^2}{L_{(2)}^2}(1 + c_1 \rho^\delta), \qquad V = c_2 \rho^\delta, \qquad \gamma = \gamma_{(2)}(1 + c_3 \rho^\delta), \tag{6.28}$$

with c_i constant, then we find an unpaired mode with $\delta = -1$, with $c_2 = c_3 = 0$, which simply corresponds to shifting r by a constant in the solution. We also find a pair of modes with $\delta = -2, 1$. The mode with $\delta = -2$ also has $c_2 = c_3 = 0$ and is associated with heating up the solution. The mode with $\delta = 1$ has $c_1 = (2/3 + 8L_{(2)}^2 + \frac{\sqrt{3}}{\sqrt{-\xi}})c_3$, $c_2 = -(8L_{(2)}^2 + \frac{\sqrt{3}}{\sqrt{-\xi}})c_3$. Finally there is another pair of modes with $\delta = -\frac{1}{2} \pm \frac{1}{2}[1 - \frac{64}{\sqrt{3}}L_{(2)}^2\sqrt{-\xi}]^{1/2}$ which have $c_2 = 0$ and c_1 related to c_3. Notice that there are BF violating modes in the AdS_2 solution when $\sqrt{-\xi} \geq \frac{\sqrt{3}}{16}(1 + (1 - 4m^2)^{1/2})$.

In the remainder of this section[8] we will focus on models with parameters given by

$$m^2 = -15/4 \,, \qquad \xi = -1/4 \,. \tag{6.29}$$

Choosing $m^2 = -15/4$ (as in previous sections) implies that the UV CFT dual to the AdS_5^0 vacuum has a relevant scalar operator with dimension $\Delta_0 = 5/2$. In this case there are BF violating modes of the AdS_2 solution when $\xi \leq -75/256 \sim -0.293$,

---

[8] In appendix D.1 we will briefly consider models with $\xi = -675/512 \sim -1.32$ which display some additional new features.

and hence they are absent for (6.29). The numerical constructions of the solutions described in the following subsections are similar to those in previous sections and so we have relegated some details to appendix D.

6.5.1 RG flows

We first consider RG flows which break spatial translations (i.e. with $k \neq 0$), starting from AdS_5^0 in the UV and going to the $AdS_2 \times \mathbb{R}^3$ solution in the IR, given by (6.27). Note that with the values of the parameters given in (6.29) the value of the scalar field in the $AdS_2 \times \mathbb{R}^3$ solution is $\gamma_{(2)} = 48^{1/4} \sim 2.63$. From the point of view of the IR, we use the $\delta = 1$ mode mentioned below (6.28) to shoot out from the $AdS_2 \times \mathbb{R}^3$ solution, as described in appendix D. For future reference we note that this mode is associated with an irrelevant operator in the CFT dual to $AdS_2 \times \mathbb{R}^3$ with $\Delta = 2$. These RG flows exist for a specific value of the dimensionless deformation parameter which is numerically found to be at $\Gamma/k^{3/2} = \bar{\Gamma}$, with

$$\bar{\Gamma} \sim 19.37 \,. \tag{6.30}$$

We next consider the boomerang RG flows starting from AdS_5^0 in the UV and ending up at the same AdS_5^0 in the IR. In the coordinates we are using the index of refraction is now given by

$$n = e^{V_{IR} - V_{UV}} \,. \tag{6.31}$$

In figure 6.6 we have plotted some features of the one parameter family of boomerang RG flows that we have constructed numerically, which, interestingly, exist in the finite range $0 \leq \Gamma/k^{3/2} \leq \bar{\Gamma}$. We find that as $\Gamma/k^{3/2}$ approaches $\bar{\Gamma}$ the boomerang RG flows start to build up an intermediate scaling regime governed by the $AdS_2 \times \mathbb{R}^3$ solution. We have also calculated the holographic free energy for these RG flows and we find that as $\Gamma/k^{3/2} \to \bar{\Gamma}$ we have $T^{tt}/k^4 \to 1614$, which is in excellent numerical agreement with the value of the free energy that we directly obtain for the AdS_5^0 to $AdS_2 \times \mathbb{R}^3$ RG flow.

While satisfying, this analysis does not reveal what happens for RG flows with $\Gamma/k^{3/2} > \bar{\Gamma}$. It turns out that these flows are singular in the far IR. In order to elucidate what is going on, we use the standard technique of constructing finite temperature black holes and then cooling them down to low temperatures. As we will see this will also reveal interesting features at finite T for $\Gamma/k^{3/2} < \bar{\Gamma}$.
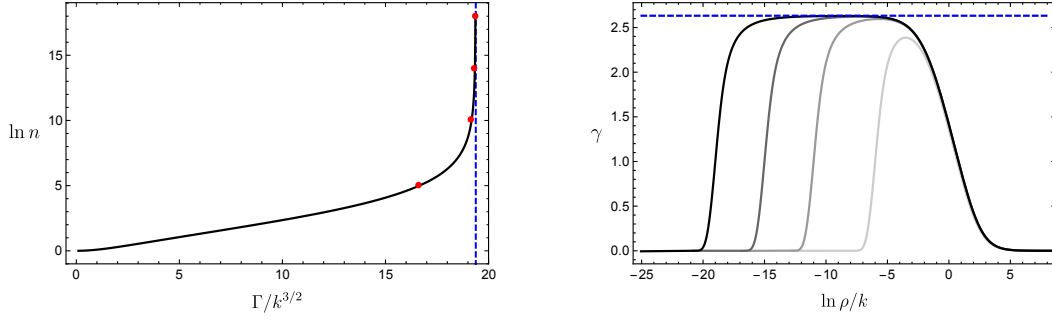
Figure 6.6: Boomerang RG flows for $m^2 = -15/4$ and $\xi = -1/4$. The left plot shows the refractive index n, defined by (6.31), as a function of the deformation parameter $\Gamma/k^{3/2}$, for the one parameter family of boomerang RG flows that exist in the finite range $0 \leq \Gamma/k^{3/2} \leq \bar{\Gamma}$. For the special value $\Gamma/k^{3/2} = \bar{\Gamma} \sim 19.37$ (dashed vertical line) we have the AdS_5^0 to $AdS_2 \times \mathbb{R}^3$ RG flow. As $\Gamma/k^{3/2}$ approaches $\bar{\Gamma}$ there is a build up of an intermediate scaling regime, determined by the $AdS_2 \times \mathbb{R}^3$ solution, as displayed by the radial behaviour of the scalar function for $\Gamma/k^{3/2} = 16.65, 19.17, 19.33$ and 19.36 (red dots on the left plot and light grey to dark grey on the right plot) and we have also marked the value of the scalar in the $AdS_2 \times \mathbb{R}^3$, $\gamma_{(2)} = 48^{1/4}$, by a horizontal dashed line.

6.5.2 Black hole solutions and thermal insulators

It is straightforward to numerically construct black hole solutions for arbitrary values of $\Gamma/k^{3/2}$ using the IR expansion as given in appendix D. We first consider the black hole solutions in the range $0 \leq \Gamma/k^{3/2} < \bar{\Gamma}$, where the boomerang RG flows exist. In the subrange $0 \leq \Gamma/k^{3/2} \leq \Gamma_C$, below a critical value Γ_C, we find that the black hole solutions can be cooled down, uneventfully, and they smoothly approach the boomerang RG flows at $T = 0$. In particular, we find that as $T \to 0$ the entropy, s, goes to zero with $s \sim T^3$. However, in the range $\Gamma_C < \Gamma/k^{3/2} < \bar{\Gamma}$ there is a first order phase transition at finite temperature. The immediate signal for this behaviour can be seen in the entropy versus temperature plots becoming multivalued, as displayed in figure 6.7. Furthermore, by calculating the free energy for the black holes in this range as a function of T, which display the characteristic swallowtail behaviour, we can determine the thermodynamically preferred black holes, again shown in 6.7.

When $\Gamma/k^{3/2} = \Gamma_C$ the line of first order phase transitions ends in a second order critical point with $\Gamma_C \sim 10.5$. When $\Gamma/k^{3/2} = \bar{\Gamma}$ the line of first order phase transitions smoothly ends at $T = 0$ at the AdS_5^0 to $AdS_2 \times \mathbb{R}^3$ RG flow solution. This behaviour is summarised in figure 6.1.

We next construct black hole solutions with $\Gamma/k^{3/2} > \bar{\Gamma}$. In this case we find no evidence of any phase transitions at finite T. When $\Gamma/k^{3/2}$ is close to $\bar{\Gamma}$, as the temperature is lowered the solutions build up a finite temperature behaviour that is governed by the $AdS_2 \times \mathbb{R}^3$ solution, before heading off to the new $T = 0$ ground
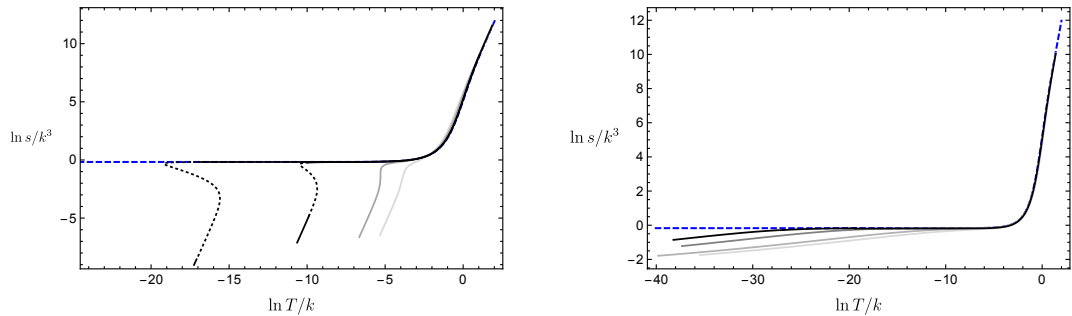
Figure 6.7: Plots of the entropy density s as a function of T for black hole solutions with various deformation parameters and for models with $m^2 = -15/4$ and $\xi = -1/4$. The left plot is for $\Gamma/k^{3/2} \leq \bar{\Gamma} \sim 19.37$, namely 5.5, 10.3, 18, and 19.3 (light grey to dark grey). The dashed blue line in both plots is for $\Gamma/k^{3/2} = \bar{\Gamma}$. For $\Gamma/k^{3/2} = 19.33$ and 19.36 we have used dotted lines on the curves to indicate the first order phase transition. As $T \to 0$, for $\Gamma/k^{3/2} < \bar{\Gamma}$ the black holes approach the boomerang RG flows, with $s \sim T^3$, and when $\Gamma/k^{3/2} = \bar{\Gamma}$ they approach the AdS_5^0 to $AdS_2 \times \mathbb{R}^3$ RG flow with, from (6.27), $s \sim 0.84 k^3$. The right plot is for $\Gamma/k^{3/2} \geq \bar{\Gamma}$, namely, 19.41, 19.75, 25 and 35 (dark grey to light grey). As $T \to 0$ the black holes have $s \to 0$, but not as a power of T. At $T \to 0$ they approach insulating ground states. In both plots the intermediate scaling regimes can be seen.

states. This is displayed in the behaviour of entropy versus temperature plots shown in figure 6.7 and also in figure 6.1. The plots in figure 6.7 also reveal some important features of the new $T = 0$ ground states. Firstly, as $T \to 0$ we have $s \to 0$. However, unlike other $s = 0$ ground states which break translations [69, 71, 72, 118], we find that the entropy density is not vanishing as a power law with T. Indeed we find that $d(\ln s)/d(\ln T)$ is decreasing as $T \to 0$. The $T = 0$ ground states are certainly singular: for example the value of the scalar field at the horizon diverges as $T \to 0$.

To determine some additional properties of the $T = 0$ ground states for $\Gamma/k^{3/2} > \bar{\Gamma}$ we can calculate the thermal DC conductivity matrix, κ^{ij}. For general holographic lattices this can be calculated by solving a Stokes flow at the horizon [92]. In fact, for this case we can use the results presented in [91] which showed that for all of the black hole solutions that we have constructed we have $\kappa^{ij} = \kappa \delta^{ij}$ with

$$\kappa = \frac{4\pi s T}{\gamma_H^2 k^2} \, , \tag{6.32}$$

where γ_H is the value of the scalar field at the black hole horizon. Plotting this as a function of T we find the behaviour shown in the right panel of figure 6.8, clearly revealing that, for $\Gamma/k^{3/2} > \bar{\Gamma}$, $\kappa \to 0$ as $T \to 0$. By examining the $d\ln\kappa/d\ln T$ we deduce that κ is not going to zero as a power law, in line with the radial behaviour of the metric mentioned previously. This thermal insulating behaviour arises because $sT/\gamma_H^2 \to 0$ as $T \to 0$ i.e. the number of degrees of freedom available to transport heat, captured by s, is going to zero rapidly enough as $T \to 0$.

For $\Gamma/k^{3/2} = \bar{\Gamma}$, associated with the AdS_5^0 to $AdS_2 \times \mathbb{R}^3$ RG flow, we have $\kappa \sim T$.
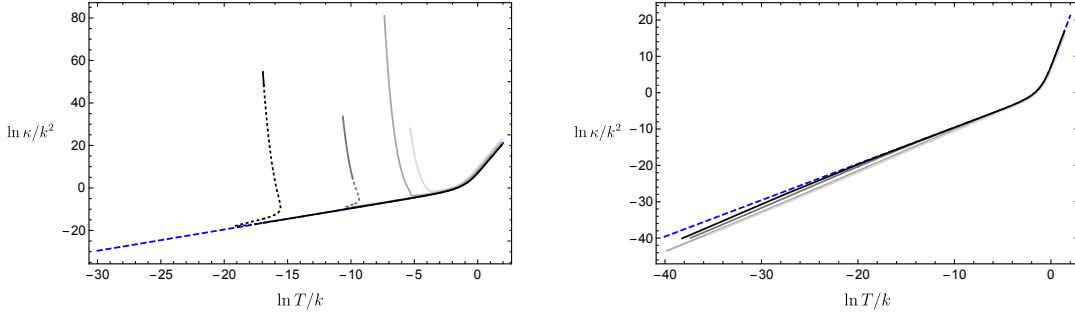
Figure 6.8: Plots of the temperature dependence of the thermal conductivity κ for the black hole solutions constructed for $m^2 = -15/4$ and $\xi = -1/4$. The left plot is for $\Gamma/k^{3/2} \leq \bar{\Gamma} \sim 19.37$, namely 5.5, 10.3, 18, and 19.3 (light grey to dark grey), as in figure 6.7, and we see thermal conducting behaviour with $\kappa \to \infty$ as $T \to 0$. The dashed blue line in both plots is for $\Gamma/k^{3/2} = \bar{\Gamma}$ with $\kappa \sim T$ as $T \to 0$. The right plot is for $\Gamma/k^{3/2} \geq \bar{\Gamma}$, namely, 19.41, 19.75, 25 and 35 (dark grey to light grey), as in figure 6.7, and we see thermal insulating behaviour with $\kappa \to 0$ as $T \to 0$.

For $\Gamma/k^{3/2} < \bar{\Gamma}$ the $T = 0$ ground states are the boomerang RG flows which have translation-invariant horizons and hence $\kappa(T) \to \infty$ as $T \to 0$, as we see in figure 6.8. We can be slightly more precise about this behaviour, generalising arguments in [1, 78], essentially by heating up the boomerang RG flow. By considering the *AdS*-Schwarzschild black hole we deduce that the location of the black hole horizon is related to the temperature via $\rho_+ = \pi T$. Next, by considering (D.3) we deduce that we can obtain the renormalisation of length scales[9] in the boomerang RG flow, $\bar{L}$, by taking the following limit of the black hole solutions: $\bar{L} = \lim_{T/k \to 0}[e^V|_{\rho=\rho_+}/(\pi T)]$. Using (D.3) and (6.32), we then anticipate that as $T/k \to 0$, the thermal conductivity blows up as an exponential multiplied by a factor of T^7. We have verified that this is the case for several branches of black holes with $\Gamma/k^{3/2} < \bar{\Gamma}$.

Finally, although not displayed in figure 6.8, as $T \to \infty$ we find that $\kappa \to T^7$. This behaviour can be understood using a similar argument, as given[10] in section 3.3 of [91], to show that the high temperature behaviour of κ is given by $\kappa \to T^{2(6-\Delta)}$, where $\Delta = 5/2$ is the scaling deformation of the operator dual to the complex scalar fields in (6.3) for the UV AdS_5^0 vacuum.

6.5.3 Diffusion and butterfly velocity

The black hole solutions that we have constructed all explicitly break translation invariance in the dual field theory. On general grounds [142, 143], the black holes necessarily have a quasi-normal hydrodynamic mode associated with diffusion of

---

[9]For the coordinates we are using, $\bar{L}$ is the same as the index of refraction for the boomerang RG flow given in (6.31).

[10]Note that the $T \to \infty$ expression for κ given in eq. (3.30) of [91] is only valid for non-vanishing charge density.

heat. From the results of [143] this mode has a diffusion constant, D, which governs the dispersion relation of the mode, which can be obtained via the Einstein relation $D = \kappa/c$, where $c \equiv T\partial s/\partial T$ is the specific heat (holding the deformation parameter $\Gamma/k^{3/2}$ fixed). Since we have already calculated, numerically, both $\kappa(T)$ and $s(T)$ it is therefore straightforward to obtain $D(T)$.

We next consider the calculation of the butterfly velocity v_B. This can be obtained by studying the construction of a shock-wave geometry on the black hole horizon [135, 136]. For the class of metrics we are considering, from [120] we have

$$v_B^2 = \frac{4\pi T}{6[e^{2V}\dot{V}]_H}\,.$$
(6.33)

We now consider the possibility that we have a relationship of the form

$$D = E\frac{v_B^2}{2\pi T}\,,$$
(6.34)

where we are interested in the low temperature behaviour of the dimensionless quantity $E(T)$

For $\Gamma/k^{3/2} = \bar{\Gamma}$ we see from figure 6.9 that as $T \to 0$ we have $E \to 1$, in agreement with the results of [124], where we recall that the AdS_5^0 to $AdS_2 \times \mathbb{R}^3$ domain wall solution is being driven by an irrelevant operator in the locally quantum critical CFT dual to $AdS_2 \times \mathbb{R}^3$ with scaling dimension $\Delta = 2$. For $\Gamma/k^{3/2} < \bar{\Gamma}$ (not shown in figure 6.8) we have the boomerang RG flows and the $T = 0$ ground states are AdS_5^0. Since these ground states are translation-invariant, the diffusion mode is absent: as $T \to 0$ we have $\kappa \to \infty$, $D \to \infty$ and $E \to \infty$. However for boomerang RG flows with intermediate scaling governed by the $AdS_2 \times \mathbb{R}^3$ solution, we find that there is a range of temperatures where $E \sim 1$.

Finally, of most interest, we consider the low temperature behaviour of E for for $\Gamma/k^{3/2} > \bar{\Gamma}$, associated with the thermally insulating ground states. Remarkably, to good numerical accuracy, we find that $E \to 0.5$ as $T \to 0$, as shown in figure 6.8.

6.6 | Final comments

Within a Q-lattice framework, in sections 6.2-6.4 we constructed simple holographic solutions which describe boomerang RG flows from a CFT in the UV, deformed by spatially dependent relevant operators, to the same CFT in the IR. For large enough deformation the solutions approach an intermediate scaling regime with a new conformal symmetry appearing at intermediate scales, which is governed by another AdS_5 solution.
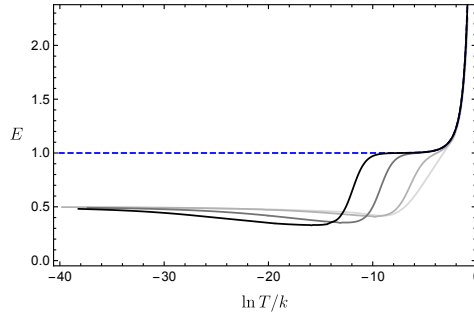
Figure 6.9: Behaviour of the ratio of the the thermal diffusion constant to the butterfly velocity, $E \equiv D/(v_B^2/2\pi T)$, as a function of T for the black hole solutions constructed for $m^2 = -15/4$ and $\xi = -1/4$ and $\Gamma/k^{3/2} \geq \bar{\Gamma}$. For $\Gamma/k^{3/2} = \bar{\Gamma}$, dashed blue line, we see $E \to 1$ as $T \to 0$. For the thermal insulators with $\Gamma/k^{3/2}$ equal to 19.75, 25 and 35 (dark grey to light grey), as in the right panels of figure 6.7 and 6.8, we see that $E \to 1/2$ as $T \to 0$.

The main features of this construction, combined with insights obtained in [2], indicate that within a bottom up framework there is significant freedom to construct 'designer boomerang flows'. In particular, suppose that we want to construct a boomerang flow from a holographic fixed point in the UV to the same fixed point in the IR. This fixed point does not have to be conformal and could be, for example, of Lifshitz type. Suppose also that we want an intermediate scaling regime governed by some other holographic geometry which could be AdS, Lifshitz or even hyperscaling violation form, which does not break translations. Then one looks for a gravitational model in which there is a standard RG flow from the UV fixed point to the intermediate scaling geometry driven by a relevant deformation, which we suppose is driven by bulk scalar fields. In addition we demand that the gravitational model allows for a Q-lattice ansatz in which the bulk scalar fields depend on the spatial coordinates. Then, much as in this chapter, there should be RG flows parametrised by a dimensionless parameter of the form Γ/k^α, where k is the characteristic wave number of the spatial deformation and Γ characterises the strength of the deformation of the relevant operator. For small Γ/k^α one expects a boomerang RG flow as the perturbative mode rapidly dies out in the IR[11]. If the boomerang RG flow exists for large values of Γ/k^α then the desired intermediate scaling will also appear. In simple models the latter feature should be present, but on the other hand it is not guaranteed. For example, if there were additional fixed point solutions in the model, then one may be driven away from the boomerang flows by a quantum phase transition at some value of Γ/k^α before intermediate scaling is seen.

In section 6.5 we also constructed boomerang flows for models in which there was

---

[11]An exception would be if the perturbative expansion generates zero mode terms at higher orders which change the IR. Such behaviour can be eliminated by imposing discrete symmetries.

an $AdS_2 \times \mathbb{R}^3$ solution which breaks translation invariance. In this case, for a specific value of $\Gamma/k^{3/2} = \bar{\Gamma}$ there is an RG flow solution from AdS_5^0 in the UV to $AdS_2 \times \mathbb{R}^3$ in the IR. We found that as $\Gamma/k^{3/2}$ approached $\bar{\Gamma}$ from below, the boomerang RG flow solutions build up an increasingly large $AdS_2 \times \mathbb{R}^3$ intermediate scaling region. *A priori*, it is unclear what might happen for $\Gamma/k^{3/2} > \bar{\Gamma}$. However, by constructing finite temperature black holes, in addition to finding an interesting line of first order phase transitions for $\Gamma/k^{3/2} < \bar{\Gamma}$, we found a new class of thermally insulating ground states for $\Gamma/k^{3/2} > \bar{\Gamma}$. A particularly interesting feature of these new ground states is that $s(T) \to 0$ but not as a power law. We also showed, numerically, that these ground states exhibit a simple relationship between the thermal diffusion constant and the butterfly velocity of the form $D = Ev_B^2/(2\pi T)$ with $E(T) \to 0.5$ as $T \to 0$. It would certainly be interesting to have a better analytic understanding of these ground state solutions, which should also allow us to confirm this result for $E(T)$. An interrelated point would be to obtain a better understanding of these insulating ground states in the limit of large $\Gamma/k^{3/2}$. A more general point is that it is not at all clear how one can directly construct such novel ground state solutions, without power law behaviour, in holography. What we have shown in this chapter is that for at least one class of models, analysing models with boomerang RG flows can reveal them.

In the above discussion we have been considering deformations associated with relevant operators of the UV fixed point. However, we note that boomerang RG flows with intermediate scaling and within a Q-lattice framework do not require the deformations to be associated with relevant operators: indeed the examples in [1] were driven by marginal operators. It is also worth emphasising that boomerang RG flows do not require Q-lattices and can also arise for what are called inhomogeneous lattices. For example, in [77] boomerang RG flows were driven by a deformation involving a spatially varying chemical potential of CFT in $d = 3$ of the form $V \cos kx$. For these deformations with $k = 0$ and $V \neq 0$, we have the standard zero temperature AdS-Reissner-Nordstrom black hole, which approaches $AdS_2 \times \mathbb{R}^2$ in the IR. It is therefore natural to conjecture that for sufficiently large V/k the boomerang RG flows could have an intermediate scaling regime approaching $AdS_2 \times \mathbb{R}^2$. It would be of interest to examine this in more detail, and more generally, analyse boomerang RG flows for other inhomogeneous lattices.

7 | Outlook

In this thesis we have investigated the RG flows for families of strongly coupled theories that have been deformed by a lattice. We have done this using the gauge/gravity correspondence, which allows us to bypass the need for a perturbative approach. For the lattices constructed in chapters 4 and 5 we took a top-down approach, by studying a consistent truncation of $D = 10$ and $D = 11$ supergravity. The consistency of the truncation ensures that the dual field theory is always a well defined QFT. The intuition developed in these chapters allowed us to write chapter 6. Therein, we have taken a phenomenological approach (bottom-up), engineering a gravity model that allows to construct a holographic lattice in which we can model an RG flow with intermediate conformal invariance and furthermore, the possibility of a thermal conductor-insulator phase transition.

On general grounds, constructing holographic lattices will require solving a coupled system of non-linear PDEs. Needless to say, such task requires the implementation of computational methods and, even with the aid of a computer, this is at the moment a difficult endeavour. A significant simplification to this problem is provided by the Q-lattice type of constructions, which can be used whenever the gravity system possesses some global symmetry. In such cases, an ansatz that breaks translations for the boundary theory can be built whilst preserving bulk homogeneity. Thus, the problem of PDEs is turned into a system of ODEs, which is now much simpler, albeit still challenging, to handle. All of the lattices that we have constructed are Q-lattices, and the method of choice used to solve the resulting system of ODEs has been a double-sided shooting, and we have explained this method in the appendix.

In both constructions of chapters 4 and 5 and in the ones studied in the first half of chapter 6, we observed boomerang RG flows that persisted for arbitrarily large values of the lattice deformation[1], Γ. The appearance of Boomerang RG flows is not inconsistent with the spirit of c-theorems because the lattice deformation that triggers the flow is not a Poincaré invariant deformation. In contrast, the black holes constructed in the second part of chapter 6 were Boomerang flows only for values of Γ that were below a specific finite critical value, which we denoted $\bar{\Gamma}$.

A remarkable feature of all of our lattices is that the RG flows could exhibit regimes of intermediate scaling. Again, for the models studied in chapters 4 and 5 and in the ones in the first half of chapter 6, the intermediate scaling became evident

---

[1]Here only, we will use Γ to denote the dimensionless lattice defomation of any of our models

(a) $AdS_5 \circlearrowleft (Lif_{3/2})$

(b) $AdS_4 \circlearrowleft (H(1,-2), H(5/2,1))$

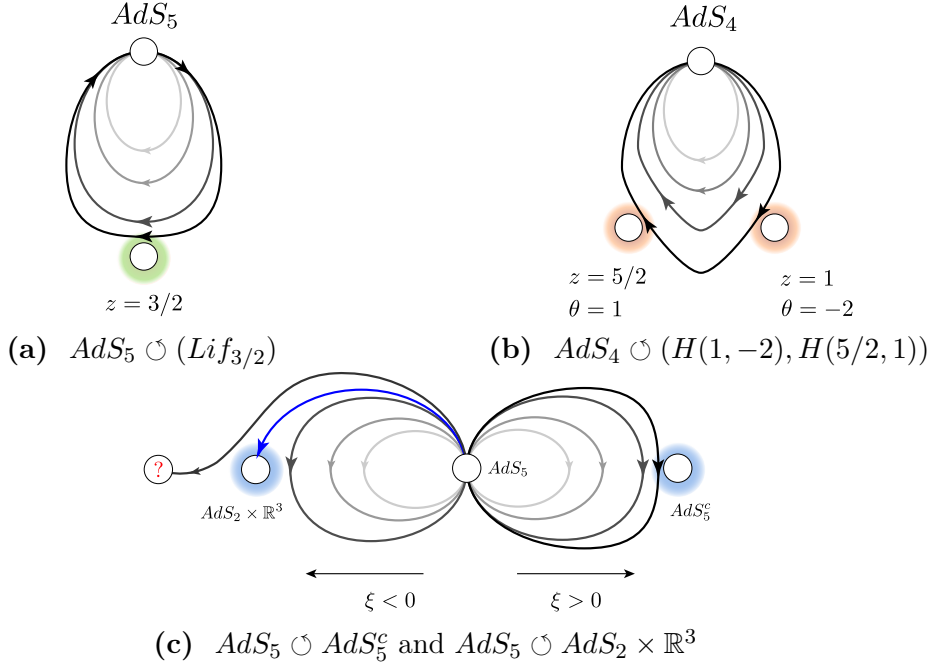**(c)** $AdS_5 \circlearrowleft AdS_5^c$ and $AdS_5 \circlearrowleft AdS_2 \times \mathbb{R}^3$

Figure 7.1: A recap of the RG flows investigated in this thesis. 7.1a shows the flow in the type IIB supergravity theory of chapter 4, for which large values of the lattice deformation drive the theory arbitrarily close to a Lifshitz-like fixed point with $z = 3/2$. 7.1b show the flow for the $D = 11$ supergravity model of chapter 5. This time two intermediate scaling regimes are present for large deformations, each is a hyperscaling violating geometry $H(z, \theta)$; there exists a Poincaré invariant flow connecting $AdS_4 \to H(1, -2)$. Finally, figure 7.1c shows the RG flows for the bottom-up model of chapter 6. For positive values of the parameter ξ (see (6.3)), large values of the lattice deformation show an intermediate conformal invariance because the flow is being driven arbitrarily close to an AdS_5^c geometry. There also exists a Poincaré invariant flow $AdS_5 \to AdS_5^c$. For negative values of ξ, the flow can be driven to an $AdS_2 \times \mathbb{R}^3$ when the lattice deformation, Γ, reaches a critical value, Γ_c. The effects of this fixed point are visible as an intermediate scaling when $\Gamma \approx \Gamma_c$. For $\Gamma > \Gamma_c$, the flow transitions into a novel insulating ground state for which the precise geometry remains unknown.

at large Γ and, furthermore, we noticed that such intermediate scaling could extend over an arbitrarily large range of scales as long as Γ was sufficiently large. The black holes constructed in the second part of chapter 6 also exhibit intermediate scaling but, instead of appearing at large lattice deformations, the intermediate scaling appeared as we approached the critical value $\Gamma \sim \bar{\Gamma}$. In fact the boomerang-like behaviour of these flows was lost for $\Gamma > \bar{\Gamma}$ and instead, a new insulating geometry appeared in the deep IR, for which the precise details remain unknown. Interestingly, however, these new ground states are thermal insulators for which the entropy vanishes as $T \to 0$ but not as a power-law scaling. This is the first example of such type of behaviour in a holographic model. A summary of the RG flows found in this thesis is given in figure 7.1.

Another interesting avenue to pursue would be to consider the charged versions of the models that we have studied. This would allow us to investigate to what extent
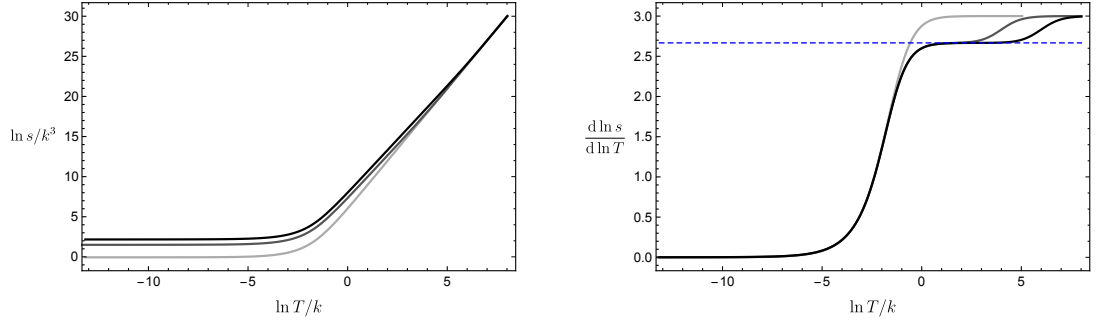
Figure 7.2: Entropy vs. Temperature plots for the charged version of the Black holes we have constructed in chapter 4. The value of the chemical potential is held fixed, while the lattice deformation, λ, is strengthened ($\lambda = 1, 6, 8$ from lightest to darkest). At large enough values of λ the intermediate intermediate scaling that was present for the neutral black holes also appears in this scenario. However, at low temperatures, the solution moves to a $AdS_2 \times \mathbb{R}^3$ geometry where the entropy reaches a constant value. The plot on the right is the logarithmic derivative of the left plot. Plateaus indicate scaling regimes. The dashed blue line highlights the expected position of the Lifshitz-like scaling.

the intermediate scalings get imprinted into the full matrix of transport coefficients. Some work in this direction has already started. For instance, it is straightforward to extend the model of chapter 4 to include a $U(1)$ gauge field, by adding a Maxwell term, as was done in [100]. This allows us to also deform the dual field theory by a chemical potential, μ, which is given by the boundary value of the gauge field,

$$A_t \to \mu + ... \quad (\text{as } r \to \infty) \tag{7.1}$$

while the ansatz for the remaining fields remains as in section 4.3, eq. (4.13). One can show that the inclusion of the Maxwell term will necessarily spoil the boomerang like behaviour of our flows because the $T \to 0$ limit will now approach an $AdS_2 \times \mathbb{R}^3$ geometry. However, by building the black holes numerically, we will find that the intermediate Lifshitz-like scaling is still present, as shown in figure 7.2. The transport coefficients, which can be obtained from the black hole horizon data following the recipe developed in [91], are indeed affected by intermediate Lifshitz-scaling as we show in figure 7.3.

The immediate next task is to introduce an oscillating perturbation on top of these black holes in order to study the AC conductivities. As with the neutral case, investigating the stability of these solutions could leads us to find interesting novel ground states. The charged case for the model of chapter 5 remains to be investigated and details for a plausible ansatz are given in appendix C.

Finally, a follow-up work on the lattices investigated in chapter 6 would be to have a better analytic understanding of the insulating ground states. So far, the precise reason on why one is able to obtain non-power-law scaling remains unclear.
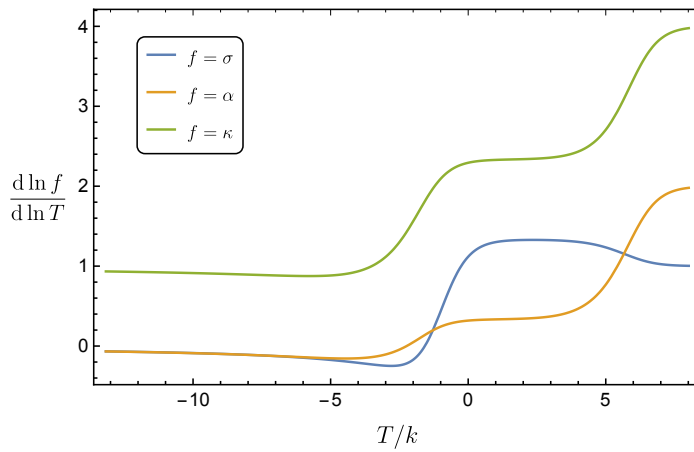
Figure 7.3: Logarithmic derivatives of the electrical conductivity, σ (blue), the thermo-electrical conductivity, α (yellow), and the thermal conductivity κ (green), for a strong lattice deformation corresponding to the darkest plot in figure 7.2. The intermediate scaling is evident.

A | Numerical shooting

We will use the technique here presented to solve boundary value problems (BVP) for systems of *nonlinear*, second order, ordinary differential equations. Beyond the fact that we are dealing with a BVP rather than an initial value problem, the nonlinear nature of the ODEs make this a delicate topic. Theorems on existence and uniqueness do not stand as strongly as they do in the linear case. Some nice discussion on the mathematical details can be found in [144, 145] and in the textbook [146]. Our discussion here mainly follows [147] and it is necessarily not rigorous.

Suppose we are given a second order differential equation for the function $f(r)$, with $r \in [a, b]$. Furthermore, we will assume that the ODE is singular at a and/or b since such is the situation in all of our applications. The singular behaviour means that our BVP cannot be phrased in terms of $f(a)$ and $f(b)$ as this would cause our code to *overflow*. Instead, our BVP should be posed in the interval $[a + \epsilon, b - \epsilon]$, $\epsilon > 0$, and rephrased in terms of an asymptotic power series for the function $f(r)$. The asymptotic power series of f will usually take the form

$$f_a^S(\epsilon) = \sum_{i,j} A_{ij} \epsilon^i (\ln \epsilon)^j \quad , \quad \epsilon = r - a, \tag{A.1}$$

$$f_b^S(\epsilon) = \sum_{i,j} B_{ij} \epsilon^i (\ln \epsilon)^j \quad , \quad \epsilon = b - r, \tag{A.2}$$

but it might be more complicated depending on the nature of the singular point (see, for instance, the expansion used in eq. (5.16)). The presence of the terms proportional to $\ln \epsilon$ will depend on the particular problem. Mathematically, these are related to the roots of the indicial equation; in the AdS/CFT correspondence, log terms will be related to anomalies. Most of the coefficients A_{ij} and B_{ij} in (A.1) will already be determined by the boundary conditions imposed. For example, we will be interested in problems where the spacetime metric asymptotes to a unit radius AdS which means that the leading behaviour as $r \to \infty$ should be $g_{tt} = -r^2 + \mathcal{O}(r)$. Solving the equations of motion order by order we will be left with a set of undetermined parameters at each endpoint, $\{A\}$ and $\{B\}$. Numerical integration can be carried out from each endpoint up to a mid point r_{mid} using, for instance, the built-in function `NDSolve` in *Mathematica*. Denote the solution obtained when integrating from a and b by $f_a(r, A)$ and $f_b(r, B)$ respectively. These solutions depend on the initial data

and therefore the matching condition

$$f_a(r_{\text{mid}}, A_{ij}) = f_b(r_{\text{mid}}, B_{ij}) \tag{A.3}$$

$$f'_a(r_{\text{mid}}, A_{ij}) = f'_b(r_{\text{mid}}, B_{ij}), \tag{A.4}$$

can be understood as imposing further restrictions on the parameters A_{ij} and B_{ij}. This will leave us with a subset of undetermined coefficients that parametrises our space of solutions.

Example. As a very simple example, consider this modification of the pendulum problem,

$$u''(r) + \frac{\sin u(r)}{r} = 0, \tag{A.5}$$

for which we would like to find regular solutions in the interval $[0, 2\pi]$. Regularity means that $u(r)$ should vanish as $r \to 0$. To feed this into a computer, we develop a power series as in (A.1), taking into account our regularity condition. Solving (A.5) order by order one finds that

$$u(\delta r) = A_{11}\delta r - \frac{A_{11}}{2}\delta r^2 + \frac{A_{11}}{12}\delta r^3 - \frac{A_{11} - 2A_{11}^3}{144}\delta r^4 + \dots \tag{A.6}$$

as $\delta r \to 0$. We see that the regularity condition imposes such restriction on our function that its power series around $r = 0$ can be found to arbitrary order in terms of a single parameter: A_{11}. However, demanding regularity at $r = 0$ gives no restriction on the behaviour of $u(2\pi)$. Lets then write

$$u(2\pi) = \lambda \tag{A.7}$$

$$u'(2\pi) = B_{11}. \tag{A.8}$$

Out of the three parameters, $\{A10, \lambda, B10\}$, the matching conditions (A.3) will further restrict two, so that our solutions will be labelled by one free parameter. Without loss of generality, we choose λ to be the free parameter. The relevant lines of code in *Mathematica* would look like

```
uA[A10_] :=
NDSolve[{eq==0, u[dr]==serU[dr,A10], u'[dr]==dSerU[dr,A10]},u,{r,dr,rmid}]


uB[l_,B10_] :=
NDSolve[{eq==0, u[2 Pi]== l, u'[2 Pi]==B10},u,{r,rmid,2 Pi}]
```

where `serU` and `dSerU` are the the series expansion (A.7) and its derivative respectively. To implement the matching condition (A.3) we simply use the function `FindRoot`, which uses a variant of the Newton method.
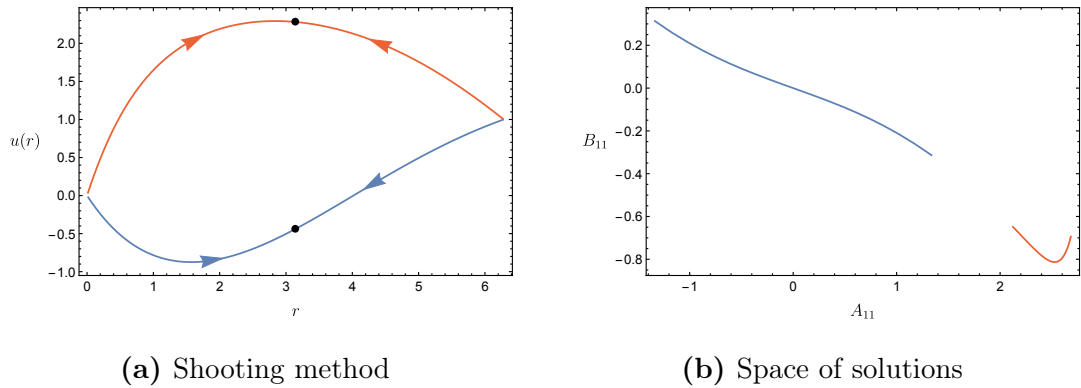
(a) Shooting method

(b) Space of solutions

Figure A.1: Double sided shooting for the modified pendulum. Figure A.1a shows two solutions found for $\lambda = 1$ when two different seeds are given to `FindRoot`. The black dot shows the value of r_{mid}, where the matching condition is imposed. To the right, figure A.1b shows two branches of solutions that exist for $\lambda \in [-1, 1]$

```
match[l_,A10_,B10_]:=
({u[rmid],u'[rmid])}/.uA[A10])-({u[rmid],u'[rmid]}/.uB[l,B10])


bndData[l_]:=
FindRoot[match[l,A10,B10],{A10,-1},{B10,1},Evaluated -> False]
```

It should be noted that `FindRoot` needs to be fed an initial guess. While there is no standard way of obtaining such initial guess, in practice one usually draws experience from a known solution. Depending on the guess `FindRoot` might converge to different solutions or it may not converge at all. This is exemplified in figure A.1, where two solutions are found for the same value of λ. The option "`Evaluated` →`False`" is included to prevent `FindRoot` from attempting a symbolic calculation; an error is produced without this option[1].

Having found a solution, it is important to verify it through different tests. For instance, the solution found should not depend on the value of r_{mid} nor δr. Numerically this means that the solution found with `FindRoot` should not be too sensible to these changes.

While the modified pendulum is a single ODE, the above procedure is easily generalised to systems of coupled ODEs. As a final remark we note that the ODEs that we encounter in this thesis have the additional complication of being highly oscillatory near the singular points. A typical Runge-Kutta method will therefore fail to converge or else converge only after a very long CPU time, because the step size has to be very restricted. A convenient way to deal with this problem is to alternate between an explicit and an implicit solving method. *Mathematica* can easily implement this by explicitly specifying the `NDSolve` method to be `StiffnessSwitching`.

---

[1]Alternatively, one can specify in each function that the parameters should be numbers.

B | Q-lattices and $SL(2, R)$ classes

The holographic lattices of [62, 65, 73, 74], and the ones studied here, are all examples of Q-lattices [60] in which one exploits the fact that the scalars parametrise the group manifold $SL(2, R)$ and consequently the gravity model admits a global $SL(2, R)$ symmetry. In particular, the spatial dependence of the scalars on the z direction is given by a specific orbit of the $SL(2, R)$ action. There are three distinct cases to consider corresponding to the three different conjugacy classes of $SL(2, R)$.

Write a general $SL(2, R)$ matrix as

$$\mathcal{M} = \begin{pmatrix} a & b \\ c & d \end{pmatrix}, \qquad ad - bc = 1 \,. \tag{B.1}$$

The three conjugacy classes are determined by the trace: the parabolic class has $|Tr\mathcal{M}| = 2$, the hyperbolic class has $|Tr\mathcal{M}| > 2$ and the elliptic class has $|Tr\mathcal{M}| < 2$.

The $SL(2, R)$ action on $\tau = \chi + ie^{-\phi}$ is given by $\tau \to (a\tau + b)/(c\tau + d)$. Suppose we start with $\chi = 0$ and $\phi = \phi_0$. Then acting with the one-parameter family of $SL(2, R)$ transformations in the parabolic conjugacy class given by

$$\mathcal{M} = \begin{pmatrix} 1 & kz \\ 0 & 1 \end{pmatrix}, \tag{B.2}$$

induces $\chi \to kz$ with ϕ_0 unchanged. This generates the ansatz for scalar fields given by $\phi = \phi(r)$ and $\chi = kz$ that was used in [62, 73, 74].

Next we consider the transformations in the hyperbolic conjugacy class of the form

$$\mathcal{M} = \begin{pmatrix} e^{-kz/2} & 0 \\ 0 & e^{kz/2} \end{pmatrix} \,. \tag{B.3}$$

This induces $\phi_0 \to \phi_0 + kz$ with $\chi = 0$ unchanged. This generates the ansatz $\phi = kz$ and $\chi = 0$ used in [65].

Finally, we consider the transformations in the elliptic conjugacy class of the form

$$\mathcal{M} = \begin{pmatrix} \cos(\frac{kz}{2}) & \sin(\frac{kz}{2}) \\ -\sin(\frac{kz}{2}) & \cos(\frac{kz}{2}) \end{pmatrix} \,. \tag{B.4}$$

After writing $\phi_0 = \varphi_0$ we find that this induces the transformation

$$\chi \to \frac{\sinh \varphi_0 \, \sin kz}{\cosh \varphi_0 + \sinh \varphi_0 \, \cos kz} \, ,$$

$$e^{\phi} \to \cosh \varphi_0 + \sinh \varphi_0 \, \cos kz \, . \tag{B.5}$$

This generates $\varphi = \varphi(r)$, and $\alpha = k \, z$, exactly as in (4.6) and (4.13). Notice that as we traverse once in the Poincaré disc via $z \to z + 2\pi/k$, we see from (B.4) that we move from $\mathcal{M} = 1$ to $\mathcal{M} = -1$. In other words we have a closed orbit in $PSL(2, R)$.

C | STU gauged supergravity and some truncations

The bosonic part of the Lagrangian for the $N = 2$ STU gauged supergravity theory is given by

$$\mathcal{L} = R - \frac{1}{2} \sum_{i=1}^{3} \left((\partial \lambda_i)^2 + \sinh^2 \lambda_i (\partial \sigma_i)^2 \right) - \sum_{a}^{4} \text{Re}\left(F_{\mu\nu}^{(a)+} \mathcal{M}_{ab} F^{(b)+\,\mu\nu} \right) - \text{g}^2 V \,,$$

(C.1)

where $F_{\mu\nu}^{(a)+} = \frac{1}{2}(F_{\mu\nu}^{(a)} - i * F_{\mu\nu}^{(a)})$, V is the potential just depending on the scalar fields

$$V = -8 \sum_{i}^{3} \cosh \lambda_i,$$

(C.2)

and $\mathcal{M}$ is a rather complicated matrix that depends on both the modulus and the phase of the complex scalars $\Phi_i = \lambda_i e^{\sigma_i}$. An explicit expression can be found in [101–103]. It is clearly consistent with the equations of motion to set all of the gauge-fields to zero. It is also not difficult to see that we can consistently set $\lambda_1 = \sigma_1 = 0$. Finally we can set $\lambda_2 = \lambda_3$ provided that we have an ansatz in which $(\partial \sigma_2)^2 = (\partial \sigma_3)^2$ and this what we studied in the main part of this chapter, and we also set $g^2 = 1/4$.

It is also of interest to look for simple frameworks in which we can have Q-lattice constructions that also carry electric charge. We have found the following ansatz that can be used to construct RG flows with charge that depend on just one of the spatial directions. Introducing coordinates (t, r, x, y) we can take the only dependence on the x direction to be via two of the periodic σ_i fields, as in the ansatz:

$$\lambda_1 = \alpha, \qquad \lambda_2 = \lambda_3 = \gamma, \qquad \sigma_1 = 0, \qquad \sigma_2 = -\sigma_3 = kx \qquad \text{(C.3)}$$

and

$$F^{(1)} = F^{(2)} = 0, \qquad F^{(3)} = F^{(4)} \equiv F \qquad \text{with} \qquad F \wedge F = 0 \,, \qquad \text{(C.4)}$$

The equations of motion of the STU theory can then be obtained from the Lagrangian

$$\mathcal{L} = R - \frac{1}{2}(\partial \alpha)^2 - (\partial \gamma)^2 - g^{xx} k^2 \sinh^2 \gamma - e^{-\alpha} F^2 + 8\,\text{g}^2 (\cosh \alpha + 2 \cosh \gamma). \quad \text{(C.5)}$$

with all fields just depending on (t, r, y). One can now restrict to an electric ansatz for

the fields in (C.5) that just depend on the radial direction. For the scalar fields we take γ, α to be functions of r and for the gauge-field we take $F = dA$ with $A = A_t(r)$. A suitable anisotropic metric ansatz is given by $ds^2 = U dt^2 + U^{-1} dr^2 + e^{2V_1} dx^2 + e^{2V_2} dy^2$ with U, V_1, V_2 functions of r.

Finally, we point out that there is a closely related ansatz which leads to (C.5) but with $\alpha \to -\alpha$. One way this can arise is by taking $\lambda_1 = \alpha$, $\lambda_2 = \lambda_3 = \gamma$, $\sigma_1 = \pi$, $\sigma_2 = \sigma_3 = kx$, $F^{(1)} = F^{(2)} = 0$ and $F^{(3)} = -F^{(4)} \equiv F$.

D | Some details for section 6.5

For the ansatz used in (6.26) the equations of motion are given by

$$0 = \dot{U} + U\left(2\dot{V} - \frac{\dot{\gamma}^2}{2\dot{V}}\right) - \frac{1}{\dot{V}}\left(4 - \frac{1}{2}(e^{-2V}k^2 + m^2)\gamma^2 - \frac{\xi}{3}\gamma^4\right),$$

$$0 = \ddot{\gamma} + \dot{\gamma}\left(\frac{\dot{U} + 3U\dot{V}}{U}\right) - \gamma\left(\frac{e^{-2V}k^2 + m^2}{U}\right) - \frac{4\xi}{3U}\gamma^3,$$

$$0 = \ddot{V} + \dot{V}^2 + \frac{1}{2}\dot{\gamma}^2. \tag{D.1}$$

Restricting to $m^2 = -15/4$ we have the following UV expansion as $\rho \to \infty$,

$$U = (\rho + \rho_+)^2(1 - \frac{3\Gamma^2}{8(\rho + \rho_+)^3} + \frac{M}{(\rho + \rho_+)^4} + \dots),$$

$$e^{2V} = (\rho + \rho_+)^2(1 - \frac{3\Gamma^2}{8(\rho + \rho_+)^3} - \frac{5\Gamma\Gamma_2}{8(\rho + \rho_+)^4} + \dots),$$

$$\gamma = \frac{\Gamma}{(\rho + \rho_+)^{3/2}} + \frac{\Gamma_2}{(\rho + \rho_+)^{5/2}} + \frac{\Gamma k^2}{2(\rho + \rho_+)^{7/2}} + \dots. \tag{D.2}$$

where the parameter ρ_+, obtained by shifting the radial coordinate is included to conveniently place the IR in the RG flows at $\rho = 0$.

For the boomerang RG flows the IR expansion, at $\rho \to 0$, is given by

$$U = \rho^2\left[1 + \frac{3}{16}e^{-\frac{2k}{\rho c_V}}\left(2c_V\frac{k^2}{\rho^2} + c_V^2\frac{k}{\rho}\right)\left(\frac{c_\gamma}{k^{3/2}}\right)^2 + \dots\right],$$

$$e^{2V} = \rho^2 c_V^2\left(1 - \frac{1}{16}e^{-\frac{2k}{\rho c_V}}\left(4\frac{k^3}{\rho^3} + 3c_V^2\frac{k}{\rho} + 3c_V^3\right)\left(\frac{c_\gamma}{k^{3/2}}\right)^2 + \dots\right),$$

$$\gamma = \frac{k^{3/2}}{\rho^{3/2}}e^{-k/\rho c_V}\left(\frac{c_\gamma}{k^{3/2}}\right) + \dots, \tag{D.3}$$

fixed by two parameters c_γ and c_V. For the RG flow from AdS_5^0 to $AdS_2 \times \mathbb{R}^3$ solution we use the IR expansion

$$U = \frac{\rho^2}{L_{(2)}^2}(1 + c_1\rho + \dots),$$

$$e^{2V} = c_V(1 + 2c_2\rho + \dots),$$

$$\gamma = \gamma_{(2)}(1 + c_3\rho + \dots), \tag{D.4}$$

with the c_i as given for the $\delta = 1$ mode in section 6.5, and hence, with c_V, (D.4)

depends on two free constants.

Finally, for the black hole solutions we use the expansion as $\rho \to 0$ given by

$$U = 4\pi T \rho - \rho^2 \frac{1}{48} \left(96 + 45\gamma_H^2 - 8\xi\gamma_H^4 - 36\gamma_H^2(k/V_H)^2\right) + \dots,$$

$$e^{2V} = V_H^2 + \rho \frac{V_H^2}{48\pi T} \left(96 + 45\gamma_H^2 - 8\xi\gamma_H^4 - 12\gamma_H^2(k/V_H)^2\right) + \dots,$$

$$\gamma = \gamma_H + \rho \frac{\gamma_H}{48\pi T} \left(-45 + 16\xi\gamma_H^2 + 12(k/V_H)^2\right) + \dots. \tag{D.5}$$

In order to calculate the holographic energy of the domain wall solutions, we need to calculate the holographic stress tensor. To do this, we need to supplement the bulk action (6.2) with boundary terms including the usual Gibbons-Hawking term and a counter-term action given by $S_{ct} = \frac{1}{16\pi G} \int d^4x \sqrt{-\gamma}(6 + \sum_\alpha \frac{3}{4} z^\alpha \bar{z}^\alpha + \dots)$, where γ_{ij} is the pull back of the bulk metric to the regulating UV boundary and the neglected terms are not important for the calculation of interest. After a little calculation we find that the energy density of the dual field theory is given in terms of the UV expansion of (D.2) as

$$T^{tt} = -3(M + \Gamma\Gamma_2). \tag{D.6}$$

In order to determine the thermodynamically preferred black holes we also need to calculate the free energy density, w, and we have

$$w = T^{tt} - Ts. \tag{D.7}$$

D.1 | RG flows and Black holes for $m^2 = -15/4$, $\xi = -675/512$

In section 6.5 we focussed on models with $m^2 = -15/4$ and $\xi = -1/4$. Here we briefly discuss models with $m^2 = -15/4$, $\xi = -675/512 \sim -1.32$ which exhibit some interesting different behaviour. It is worth noting that for these values, the $AdS_2 \times \mathbb{R}^3$ solution given in (6.27) has a BF violating mode (see the discussion below (6.28)) and this seems to be at least partially responsible for the differing behaviour.

The AdS_5^0 to $AdS_2 \times \mathbb{R}^3$ RG flow now exists for the special value $\Gamma/k^{3/2} = \bar{\Gamma} \sim 1.8466$. We can also construct boomerang RG flows from AdS_5^0 to AdS_5^0 for a finite range of $\Gamma/k^{3/2}$ but unlike when $m^2 = -15/4$, $\xi = -1/4$, and surprisingly, this range now extends further than $\bar{\Gamma}$ as shown in figure D.1. In particular, there is now a range of $\Gamma/k^{3/2}$ where the boomerang RG flows are not uniquely determined by the UV deformation parameter $\Gamma/k^{3/2}$, but instead by the refractive index n.
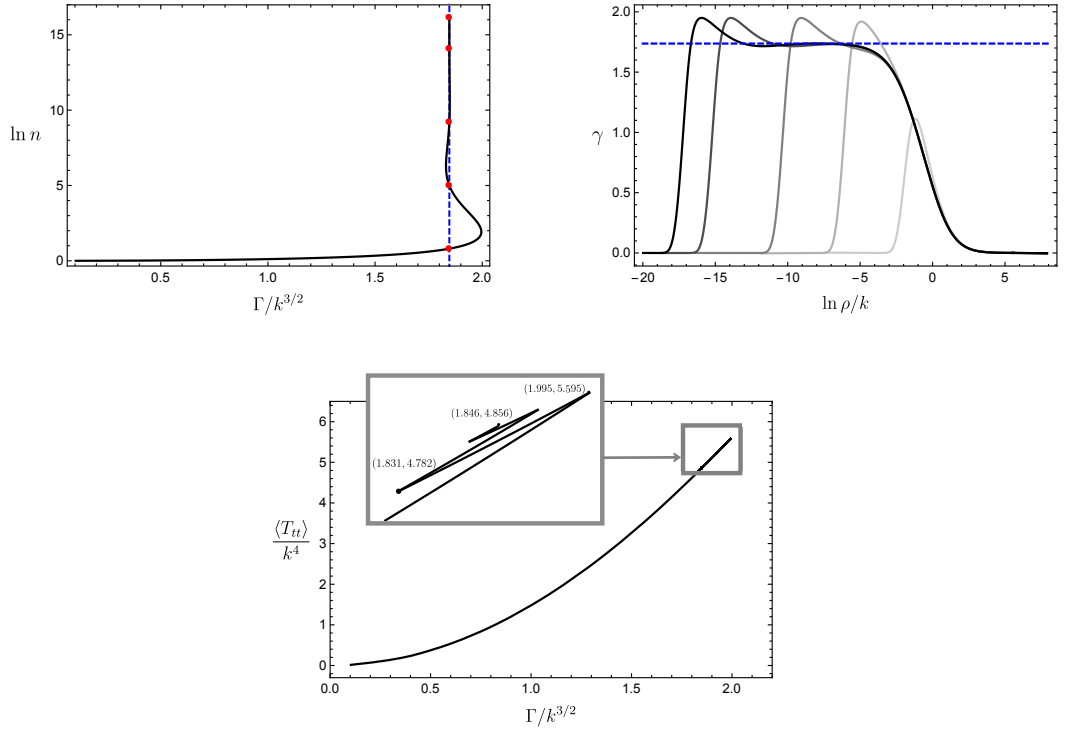
Figure D.1: Boomerang RG flows for $m^2 = -15/4$ and $\xi = -675/512$. The upper left plot shows the refractive index n, defined by (6.31), as a function of the deformation parameter $\Gamma/k^{3/2}$, for a one parameter family of boomerang RG flows. For the special value $\Gamma/k^{3/2} = \bar{\Gamma} \sim 1.8466$ (dashed vertical line) there is also an AdS_5^0 to $AdS_2 \times \mathbb{R}^3$ RG flow. Near $\Gamma/k^{3/2} = \bar{\Gamma}$ the boomerang flows are not uniquely specified by the value of $\Gamma/k^{3/2}$. As n becomes large the boomerang flows build up a large intermediate scaling regime dominated by the $AdS_2 \times \mathbb{R}^3$ solution: for several boomerang flows with $\Gamma/k^{3/2} \sim 1.8466$, denoted by red dots, we have plotted the radial behaviour of the scalar function in the upper right plot, with light grey to dark grey associated with increasing n, and the dashed horizontal line indicates the constant value of γ in the $AdS_2 \times \mathbb{R}^3$ fixed solution. The bottom plot shows the value of the energy for the boomerang flows and we see that for values of $\Gamma/k^{3/2}$ where there is non-uniqueness, it is the solution with the smallest value of n that is preferred (the lightest grey in the upper right plot), and hence the intermediate $AdS_2 \times \mathbb{R}^3$ scaling is frustrated.

These are perhaps the first examples of holographic RG flows which have the same fixed point solution in the IR and yet they are not uniquely specified by their UV deformation data[1]. Furthermore, for the specific value $\Gamma/k^{3/2} = \bar{\Gamma}$ there is also the AdS_5^0 to $AdS_2 \times \mathbb{R}^3$ RG flow solution, giving rise to an additional non-uniqueness for this specific value of the UV deformation. As $n \to \infty$ we find that $\Gamma/k^{3/2} \to \bar{\Gamma}$. Furthermore, as n gets larger the boomerang RG flows build up an increasingly larger intermediate scaling regime that is determined by the $AdS_2 \times \mathbb{R}^3$ solution, as also displayed in the radial behaviour of the scalar field γ in figure D.1.

For the values of $\Gamma/k^{3/2}$ where there is not a unique solution, the physical RG flow solution is the one that has the smallest energy. In figure D.1 we have plotted T^{tt} for the boomerang flows and we find that for a given value of $\Gamma/k^{3/2}$ the energetically preferred solution is given by the smallest value of n. In particular, the amount of build up of an intermediate scaling regime determined by the $AdS_2 \times \mathbb{R}^3$ solution is frustrated for energetic reasons.

We have constructed some finite temperature black hole solutions, but the full phase diagram is rather involved due to the presence of multiple branches of solutions in the region of $\Gamma/k^{3/2}$ where there is non-uniqueness of the boomerang RG flows. While we leave a full analysis to future work, we note that we have constructed some black hole solutions for values of $\Gamma/k^{3/2}$ significantly larger than $\bar{\Gamma}$ and we find that as $T \to 0$ the ground states have $s(T) \to 0$, not as a power law, and they are again thermal insulators. Furthermore, we also find that they satisfy the diffusion-butterfly velocity relation given in (6.34) with again, remarkably, $E(T) \to 0.5$ as $T \to 0$.

---

[1]Examples of holographic RG flows which are not uniquely specified by their UV data but with *different* IR fixed point solutions arise in many situations including in the context of the $T \to 0$ limit of spontaneously broken phases.

Bibliography

[1] A. Donos, J. P. Gauntlett and O. Sosa-Rodriguez, *Anisotropic plasmas from axion and dilaton deformations*, *JHEP* **11** (2016) 002, [1608.02970].

[2] A. Donos, J. P. Gauntlett, C. Rosen and O. Sosa-Rodriguez, *Boomerang RG flows in M-theory with intermediate scaling*, *JHEP* **07** (2017) 128, [1705.03000].

[3] A. Donos, J. P. Gauntlett, C. Rosen and O. Sosa-Rodriguez, *Boomerang RG flows with intermediate conformal invariance*, *JHEP* **04** (2018) 017, [1712.08017].

[4] J. M. Maldacena, *The Large N limit of superconformal field theories and supergravity*, *Int. J. Theor. Phys.* **38** (1999) 1113–1133, [hep-th/9711200].

[5] E. Witten, *Anti-de Sitter space and holography*, *Adv. Theor. Math. Phys.* **2** (1998) 253–291, [hep-th/9802150].

[6] P. Coleman, *Condensed matter: strongly correlated electrons*, *Physics World* **8** (1995) 29.

[7] K. G. Wilson, *The Renormalization Group: Critical Phenomena and the Kondo Problem*, *Rev. Mod. Phys.* **47** (1975) 773.

[8] A. B. Zamolodchikov, *Irreversibility of the flux of renormalization group in 2d field theory*, *JETP Lett.* **43** (1986) .

[9] J. L. Cardy, *Is There a c Theorem in Four-Dimensions?*, *Phys. Lett.* **B215** (1988) 749–752.

[10] Z. Komargodski and A. Schwimmer, *On Renormalization Group Flows in Four Dimensions*, *JHEP* **12** (2011) 099, [1107.3987].

[11] D. L. Jafferis, I. R. Klebanov, S. S. Pufu and B. R. Safdi, *Towards the F-Theorem: N=2 Field Theories on the Three-Sphere*, *JHEP* **06** (2011) 102, [1103.1181].

[12] M. Taylor and W. Woodhead, *The holographic F theorem*, 1604.06809.

[13] H. Casini and M. Huerta, *A Finite entanglement entropy and the c-theorem*, *Phys. Lett.* **B600** (2004) 142–150, [hep-th/0405111].

[14] H. Casini and M. Huerta, *A c-theorem for entanglement entropy*, *Journal of Physics A Mathematical General* **40** (June, 2007) 7031–7036, [cond-mat/0610375].

[15] D. Z. Freedman, S. S. Gubser, K. Pilch and N. P. Warner, *Renormalization group flows from holography supersymmetry and a c theorem*, *Adv. Theor. Math. Phys.* **3** (1999) 363–417, [`hep-th/9904017`].

[16] R. C. Myers and A. Sinha, *Holographic c-theorems in arbitrary dimensions*, `1011.5819`.

[17] J. Cardy, *Scaling and renormalization in statistical physics*, vol. 5. Cambridge university press, 1996.

[18] D. S. Fisher, *Scaling and critical slowing down in random-field Ising systems*, *Phys. Rev. Lett.* **56** (1986) 416–419.

[19] P. Francesco, P. Mathieu and D. Senechal, *Conformal Field Theory*. Island Press, 1996.

[20] R. Blumenhagen and E. Plauschinn, *Introduction to Conformal Field Theory*. Lecture Notes in Physics. Springer-Verlag Berlin Heidelberg, 1 ed., 2009, 10.1007/978-3-642-00450-6.

[21] G. Mack and A. Salam, *Finite-component field representations of the conformal group*, *Annals of Physics* **53** (1969) 174 – 202.

[22] S. Coleman and J. Mandula, *All possible symmetries of the s matrix*, *Phys. Rev.* **159** (Jul, 1967) 1251–1256.

[23] S. Minwalla, *Restrictions imposed by superconformal invariance on quantum field theories*, *Adv. Theor. Math. Phys.* **2** (1998) 783–851, [`hep-th/9712074`].

[24] M. F. Sohnius, *Introducing supersymmetry*, *Physics Reports* **128** (1985) 39 – 204.

[25] S. Sachdev, *Quantum Phase Transitions*. Cambridge University Press, 2011.

[26] A. Lucas, T. Sierens and W. Witczak-Krempa, *Quantum critical response: from conformal perturbation theory to holography*, *JHEP* **07** (2017) 149, [`1704.05461`].

[27] M. J. Duff, *Twenty years of the Weyl anomaly*, *Class. Quant. Grav.* **11** (1994) 1387–1404, [`hep-th/9308075`].

[28] J. L. Cardy, *Anisotropic corrections to correlation functions in finite-size systems*, *Nuclear Physics B* **290** (1987) 355 – 362.

[29] J. L. Cardy, *Operator Content of Two-Dimensional Conformally Invariant Theories*, *Nucl. Phys.* **B270** (1986) 186–204.

[30] E. P. Verlinde, *On the holographic principle in a radiation dominated universe*, `hep-th/0008140`.

[31] S. W. Hawking and G. F. R. Ellis, *The Large Scale Structure of Space-Time*. Cambridge Monographs on Mathematical Physics. Cambridge University Press, 1973, 10.1017/CBO9780511524646.

[32] P. Breitenlohner and D. Z. Freedman, *Positive energy in anti-de sitter backgrounds and gauged extended supergravity*, Physics Letters B **115** (1982) 197 – 201.

[33] M. Guica, K. Skenderis, M. Taylor and B. C. van Rees, *Holography for Schrodinger backgrounds*, JHEP **02** (2011) 056, [`1008.1991`].

[34] B. C. van Rees, *Irrelevant deformations and the holographic Callan-Symanzik equation*, JHEP **10** (2011) 067, [`1105.5396`].

[35] D. Marolf and S. F. Ross, *Boundary Conditions and New Dualities: Vector Fields in AdS/CFT*, JHEP **11** (2006) 085, [`hep-th/0606113`].

[36] S. W. Hawking and D. N. Page, *Thermodynamics of Black Holes in anti-De Sitter Space*, Commun. Math. Phys. **87** (1983) 577.

[37] M. J. Duff, *TASI lectures on branes, black holes and Anti-de Sitter space*, in *Theoretical physics at the end of the twentieth century. Proceedings, Summer School, Banff, Canada, June 27-July 10, 1999*, pp. 3–125, 1999. `hep-th/9912164`.

[38] G. T. Horowitz and A. Strominger, *Black strings and P-branes*, Nucl. Phys. **B360** (1991) 197–209.

[39] G. 't Hooft, *A Planar Diagram Theory for Strong Interactions*, Nucl. Phys. **B72** (1974) 461.

[40] O. Aharony, S. S. Gubser, J. M. Maldacena, H. Ooguri and Y. Oz, *Large N field theories, string theory and gravity*, Phys. Rept. **323** (2000) 183–386, [`hep-th/9905111`].

[41] E. Witten, *String theory dynamics in various dimensions*, Nucl. Phys. **B443** (1995) 85–126, [`hep-th/9503124`].

[42] O. Aharony, O. Bergman, D. L. Jafferis and J. Maldacena, *N=6 superconformal Chern-Simons-matter theories, M2-branes and their gravity duals*, JHEP **10** (2008) 091, [`0806.1218`].

[43] I. R. Klebanov and A. M. Polyakov, *AdS dual of the critical O(N) vector model*, Phys. Lett. **B550** (2002) 213–219, [`hep-th/0210114`].

[44] S. Benvenuti, S. Franco, A. Hanany, D. Martelli and J. Sparks, *An Infinite family of superconformal quiver gauge theories with Sasaki-Einstein duals*, JHEP **06** (2005) 064, [`hep-th/0411264`].

[45] S. S. Gubser, I. R. Klebanov and A. M. Polyakov, *Gauge theory correlators from noncritical string theory*, Phys. Lett. **B428** (1998) 105–114, [`hep-th/9802109`].

[46] J. W. York, *Boundary terms in the action principles of general relativity*, *Foundations of Physics* **16** (1986) 249–2577.

[47] K. Skenderis, *Lecture notes on holographic renormalization*, *Class.Quant.Grav.* **19** (2002) 5849–5876, [`hep-th/0209067`].

[48] C. Fefferman and C. R. Graham, *The ambient metric*, *Ann. Math. Stud.* **178** (2011) 1–128, [`0710.0919`].

[49] S. de Haro, S. N. Solodukhin and K. Skenderis, *Holographic reconstruction of space-time and renormalization in the AdS / CFT correspondence*, *Commun.Math.Phys.* **217** (2001) 595–622, [`hep-th/0002230`].

[50] D. T. Son and A. O. Starinets, *Minkowski space correlators in AdS / CFT correspondence: Recipe and applications*, *JHEP* **0209** (2002) 042, [`hep-th/0205051`].

[51] K. Skenderis and B. C. van Rees, *Real-time gauge/gravity duality: Prescription, Renormalization and Examples*, *JHEP* **05** (2009) 085, [`0812.2909`].

[52] M. Bianchi, D. Z. Freedman and K. Skenderis, *How to go with an RG flow*, *JHEP* **08** (2001) 041, [`hep-th/0105276`].

[53] J. de Boer, *The Holographic renormalization group*, *Fortsch. Phys.* **49** (2001) 339–358, [`hep-th/0101026`].

[54] R. Kubo, *The fluctuation-dissipation theorem*, *Reports on Progress in Physics* **29** (1966) 255.

[55] S. A. Hartnoll, *Lectures on holographic methods for condensed matter physics*, *Class.Quant.Grav.* **26** (2009) 224002, [`0903.3246`].

[56] Z. Q. Li, E. A. Henriksen, Z. Jiang, Z. Hao, M. C. Martin, P. Kim et al., *Dirac charge dynamics in graphene by infrared spectroscopy*, *Nature Physics* **4** (06, 2008) 532 EP –.

[57] S. A. Hartnoll, P. K. Kovtun, M. Muller and S. Sachdev, *Theory of the Nernst effect near quantum phase transitions in condensed matter, and in dyonic black holes*, *Phys. Rev.* **B76** (2007) 144502, [`0706.3215`].

[58] R. Mahajan, M. Barkeshli and S. A. Hartnoll, *Non-Fermi liquids and the Wiedemann-Franz law*, *Phys.Rev.* **B88** (2013) 125107, [`1304.4249`].

[59] G. T. Horowitz, J. E. Santos and D. Tong, *Optical Conductivity with Holographic Lattices*, *JHEP* **1207** (2012) 168, [`1204.0519`].

[60] A. Donos and J. P. Gauntlett, *Holographic Q-lattices*, *JHEP* **1404** (2014) 040, [`1311.3292`].

[61] E. Bergshoeff, C. Hull and T. Ortin, *Duality in the type-ii superstring effective action*, *Nucl.Phys.* **B451** (1995) 547–578, [`hep-th/9504081`].

[62] D. Mateos and D. Trancanelli, *The anisotropic N=4 super Yang-Mills plasma and its instabilities*, *Phys.Rev.Lett.* **107** (2011) 101601, [`1105.3472`].

[63] K. Iwasawa, *On some types of topological groups*, *Annals of Mathematics* **50** (1949) 507–558.

[64] M. Naimark and A. Shtern, *Theory of group representations*. Grundlehren der mathematischen Wissenschaften. Heidelberg, 1982.

[65] S. Jain, N. Kundu, K. Sen, A. Sinha and S. P. Trivedi, *A Strongly Coupled Anisotropic Fluid From Dilaton Driven Holography*, *JHEP* **1501** (2015) 005, [`1406.4874`].

[66] I. R. Klebanov and E. Witten, *Superconformal field theory on three-branes at a Calabi-Yau singularity*, *Nucl.Phys.* **B536** (1998) 199–218, [`hep-th/9807080`].

[67] J. P. Gauntlett, D. Martelli, J. Sparks and D. Waldram, *Sasaki-Einstein metrics on S**2 x S**3*, *Adv. Theor. Math. Phys.* **8** (2004) 711–734, [`hep-th/0403002`].

[68] S. A. Hartnoll and D. M. Hofman, *Locally Critical Resistivities from Umklapp Scattering*, *Phys.Rev.Lett.* **108** (2012) 241601, [`1201.3917`].

[69] A. Donos and S. A. Hartnoll, *Interaction-driven localization in holography*, *Nature Phys.* **9** (2013) 649–655, [`1212.2998`].

[70] T. Andrade and B. Withers, *A simple holographic model of momentum relaxation*, *JHEP* **1405** (2014) 101, [`1311.5157`].

[71] A. Donos and J. P. Gauntlett, *Novel metals and insulators from holography*, *JHEP* **1406** (2014) 007, [`1401.5077`].

[72] B. Goutéraux, *Charge transport in holography with momentum dissipation*, *JHEP* **1404** (2014) 181, [`1401.5436`].

[73] T. Azeyanagi, W. Li and T. Takayanagi, *On String Theory Duals of Lifshitz-like Fixed Points*, *JHEP* **0906** (2009) 084, [`0905.0688`].

[74] D. Mateos and D. Trancanelli, *Thermodynamics and Instabilities of a Strongly Coupled Anisotropic Plasma*, *JHEP* **1107** (2011) 054, [`1106.1637`].

[75] E. Banks and J. P. Gauntlett, *A new phase for the anisotropic N=4 super Yang-Mills plasma*, *JHEP* **09** (2015) 126, [`1506.07176`].

[76] E. Banks, *Phase transitions of an anisotropic N=4 super Yang-Mills plasma via holography*, *JHEP* **07** (2016) 085, [`1604.03552`].

[77] P. Chesler, A. Lucas and S. Sachdev, *Conformal field theories in a periodic potential: results from holography and field theory*, *Phys.Rev.* **D89** (2014) 026005, [`1308.0329`].

[78] A. Donos, J. P. Gauntlett and C. Pantelidou, *Conformal field theories in d = 4 with a helical twist*, *Phys.Rev.* **D91** (2015) 066003, [1412.3446].

[79] S. Harrison, S. Kachru and H. Wang, *Resolving Lifshitz Horizons*, *JHEP* **02** (2014) 085, [1202.6635].

[80] J. Bhattacharya, S. Cremonini and A. Sinkovics, *On the IR completion of geometries with hyperscaling violation*, *JHEP* **02** (2013) 147, [1208.1752].

[81] N. Kundu, P. Narayan, N. Sircar and S. P. Trivedi, *Entangled Dilaton Dyons*, *JHEP* **03** (2013) 155, [1208.2008].

[82] J. Bhattacharya, S. Cremonini and B. Goutraux, *Intermediate scalings in holographic RG flows and conductivities*, *JHEP* **02** (2015) 035, [1409.4797].

[83] A. Donos, J. P. Gauntlett and C. Pantelidou, *Semi-local quantum criticality in string/M-theory*, *JHEP* **1303** (2013) 103, [1212.1462].

[84] G. Policastro, D. T. Son and A. O. Starinets, *The Shear viscosity of strongly coupled N=4 supersymmetric Yang-Mills plasma*, *Phys.Rev.Lett.* **87** (2001) 081601, [hep-th/0104066].

[85] P. Kovtun, D. T. Son and A. O. Starinets, *Viscosity in strongly interacting quantum field theories from black hole physics*, *Phys.Rev.Lett.* **94** (2005) 111601, [hep-th/0405231].

[86] A. Rebhan and D. Steineder, *Violation of the Holographic Viscosity Bound in a Strongly Coupled Anisotropic Plasma*, *Phys. Rev. Lett.* **108** (2012) 021601, [1110.6825].

[87] K. A. Mamo, *Holographic RG flow of the shear viscosity to entropy density ratio in strongly coupled anisotropic plasma*, *JHEP* **10** (2012) 070, [1205.1797].

[88] R. Critelli, S. I. Finazzo, M. Zaniboni and J. Noronha, *Anisotropic shear viscosity of a strongly coupled non-Abelian plasma from magnetic branes*, *Phys. Rev.* **D90** (2014) 066006, [1406.6019].

[89] S. Jain, R. Samanta and S. P. Trivedi, *The Shear Viscosity in Anisotropic Phases*, 1506.01899.

[90] J. Erdmenger, P. Kerner and H. Zeller, *Non-universal shear viscosity from Einstein gravity*, *Phys. Lett.* **B699** (2011) 301–304, [1011.5912].

[91] A. Donos and J. P. Gauntlett, *Thermoelectric DC conductivities from black hole horizons*, *JHEP* **1411** (2014) 081, [1406.4742].

[92] A. Donos and J. P. Gauntlett, *Navier-Stokes Equations on Black Hole Horizons and DC Thermoelectric Conductivity*, *Phys. Rev.* **D92** (2015) 121901, [1506.01360].

[93] E. Banks, A. Donos and J. P. Gauntlett, *Thermoelectric DC conductivities and Stokes flows on black hole horizons*, JHEP **10** (2015) 103, [1507.00234].

[94] A. Donos, J. P. Gauntlett, T. Griffin and L. Melgar, *DC Conductivity of Magnetised Holographic Matter*, JHEP **01** (2016) 113, [1511.00713].

[95] S. A. Hartnoll and E. Shaghoulian, *Spectral weight in holographic scaling geometries*, JHEP **1207** (2012) 078, [1203.4236].

[96] S. Benvenuti and A. Hanany, *Conformal manifolds for the conifold and other toric field theories*, JHEP **08** (2005) 024, [hep-th/0502043].

[97] G. T. Horowitz and M. M. Roberts, *Zero Temperature Limit of Holographic Superconductors*, JHEP **0911** (2009) 015, [0908.3677].

[98] P. Basu, J. He, A. Mukherjee and H.-H. Shieh, *Hard-gapped Holographic Superconductors*, Phys.Lett. **B689** (2010) 45–50, [0911.4999].

[99] A. Donos, J. P. Gauntlett and C. Pantelidou, *Competing p-wave orders*, Class.Quant.Grav. **31** (2014) 055007, [1310.5741].

[100] L. Cheng, X.-H. Ge and S.-J. Sin, *Anisotropic plasma at finite $U(1)$ chemical potential*, JHEP **1407** (2014) 083, [1404.5027].

[101] M. Cvetic et al., *Embedding AdS black holes in ten and eleven dimensions*, Nucl. Phys. **B558** (1999) 96–126, [hep-th/9903214].

[102] M. Cvetic, H. Lu and C. N. Pope, *Geometry of the embedding of supergravity scalar manifolds in $D = 11$ and $D = 10$*, Nucl. Phys. **B584** (2000) 149–170, [hep-th/0002099].

[103] A. Azizi, H. Godazgar, M. Godazgar and C. N. Pope, *Embedding of gauged STU supergravity in eleven dimensions*, Phys. Rev. **D94** (2016) 066003, [1606.06954].

[104] C. Charmousis, B. Goutéraux, B. Kim, E. Kiritsis and R. Meyer, *Effective Holographic Theories for low-temperature condensed matter systems*, JHEP **1011** (2010) 151, [1005.4690].

[105] N. Ogawa, T. Takayanagi and T. Ugajin, *Holographic Fermi Surfaces and Entanglement Entropy*, JHEP **1201** (2012) 125, [1111.1023].

[106] L. Huijse, S. Sachdev and B. Swingle, *Hidden Fermi surfaces in compressible states of gauge-gravity duality*, Phys.Rev. **B85** (2012) 035121, [1112.0573].

[107] M. J. Duff and J. T. Liu, *Anti-de Sitter black holes in gauged $N = 8$ supergravity*, Nucl. Phys. **B554** (1999) 237–253, [hep-th/9901149].

[108] S. S. Gubser, S. S. Pufu and F. D. Rocha, *Quantum critical superconductors in string theory and M- theory*, Phys. Lett. **B683** (2010) 201–204, [0908.0011].

[109] S. S. Gubser, *Curvature singularities: The Good, the bad, and the naked*, *Adv. Theor. Math. Phys.* **4** (2000) 679–745, [`hep-th/0002160`].

[110] H. A. Chamblin and H. S. Reall, *Dynamic dilatonic domain walls*, *Nucl. Phys.* **B562** (1999) 133–157, [`hep-th/9903225`].

[111] T. Faulkner, N. Iqbal, H. Liu, J. McGreevy and D. Vegh, *Holographic non-Fermi liquid fixed points*, *Phil. Trans. Roy. Soc.* **A 369** (2011) 1640, [`1101.0597`].

[112] A. Donos and J. P. Gauntlett, *Superfluid black branes in $AdS_4 \times S^7$*, *JHEP* **06** (2011) 053, [`1104.4478`].

[113] N. Bobev, K. Pilch and N. P. Warner, *Supersymmetric Janus Solutions in Four Dimensions*, *JHEP* **06** (2014) 058, [`1311.4883`].

[114] N. Bao, X. Dong, S. Harrison and E. Silverstein, *The Benefits of Stress: Resolution of the Lifshitz Singularity*, *Phys. Rev.* **D86** (2012) 106008, [`1207.0171`].

[115] T. Nishioka, S. Ryu and T. Takayanagi, *Holographic Entanglement Entropy: An Overview*, *J. Phys.* **A42** (2009) 504008, [`0905.0932`].

[116] R. C. Myers and A. Singh, *Comments on Holographic Entanglement Entropy and RG Flows*, *JHEP* **04** (2012) 122, [`1202.2068`].

[117] H. Liu and M. Mezei, *A Refinement of entanglement entropy and the number of degrees of freedom*, *JHEP* **04** (2013) 162, [`1202.2070`].

[118] A. Donos, B. Goutéraux and E. Kiritsis, *Holographic Metals and Insulators with Helical Symmetry*, *JHEP* **1409** (2014) 038, [`1406.6351`].

[119] S. A. Hartnoll, *Theory of universal incoherent metallic transport*, *Nature Phys.* **11** (2015) 54, [`1405.3651`].

[120] M. Blake, *Universal Charge Diffusion and the Butterfly Effect in Holographic Theories*, *Phys. Rev. Lett.* **117** (2016) 091601, [`1603.08510`].

[121] M. Blake, *Universal Diffusion in Incoherent Black Holes*, *Phys. Rev.* **D94** (2016) 086014, [`1604.01754`].

[122] A. Lucas and J. Steinberg, *Charge diffusion and the butterfly effect in striped holographic matter*, *JHEP* **10** (2016) 143, [`1608.03286`].

[123] Y. Ling, P. Liu and J.-P. Wu, *Holographic Butterfly Effect at Quantum Critical Points*, *JHEP* **10** (2017) 025, [`1610.02669`].

[124] M. Blake and A. Donos, *Diffusion and Chaos from near AdS_2 horizons*, *JHEP* **02** (2017) 013, [`1611.09380`].

[125] R. A. Davison, W. Fu, A. Georges, Y. Gu, K. Jensen and S. Sachdev, *Thermoelectric transport in disordered metals without quasiparticles: The Sachdev-Ye-Kitaev models and holography*, Phys. Rev. **B95** (2017) 155131, [1612.00849].

[126] M. Baggioli, B. Goutraux, E. Kiritsis and W.-J. Li, *Higher derivative corrections to incoherent metallic transport in holography*, JHEP **03** (2017) 170, [1612.05500].

[127] S.-F. Wu, B. Wang, X.-H. Ge and Y. Tian, *Collective diffusion and quantum chaos in holography*, Phys. Rev. **D97** (2018) 106018, [1702.08803].

[128] K.-Y. Kim and C. Niu, *Diffusion and Butterfly Velocity at Finite Density*, JHEP **06** (2017) 030, [1704.00947].

[129] M. Baggioli and W.-J. Li, *Diffusivities bounds and chaos in holographic Horndeski theories*, JHEP **07** (2017) 055, [1705.01766].

[130] M. Blake, R. A. Davison and S. Sachdev, *Thermal diffusivity and chaos in metals without quasiparticles*, Phys. Rev. **D96** (2017) 106008, [1705.07896].

[131] S.-F. Wu, B. Wang, X.-H. Ge and Y. Tian, *Holographic RG flow of thermoelectric transport with momentum dissipation*, Phys. Rev. **D97** (2018) 066029, [1706.00718].

[132] D. Giataganas, U. Grsoy and J. F. Pedraza, *Strongly-coupled anisotropic gauge theories and holography*, 1708.05691.

[133] S. Grozdanov, K. Schalm and V. Scopelliti, *Black hole scrambling from hydrodynamics*, 1710.00921.

[134] A. Lucas, *Constraints on hydrodynamics from many-body quantum chaos*, 1710.01005.

[135] S. H. Shenker and D. Stanford, *Black holes and the butterfly effect*, JHEP **03** (2014) 067, [1306.0622].

[136] J. Maldacena, S. H. Shenker and D. Stanford, *A bound on chaos*, JHEP **08** (2016) 106, [1503.01409].

[137] K. Sfetsos, *On gravitational shock waves in curved space-times*, Nucl. Phys. **B436** (1995) 721–745, [hep-th/9408169].

[138] I. R. Klebanov and E. Witten, *AdS/CFT correspondence and symmetry breaking*, Nucl. Phys. **B556** (1999) 89–114, [hep-th/9905104].

[139] S. Ryu and T. Takayanagi, *Holographic derivation of entanglement entropy from AdS/CFT*, Phys. Rev. Lett. **96** (2006) 181602, [hep-th/0603001].

[140] S. Ryu and T. Takayanagi, *Aspects of Holographic Entanglement Entropy*, JHEP **08** (2006) 045, [hep-th/0605073].

[141] T. Albash and C. V. Johnson, *Holographic Entanglement Entropy and Renormalization Group Flow*, JHEP **02** (2012) 095, [1110.1074].

[142] A. Donos, J. P. Gauntlett and V. Ziogas, *Diffusion in inhomogeneous media*, Phys. Rev. **D96** (2017) 125003, [1708.05412].

[143] A. Donos, J. P. Gauntlett and V. Ziogas, *Diffusion for Holographic Lattices*, JHEP **03** (2018) 056, [1710.04221].

[144] P. B. Bailey and L. Shampine, *Existence from uniqueness for two point boundary value problems*, Journal of Mathematical Analysis and Applications **25** (1969) 569 – 574.

[145] J. V. Baxley, *Existence theorems for nonlinear second order boundary value problems*, Journal of Differential Equations **85** (1990) 125 – 150.

[146] D. Jordan and P. Smith, *Nonlinear Ordinary Differential Equations: An Introduction for Scientists and Engineers*. Oxford applied and engineering mathematics. Oxford University Press, 2007.

[147] T. Andrade, *Holographic lattices and numerical techniques*, 2017. 1712.00548.